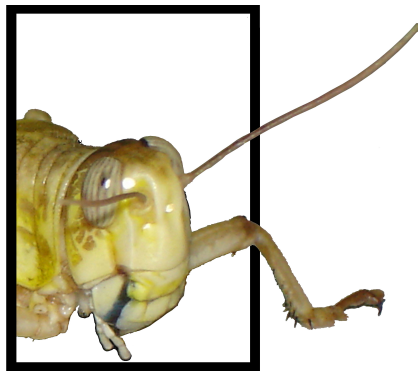# Coding of sky-compass information in neurons of the anterior optic tubercle of the desert locust
Schistocerca gregaria

Kodierung von Himmelskompassinformationen in Neuronen des anterioren optischen Tuberkels der Wüstenheuschrecke
Schistocerca gregaria

Coding of sky-compass information in neurons of the anterior optic tubercle of the desert locust *Schistocerca gregaria*

Kodierung von Himmelskompassinformationen in Neuronen des anterioren optischen Tuberkels der Wüstenheuschrecke
Schistocerca gregaria

Dissertation zur Erlangung des
Doktorgrades der Naturwissenschaften
(Dr. rer. nat.)

dem Fachbereich Biologie
der Philipps-Universität Marburg
vorgelegt von
Keram Pfeiffer
aus Mönchengladbach
Marburg/Lahn 2006

Contents

Erklärung: Eigene Beiträge und veröffentlichte Teile der Arbeit

Laut §8, Absatz 3 der Promotionsordnung der Philipps-Universität Marburg (Fassung vom 28.4.1993) müssen bei den Teilen der Dissertation, die aus gemeinsamer Forschungsarbeit entstanden sind, „die individuellen Leistungen des Doktoranden deutlich abgrenzbar und bewertbar sein." Dies betrifft die Kapitel 1-3. Die Beiträge werden im folgenden näher erläutert.

Kapitel 1: Polarization-sensitive and light-sensitive neurons in two parallel pathways passing through the anterior optic tubercle in the locust brain

- Durchführung von 43% der Experimente (48 von 112 Ableitungen)

- Einarbeitung und Betreuung von Dr. Michiyo Kinoshita. Dr. Kinoshita war Gastwissenschaftlerin in unserem Labor und hat die restlichen Ableitungen durchgeführt.

- Auswertung aller Experimente

- Verfassen des Manuskripts in Zusammenarbeit (Korrektur) mit Prof. Dr. Uwe Homberg

- Dieses Kapitel wurde in der vorliegenden Form im Journal of Neurophysiology veröffentlicht. (Pfeiffer K, Kinoshita M, Homberg, U, Polarization-sensitive and light-sensitive neurons in two parallel pathways passing through the anterior optic tubercle in the locust brain. *J. Neurophysiol.* **94**, 3903-3915 (2005).)

Kapitel 2: Coding of spatial directions via time-compensated combination of celestial compass cues

- Planung der Reizapparatur

- Planung, Durchführung und Auswertung aller Experimente

- Verfassen des Manuskriptes in Zusammenarbeit (Korrektur) mit Prof. Dr. Uwe Homberg

- Dieses Kapitel wurde am 28.7.2006 in der vorliegenden Form bei Nature Neuroscience eingereicht.

Kapitel 3: Performance of polarization-sensitive inerneurons of the anterior optic tubercle in the locust brain at different degrees of polarization

- Planung und Umbau der Reizapparatur

- Planung, Durchführung und Auswertung aller Experimente

- Verfassen des Manuskriptes in Zusammenarbeit (Korrektur) mit Prof. Dr. Uwe Homberg

Die Abfassung des Dissertation in englischer Sprache wurde vom Dekan des Fachbereichs Biologie am 11.07.2006 genehmigt.

Zusammenfassung

Viele Insekten zeigen ein ausgeprägtes Orientierungs- bzw. Navigationsvermögen. Neben der Orientierung an Landmarken bilden die Sonne und verschiedene Aspekte des Himmelslichts, wie Farbe, Helligkeit und Polarisation, die wichtigsten Informationsquellen, die eine zielgerichtete Lokomotion erlauben. Während sich soziale Hymenopteren aufgrund ihrer guten Dressierbarkeit besonders gut für verhaltensbiologische Experimente zur Himmelskompassorientierung eignen (von Frisch, 1949; Wehner, 1997), haben sich insbesondere die Feldgrille *(Gryllus campestris)* und die Wüstenheuschrecke *(Schistocerca gregaria)* zu Modellorganismen für elektrophysiologische und morphologische Untersuchungen des Polarisationssehsystems entwickelt (Labhart et al., 2001; Homberg, 2004).

Alle Insekten, die das Polarisationsmuster des Himmelslichtes perzipieren können, besitzen einen besonderen Augenbereich, die dorsale Randregion. Ommatidien dieser dorsalen Randregion unterscheiden sich durch zahlreiche Spezialisierungen, die die Empfindlichkeit für polarisiertes Licht erhöhen, von denen des restlichen Komplexauges (Labhart & Meyer, 1999). Durch Farbstoffinjektionen und intrazelluläre Ableitungen konnte die neuronale Verbindung zwischen der dorsalen Randregion und dem Zentralkomplex (Polarisationssehbahn) bei der Wüstenheuschrecke dargestellt werden. Eine Zwischenstation dieser Sehbahn ist der anteriore optische Tuberkel (AOTu), ein etwa 200 µm großes Neuropil im Zentralhirn (Homberg et al., 2003). Unter dem Präparationsmikroskop ist der AOTu als Erhebung der frontalen Gehirnoberfläche zu erkennen und erlaubt daher ein gezieltes Einstechen einer intrazellulären Ableitelektrode. Das Ziel der Arbeit bestand zunächst darin, mit Hilfe intrazellulärer Ableitungen die Funktion des AOTu, insbesondere im Hinblick auf eine Beteiligung beim Polarisationssehen, zu untersuchen. Dabei stellte sich heraus, dass sich zwei Neuronentypen der unteren Einheit des AOTu (Typ LoTu1, Typ TuTu1) aufgrund ihres großen Faserdurchmessers hervorragend für intrazelluläre Ableitungen eignen. Beide Zelltypen kommen nur in sehr geringer Zahl im Gehirn vor (2 x LoTu1, 4 x TuTu1), so dass es möglich wurde, von individuellen Neuronen in verschiedenen Tieren wiederholt abzuleiten. Dies ermöglichte eine sehr detaillierte Untersuchung beider Zelltypen, wobei im Verlauf der Arbeit die Stimulation von polarisiertem Licht auf verschiedene unpolarisierte Lichtreize ausgedehnt wurde. Dabei wurde den Tieren während der Ableitung ein monochromatischer (grüner oder ultravioletter) Lichtpunkt präsentiert, der sich auf einer Kreisbahn in 45° Elevation um das Zentrum des Kopfes bewegte. Dies ermöglichte das Vermessen der rezeptiven Felder, die den Antworten auf unpolarisierte Lichtreize zugrunde liegen.

Bei intrazellulären Ableitungen dient eine Glaskapillare, welche unter Hitze zu einer feinen Spitze von weniger als 1 µm Durchmesser ausgezogen wird und mit einem Farbstoff und einer Elektrolytlösung gefüllt wird, als Elektrode. Wird diese in eine Nervenzelle eingestochen, können mit Hilfe eines angeschlossenen Verstärkers und eines Oszilloskops (oder eines A/D Wandlers und PCs) Aktionspotentiale gemessen werden, während dem Tier verschiedene Reize präsentiert werden. Der in der Elektrode enthaltene Farbstoff wird in das Neuron injiziert, so dass dessen Morphologie analysiert werden kann. So lassen sich zum einen identifizierte Neurone in verschiedenen Präparaten wieder erkennen, zum anderen kann man aufgrund der Verzweigungen der Zellen und ihrer Reaktionen auf die gebotenen Reize einzelnen Gehirnarealen bestimmte Funktionen zuordnen.

Die Arbeit gliedert sich in vier Kapitel.

Kapitel 1: Polarisations-empfindliche und Licht-empfindliche Neurone in zwei parallelen Bahnen durch den anterioren optischen Tuberkel im Heuschreckengehirn.
(Polarization-sensitive and light-sensitive neurons in two parallel pathways passing through the anterior optic tubercle in the locust brain)

Der AOTu der Heuschrecke gliedert sich morphologisch in eine obere und eine untere Einheit. Beide sind Teil neuronaler Bahnen, die parallel von den primären visuellen Zentren, den optischen Loben, über den AOTu in den lateralen akzessorischen Lobus und von dort in den Zentralkomplex ziehen. Durch Farbstoffinjektionen in die untere Einheit des AOTu konnten Neurone gefärbt werden, deren presumptive Ausgangsregionen mit den presumptiven Eingangsregionen polarisationsempfindlicher Tangentialzellen der unteren Zentralkörpereinheit überlappen und vermutlich mit diesen in synaptischem Kontakt stehen. In dieser Arbeit wurde untersucht, ob die morphologische Zweiteilung des AOTu einer funktionalen Teilung entspricht, insbesondere im Hinblick auf eine mögliche Bedeutung der unteren Einheit im Polarisationssehsystem der Heuschrecke.

Insgesamt wurden sieben Neuronentypen charakterisiert, davon vier Zelltypen in der unteren Einheit des AOTu. Das wichtigste Ergebnis dieser Arbeit ist, dass alle vier Neuronentypen der unteren Einheit des AOTu polarisationsempfindlich sind. Dies bestätigt die auf morphologischen Untersuchungen beruhende Annahme, dass der AOTu Teil der Polarisationssehbahn der Heuschrecke ist. Von den beiden Neuronen LoTu1 und TuTu1 konnte insgesamt über hundertmal abgeleitet werden, so dass diese Neurone sehr detailliert untersucht werden konnten. Beschattungsexperimente, bei denen die dorsale Randregion eines Auges abgedeckt oder übermalt wurde, zeigten, dass LoTu1 Polarisationsinformationen ausschließlich von dem zum Zellkörper ipsilateralen Auge erhält. Bei TuTu1 Neuronen waren die Reaktionen auf polarisiertes Licht bei Beschattung des ipsilateralen Auges nicht verschwunden, jedoch deutlich in ihrer Amplitude reduziert. Beide Neuronentypen sind spezifisch auf bestimmte E-Vektor Orientierungen abgestimmt. Das LoTu1 Neuron, dessen Zellkörper sich in der linken Gehirnhälfte befindet, antwortet maximal bei einer E-Vektor Orientierung um 134°, während die Zelle der anderen Gehirnhälfte maximal bei einer E-Vektor Orientierung um 41° erregt wird. Bei TuTu1 Neuronen gibt es in jeder Gehirnhälfte eine Zelle, deren Vorzugsvektor bei 0° liegt und jeweils eine, die maximal bei 135° (Soma links) bzw. bei 45° (Soma rechts) antwortet (vgl. aber hierzu die Bemerkungen im Abschnitt über Kapitel 2).

Alle Neurone der oberen Einheit zeigten Reaktionen auf unpolarisierte Lichtreize. Eine von fünf untersuchten Zellen war darüber hinaus leicht polarisationsempfindlich. In der oberen Einheit des AOTu werden somit hauptsächlich andere visuelle Parameter als Polarisation verarbeitet.

Ein unerwartetes Ergebnis, das die Zielrichtung der Arbeit maßgeblich beeinflusste, waren die Antworten beider Neuronentypen auf unpolarisiertes Licht. Diese Reaktionen waren stark abhängig von der Richtung des Stimulus und ließen die Vermutung zu, dass LoTu1 und TuTu1 Neurone möglicherweise auch bei der Kodierung der horizontalen Richtung der Sonne, dem Sonnenazimut, eine Rolle spielen.

Kapitel 2: Richtungskodierung durch zeitkompensierte Kombination von Himmelskompassinformationen
(Coding of spatial directions via time-compensated combination of celestial compass cues)

Himmelslicht weist neben einem Polarisationsmuster weitere Eigenschaften auf, die Hinweise auf den Sonnenstand geben. Während die Orientierung von E-Vektoren des polarisierten Lichtes keine Unterscheidung zwischen der horizontalen Position der Sonne und der der Sonne entgegen gesetzten Himmelsrichtung erlaubt, ist dies durch Hinzuziehen der im folgenden erläuterten Richtungsinformationen möglich. Die prominenteste Richtungsinformation am Taghimmel liefert die Sonne selbst. Als hellster Punkt am Himmel ist ihre Position leicht bestimmbar. Daneben weist das gestreute Himmelslicht einen Farbgradienten auf. Licht von der der Sonne zugewandten Him-

melshälfte, der solaren Hemisphäre, weist im Vergleich zu Licht aus der antisolaren Hemisphäre einen geringeren Anteil kurzwelligen Lichts auf. Ob und wie diese Informationen von Neuronen des AOTu verarbeitet werden, ist Gegenstand dieses Kapitels der Arbeit.

Um den Einfluss von Wellenlänge und Position eines unpolarisierten Lichtstimulus auf die Aktivität der Neurone zu testen, wurden monochromatische grüne (530 nm) und ultraviolette (350 nm) Lichtpunkte gleicher Photonenfluenzraten in einer Elevation von 45° auf einer Kreisbahn um den Kopf des Tieres bewegt. Die gewählten Wellenlängen entsprachen dabei den Absorptionsmaxima der lang- bzw. kurzwelligen Photorezeptoren im Komplexauge der Heuschrecken. Bei allen Ableitungen wurde vor der Stimulation mit unpolarisiertem Licht mit blauem (450 nm) linear polarisiertem Licht mit rotierendem E-Vektor stimuliert. Dies diente einerseits dem Erkennen der jeweiligen Zelltypen, die anhand ihrer Reaktion auf polarisiertes Licht identifiziert werden konnten, andererseits sollten die Vorzugsrichtungen der Neurone für die verschiedenen Reize verglichen werden. Aus Versuchen mit unbewegten, monochromatischen, unpolarisierten Lichtreizen war uns bereits bekannt, dass sowohl LoTu1 als auch TuTu1 Gegenfarben-Eigenschaften besitzen. Dies bedeutet, dass sie bei Reizung mit einer bestimmten Wellenlänge erregt werden, während sie bei Reizung mit einer anderen Wellenlänge gehemmt werden. Mit den bewegten Lichtreizen konnten nun die rezeptiven Felder und auch die Vorzugsrichtungen für die jeweiligen Stimuli bestimmt werden. LoTu1 Neurone zeigten starke Erregung, wenn sich ein grüner Lichtpunkt im ipsilateralen Sehfeld befand und wurden von ipsilateralem UV-Licht gehemmt. TuTu1 Neurone reagierten umgekehrt, d.h. sie wurden bei ipsilateralem grünem Licht gehemmt und durch ipsilaterales UV-Licht erregt. Zusätzlich zeigten sie Exzitationen bei kontralateralem grünem Licht und, in einigen Fällen, Inhibition bei kontralateralem UV-Licht.

Um zu überprüfen, ob die Reaktionen der Neurone die räumliche Beziehung zwischen dem Sonnenazimut und der Orientierung von E-Vektoren des Himmelspolarisationsmusters widerspiegelt, wurde für alle Ableitungen der Winkel zwischen der maximalen E-Vektorantwort und der maximalen Antwort auf den grünen Lichtpunkt, der die Sonne repräsentierte, berechnet. Es zeigte sich, dass dieser Winkel sich im Tagesverlauf ändert, von kleinen Werten gegen Mittag zu großen Werten (maximal 90°) gegen Abend. Da die untersuchten Neurone Polarisationsinformation ausschließlich (bei TuTu1 hauptsächlich) über die dorsalen Randregion eines Auges verarbeiten, kann man aufgrund der optischen Achse der dort vorhandenen Photorezeptoren ein rezeptives Feld erwarten, dass sein Zentrum nicht im Zenit sondern seitlich davon hat. Dies bedeutet, dass sich die perzipierte E-Vektororientierung im Tagesverlauf abhängig von der Sonnenhöhe verändert. Berechnungen zur Änderung des Polarisationsmusters im Tagesverlauf deuten darauf hin, dass durch die tageszeitliche Änderung im Antwortverhalten der Neurone diese Veränderung kompensiert wird. Dies verhindert, dass das Polarisationsmuster und der direkte Blick auf die Sonne widersprüchliche Informationen liefern.

Die Verteilung der E-Vektor Vorzugsrichtungen aller Ableitungen von LoTu1 und TuTu1 erstreckte sich bei diesen Versuchen nahezu über den gesamten möglichen Bereich von 0° bis 180° und war bei LoTu1 Neuronen nicht von einer Gleichverteilung zu unterscheiden. Die hierbei verwendeten Tiere wurden im Gegensatz zu den in Kapitel 1 verwendeten Tieren nicht im Labor unter Kunstlicht, sondern in einem Gewächshaus aufgezogen und hatten freie Sicht auf das Himmelspolarisationsmuster. Möglicherweise ist daher ein Grundwert für die E-Vektor Vorzugsrichtung genetisch fixiert (vgl. Kapitel 1), während tageszeitliche Änderungen erlernt werden müssen.

Wenn die vorgestellten Neurone den Sonnenazimut sowohl aus dem Blick auf die Sonne, dem UV/grün Kontrast des Himmelslichtes, als auch aus dem Polarisationsmuster ableiten können, ist es notwendig, dass alle Parameter entweder die gleichen Informationen liefern, oder nicht alle Parameter zu jedem Zeitpunkt ausgewertet werden. Beispielsweise ist bei LoTu1 Neuronen die

Reaktion auf ipsilaterales grünes Licht so stark, dass vermutlich bei ipsilateralem Sonnenstand die wesentlich schwächere Reaktion auf das polarisierte Licht maskiert wird. Anders verhält es sich bei TuTu1 Neuronen, die auf polarisiertes Licht ebenso stark reagieren wie auf unpolarisiertes. Da TuTu1 Neurone maximal durch kontralaterales grünes Licht erregt werden, kann vermutet werden, dass die E-Vektor Antwort aufgrund des geringen Polarisationsgrades bei kontralateralem Sonnenstand gering ist.

Kapitel 3: Antwortverhalten polarisationsempfindlicher Neurone des anterioren optischen Tuberkels im Heuschreckengehirn bei verschiedenen Polarisationsgraden
(Performance of polarization-sensitive interneurons of the anterior optic tubercle in the locust brain at different degrees of polarization)

Das Polarisationsmuster des Himmelslichtes zeichnet sich, außer durch die Anordnung der E-Vektoren tangential zu konzentrischen Kreisen um die Sonne, auch durch einen Gradienten des Polarisationsgrades (d) aus. Während direktes Sonnenlicht unpolarisiert ist, findet sich der höchste Polarisationsgrad in einem Winkel von 90° zur Sonne. Unter optimalen atmosphärischen Bedingungen kann dort das Licht bis zu 75% polarisiert sein ($d = 0,75$). Meist liegt der Polarisationsgrad jedoch niedriger, insbesondere unter Wolken. In den Versuchen sollte daher untersucht werden, wie die polarisations-sensitiven Neurone des AOTu auf polarisiertes Licht unterschiedlichen Polarisationsgrades reagieren.

In den Versuchen zu diesem Kapitel wurde wie bei den vorigen Versuchen mit einem rotierenden Polarisationsfilter stimuliert. Durch das Einbringen einer Verzögerungsfolie in den Strahlengang wurde elliptisch polarisiertes Licht unterschiedlicher Elliptizität erzeugt. Elliptisch polarisiertes Licht einer bestimmten Elliptizität (d) hat auf Photorezeptoren den gleichen Effekt wie partiell linear polarisiertes Licht gleichen d-Wertes, ist aber einfacher zu erzeugen.

Sowohl LoTu1 als auch TuTu1 Neurone zeigten eine lineare Beziehung zwischen dem d-Wert und der Antwortstärke. Dabei unterschieden sich beide Typen insofern, als bei TuTu1 Neuronen gleiche Änderungsraten im Polarisationsgrad zu größeren Änderungen in der Antwortstärke führten als bei LoTu1 Neuronen. Bei beiden Zelltypen ging die Gesamtaktivität mit sinkendem Polarisationsgrad zurück, was bei niedrigen d-Werten zu starker Inhibition und ausbleibender Modulation der Aktivität führte. Aus den Versuchen zu Kapitel 1 war bereits bekannt, dass beide Neurontypen durch unpolarisiertes dorsales Licht gehemmt werden. Diese Reaktion interferiert offensichtlich bei niedrigen Polarisationsgraden mit der E-Vektor-abhängigen Polarisationsreaktion. Die biologische Funktion dieses Zusammenspiels liegt möglicherweise darin, bestimmte Himmelsteile von der Analyse durch das Polarisationssehsystem auszuschließen, da sie andere Richtungsinformationen als das direkte Sonnenlicht und der Farbgradient des Himmels liefern würden (s. Kapitel 2). Dies würde bedeuten, dass bei kontralateralem Sonnenstand, der zu starker Erregung von TuTu1 Neuronen führen würde, Polarisationsinformation des Himmelslichtes nicht wahrgenommen wird und so auch nicht zu Fehlinformationen führen kann.

Fazit aus Kapitel 1-3

Durch die Experimente im Rahmen meiner Dissertation konnten die beiden Neurone LoTu1 und TuTu1 sehr genau charakterisiert werden. Ich konnte zeigen, dass beide Zellen Teil eines Systems sind, welches die horizontale Richtung der Sonne, den Sonnenazimut, relativ zur Körperlängsachse des Tieres signalisiert. Um Informationen über den Sonnenazimut zu erhalten, sind Photorezeptoren von verschiedenen Teilen des Komplexauges so verschaltet, dass unterschiedliche Aspekte des Himmelslichts (Intensität, spektrale Zusammensetzung, E-Vektor Orientierung) gleiche Informationen liefern. Diese Integration geschieht bereits sehr peripher, vermutlich in Tangentialzellen

der Medulla, dem zweiten optischen Ganglion. Diese Zellen erhalten wahrscheinlich sowohl direkten Eingang von Photorezeptoren als auch indirekten Eingang von Monopolarzellen der Lamina. Da der Winkel zwischen dem Sonnenazimut und dem E-Vektor-Muster im Tagesverlauf mit der Höhe der Sonne (Sonnenelevation) variiert, ändert sich die Justierung der Neurone im Tagesverlauf ebenfalls. Dies ist notwendig, damit E-Vektor Orientierung und Lichtintensität/spektrale Zusammensetzung des Lichtes denselben Sonnenazimut anzeigen. Beide Neuronentypen sind ab einem Polarisationsgrad von ca. $d = 0,3$ in der Lage, E-Vektor Orientierung zu kodieren. Damit liefern die E-Vektoren in einem Bereich von etwa $100°$ um die Sonne keine Richtungsinformationen. Dies könnte dazu dienen, Missweisungen durch die in diesem Gebiet sehr variablen E-Vektor Orientierungen zu verhindern. Die Neurone LoTu1 und TuTu1 können somit als Sonnenazimut-Detektoren betrachtet werden, die alle verfügbaren Richtungsinformationen des Himmelslichts auswerten.

Kapitel 4: Spike2 Skripte zur Datenerfassung, -auswertung und für Modellrechnungen
(Spike2 scripts for data acquisition, data evaluation and for model calculations)

Spike2 ist eine Datenerfassungs- und -analysesoftware für elektrophysiologische Experimente. Es beinhaltet eine leistungsfähige Skriptsprache, die eine flexible Anpassung des Programms an die spezifischen Bedürfnisse der Benutzer ermöglicht. Es können Arbeitsabläufe automatisiert, interaktive Dialoge erstellt oder automatische online Analysen programmiert werden.

Mit Hilfe dieser Skriptsprache habe ich im Verlauf meiner Dissertation einige Skripte erstellt, von denen die wichtigsten und umfangreichsten hier dokumentiert werden sollen. Im Folgenden möchte ich nur kurz auf die Fähigkeiten und Funktionen der beiden mächtigsten und von mir meistbenutzten Skripte eingehen. Die Besprechung aller im Rahmen der Dissertation entstandenen Skripte würde den Rahmen der Zusammenfassung sprengen. Einige weitere werden jedoch in Kapitel 4 vorgestellt.

IntraCell Dieses Skript entstand im Rahmen der Datenauswertung zum ersten Kapitel. Ursprünglich war es nur konzipiert, um automatisch Histogramme der neuronalen Aktivität während Stimulation mit polarisiertem Licht zu erstellen. Inzwischen ist es zu einem interaktiven Auswerteskript mit einer Fülle an Funktionen geworden und ist sicherlich nicht nur zur Auswertung intrazellulärer Ableitungen von polarisationsempfindlichen Interneuronen geeignet. Einige Aufgaben, die das Skript übernimmt, sind auch über die normalen Funktionen von Spike2 zugänglich; dies erfordert jedoch ein Vielfaches an Zeit. Andere Funktionen, wie zum Beispiel Änderungen der Ansichtsgröße von Kanälen, sind ausschließlich über Skriptfunktionen abrufbar.

Das Skript bietet:

- verschiedene Funktionen, die das Arbeiten mit Cursors vereinfachen und beschleunigen (Cursor holen, zwischen Cursors zoomen, Zeit zwischen Cursors berechnen)

- verschiedene Funktionen, um Einstellungen an einzelnen Kanälen vorzunehmen (löschen, Größe in der Ansicht ändern, verstecken, alle zeigen)

- Darstellung der kompletten Aufnahme und Optimierung der Y-Achsenskalierung

- Einstellen der Punktgröße für die Darstellung von Instantanfrequenzen

- automatisches oder interaktives Erstellen von Peristimulus Zeit Histogrammen für eine komplette Aufnahme, oder ausgewählte Teile davon

- interaktives Erstellen von Interevent Intervall Histogrammen für ausgewählte Bereiche

- Berechnung von Vorzugsrichtungen bei einzelnen Stimulationen (sowohl für polarisiertes, als auch für unpolarisiertes Licht)

- Berechnung des Polarisationsgrades anhand einer Aufnahmespur eines Polarimeters (interaktiv)

- interaktive Berechnung von Peristimulus Zeit Histogrammen für Stimulation mit unpolarisiertem Licht (oder einem beliebigen anderen Reiz)

Die meisten Auswertfunktionen bereiten die Daten so auf, dass sie in Tabellenkalkulationsprogrammen weiterverwendet werden können. Dabei werden die Analyseergebnisse als Textdatei gespeichert und/oder in die Zwischenablage kopiert.

Record Dieses Skript wird zur Datenerfassung verwendet. Es erfüllt zwei grundlegende Aufgaben. Zunächst ermöglicht es eine schwellenwertbasierte Online-Auswertung neuronaler Aktivität. Diese reicht von der Anzeige der mittleren Aktivität über automatische Histogramme bis zu automatischer Berechnung der Vorzugsrichtung und deren grafischer Darstellung unmittelbar nach einem Reiz, inklusive Signifikanztest. Die zweite Hauptaufgabe ist die Kommunikation mit den Programmen, welche die Reizapparatur steuern. Dabei schreiben die Programme Steuerung.exe und Beleuchtungssteuerung.exe (beide von Sebastian Richter entwickelt) aktuelle Werte zur Stimulation, wie Wellenlänge und Intensität des Lichtes, Drehgeschwindigkeit und aktuelle Position der Stimuluseinheit in die Windows Registrierung. Record liest diese Daten ständig aus und passt so zum Beispiel die Skalierung der Achsen an die Drehgeschwindigkeit an und nimmt die Stimulusparameter mit in die aktuelle Datei auf. Bei der Online-Auswertung ermöglicht dies zudem, dass die Vorzugsrichtungen verschiedener Stimuli in einem Kreisdiagramm farblich dargestellt werden können. Darüber hinaus beinhaltet es weitere nützliche Funktionen, wie zum Beispiel das automatische Benennen der aufgenommenen Dateien und das Erstellen einer übersichtlichen Ordnerstruktur, in der alle Dateien einer Ableitung gespeichert werden. Unter diesen Dateien findet sich auch eine vom Skript erstellte Log-Datei, die sowohl die Ergebnisse der Online-Auswertung, als auch sämtliche Einstellungen der Stimulusparameter enthält.

Das Skript stellt sowohl bei der Datenerfassung als auch bei der späteren Arbeit mit den erfassten Daten eine erhebliche Erleichterung dar. Zum einen hilft die Online-Auswertung, während des Experiments zu entscheiden, ob man gerade von einer polarisationsempfindlichen Zelle ableitet, bzw. ob ein bestimmter Reiz noch einmal präsentiert werden soll. Zum anderen hat man stets beim späteren Öffnen einer Aufnahme alle Informationen zur Stimulation parat, ohne auf handschriftliche Aufzeichnungen angewiesen zu sein.

Literatur

Homberg, U. (2004). In search of the sky compass in the insect brain. Naturwissenschaften, 91, 199–208.

Homberg, U., Hofer, S., Pfeiffer, K., & Gebhardt, S. (2003). Organization and neural connections of the anterior optic tubercle in the brain of the locust, Schistocerca gregaria. J Comp Neurol, 462, 415–30.

Labhart, T. & Meyer, E. P. (1999). Detectors for polarized skylight in insects: a survey of ommatidial specializations in the dorsal rim area of the compound eye. Microsc Res Tech, 47, 368–79.

Labhart, T., Petzold, J., & Helbling, H. (2001). Spatial integration in polarization-sensitive interneurones of crickets: a survey of evidence, mechanisms and benefits. J Exp Biol, 204, 2423–30.

von Frisch, K. (1949). Die Polarisation des Himmelslichtes als orientierender Faktor bei den Tänzen der Bienen. Experientia, 5, 142–148.

Wehner, R. (1997). The ant's celestial compass system: spectral and polarization channels. (Basel: Birkhäuser).

Introduction

Directed behavior of animals is often coupled to an external frame of reference. Any physical or chemical property of the environment that contains directional information and that can be perceived by an animal can serve as a guiding cue during or prior to a directed behavior. Simple examples of directed behavior are escape responses to potentially harmful stimuli, like the escape reflex of the earthworm *Lumbricus* (Roberts, 1962) or the gill withdrawl reflex of the sea snail *Aplysia* (Croll, 2003). More advanced forms of directed behavior are taxis movements like the oriented flight of a male moth toward a conspecific female along a chemical gradient of sex pheromones (Hansson, 1995). The most elaborate directed behaviors are long-range migrations of migratory birds, sea turtles, monarch butterflies, locusts and many other species (Waterman, 1989; Papi, 1992; Baker, 1978). Of particular fascination are directed behaviors that are oriented to sensory cues not perceptible by humans. Examples are the geomagnetic field and the sky-polarization pattern. Although the entoptic phenomenon called "Haidingers Brush" also enables humans to perceive the plane of polarized light (Haidinger, 1844), this phenomenon requires practice, rather large degrees of polarization, and is unknown to most people. Many animals, however, are able to perceive and make use of polarized light that surrounds us.

Polarized light

Light is the visible band of electromagnetic radiation with wavelengths ranging from about 300 nm to 800 nm. As such, it oscillates in a plane that is perpendicular to the direction of propagation (transverse wave). The plane of oscillation of polarized light is described by the orientation of its electric field-vector (E-vector). Direct light from the sun or a light bulb is unpolarized, i.e. the probability for any orientation of the E-vector is equally high. Unpolarized light can be linearly polarized by three mechanisms:

scattering, reflection and birefringence, with the latter playing practically no role in animal vision. Reflected, polarized light is ubiquitous. It emerges from any shiny, non-metallic dielectric surface, such as a body of water, a leaf or the surface of an animal's body. Both E-vector orientation and the degree of polarization depend on the orientation of the surface and on the reflection angle and thus both may rapidly change in moving, polarizing objects. Scattered, polarized light originates from the canopy. Both E-vector orientation and degree of polarization are tightly linked to the position of the sun. Underneath clouds the degree of polarization is strongly reduced which results in nearly unpolarized light underneath a closed, thick layer of clouds (Pomozi et al., 2001).

Perception of polarized light

Insects that are able to perceive polarized light, be it the sky polarization pattern or light that is reflected from bodies of water, are equipped with a specialized region of ommatidia in their compound eyes that is highly adapted for this task. In insects that detect sky-light polarization, the optical axes of the specialized ommatidia point upwards and the area of the eye is called dorsal rim area (DRA). Accordingly, insects that detect water surfaces by their polarization, possess a specialized ventral polarization-sensitive area that views downward. Compared to the ommatidia in the rest of the compound eye, those of the polarization-sensitive areas have a variety of specializations that increase polarization sensitivity. The most important property that is shared by all (invertebrate) polarization detectors is a highly parallel alignment of microvilli along the long-axis of the rhabdomer (Horváth & Varjú, 2004). Due to their shape, microvilli are inherently dichroic with a theoretical polarization sensitivity (PS) of 2. Recordings from DRA-photoreceptors, however, exhibit much higher PS-values of 5-60. It is assumed

that this results from a high degree of alignment of photopigments, that are dichroic themselves, within the microvilli (Snyder & Laughlin, 1975).

In all insects studied, each ommatidium of the DRA contains two sets of retinula cells with orthogonally arranged microvilli (Labhart & Meyer, 1999) Both sets of photoreceptors always use the same photopigment. Thus a homochromatic system is formed, that is not influenced by variations in wavelength. In addition to high PS, most DRAs have evolved specializations to increase the acceptance angle of the photoreceptors. This is done by reducing or omitting screening pigments between the ommatidia and by various alterations of the cornea, like pore canals or air cavities that are believed to scatter the light (Labhart & Meyer, 1999; Homberg & Paech, 2002). The wide acceptance angle of DRA photoreceptors serves as a spatial low-pass filter and reduces the influence of local irregularities within the sky-polarization pattern (Labhart et al., 2001).

Reflected, polarized light

The significance of polarized light that arises from surface reflection has been analyzed largely for animals that live in or in close proximity to water. Reports about butterflies that are thought to find their mating partners or host-plants for oviposition through polarized light reflected from wings or leaves are controversial (Kelber, 1999; Horváth et al., 2002; Sweeney et al., 2003; Horváth & Varjú, 2004).

Light reflected from water surfaces is linearly polarized and can be used to discriminate bodies of water from the surrounding environment. The water living backswimmer *Notonecta glauca* is dispersed by flying to new habitats. Behavioral experiments showed that these animals exhibit a so called plunge reaction upon the experience of ventrally polarized UV light (Schwind, 1984). They tilt their body upwards, possibly to maximize the perceived degree of polarization, and then close the wings and spread out their rowing legs. More recent experiments showed that

a variety of other water associated insect species (several species of water associated bugs, beetles and nematocerans; Schwind, 1991) are also attracted by ventrally polarized light.

Polarized sky-light

Most work about polarization vision involves the sky-polarization pattern. On the way from sun to earth, the unpolarized sunlight is scattered by gas molecules and particles in the atmosphere. As a consequence sky-light is partly polarized with a pattern that roughly follows the single scattering Rayleigh model (Strutt, 1871). *E*-vectors are oriented tangentially to concentric circles around the sun. The degree of polarization increases from the unpolarized direct sunlight to a maximum degree of 75% polarization (d=0.75) at 90° from the sun. This pattern is linked to the position of the sun, so in the course of the day the pattern changes according to the apparent movement of the sun. Another result of scattering is a color gradient along the celestial sphere. The ratio between long wavelength-light and short wavelength-light is larger in the solar and smaller in the antisolar half of the sky (Coemans et al., 1994).

The first documented experiment, which showed that insects can orient themselves using sky-light instead of direct view of the sun, was performed by (Santschi, 1923). He observed harvester ants *(Messor barbarus)* that walked home after a foraging trip. When he shielded the direct sunlight from the ants' view with a cardboard cylinder, the animals were still oriented properly. When he covered the top of the cylinder with a ground-glass plate, which depolarized the light, the ants became disoriented. However, Santschi was not able to properly interpret his observation.

It was Karl von Frisch, 25 years later, who showed and explained for the first time that animals (honeybees) can orient themselves according to the *E*-vector orientation of polarized light. He studied worker honeybees that were fed 200 m away from the hive. Upon their re-

turn from the feeder, the bees performed waggle dances on a comb that was oriented horizontally with open view of the sky, but without direct view of the sun. With these dances, honeybees communicate both the distance and direction of a food source to their nest mates. Although the bees could not see the sun, they indicated the correct direction of the feeder by their dances. Von Frisch concluded that the bees could perceive a phenomenon at the blue sky that is linked to the position of the sun (von Frisch, 1948). To test if this phenomenon could be polarized light, he covered the top of the comb with a polarizing sheet. By changing the orientation of this sheet he could influence the dancing direction of the bees (von Frisch, 1949).

Behavioral experiments have meanwhile shown that several other insects, including crickets, locusts, flies, and dung beetles can perceive the *E*-vector orientation of polarized light (Brunner & Labhart, 1987; von Philipsborn & Labhart, 1990; Mappes & Homberg, 2004; Dacke et al., 2004). In bees, ants, crickets, and locusts it was also demonstrated that the perception of polarized light depends on the dorsal rim area of the compound eye (Wehner & Strasser, 1985; Wehner, 1982; Fent, 1985; Brunner & Labhart, 1987; Mappes & Homberg, 2004).

Spectral cues

As already mentioned above, scattering of sunlight in the atmosphere does not only lead to a pattern of polarization, but also to a color gradient along the celestial sphere. While the intensity of short wavelength light is largely invariant at different azimuths and elevations, the long wavelength intensity depends on the angular distance from the sun (Coemans et al., 1994). The ratio between the intensity of long and short wavelength light is large in the solar hemisphere of the sky and smaller in the antisolar hemisphere. Animals that are able to see this color contrast might use it as a cue to detect the solar azimuth. This ability requires UV-sensitive photoreceptors.

Behavioral laboratory experiments with pigeons, that are known to possess a time-compensated sun compass (Schmidt-Koenig, 1958), have shown that these birds have the sensory capability of perceiving the sky color-gradient (Coemans et al., 1994). However it is unknown, whether they really employ this capability to determine the solar azimuth when the sun is not visible.

In honeybees, orientation with respect to spectral cues was shown in behavioral experiments. When returning from an artificial feeder, bees performed waggled dances under artificial lighting conditions on a horizontal platform. The orientation of the dances was dependent on the color of the artificial light. Under light in the range between 430 nm and 610 nm, the light source was always interpreted as the sun. When UV-light was used instead, the bees danced roughly in the opposite direction and thus interpreted the UV-light as the "anti-solar" direction (Edrich et al., 1979). In similar experiments, Rossel & Wehner (1984) showed that honeybees interpret any long wavelength stimulus to lie along the solar meridian in the solar half of the sky, while a stimulus of UV-light is interpreted as lying anywhere within the antisolar half of the sky.

Outdoor experiments with homing ants (genus *Cataglyphis*) showed that these animals can detect the solar azimuth without seeing the sun or the polarization pattern (Wehner, 1997).

Polarization-sensitive interneurons

While the fact that insects can use polarized light as an orientational cue has been known since the seminal work of von Frisch (1949), the knowledge about the neuronal basis that underlies this behavior is still fragmentary.

The first data on polarization-sensitive interneurons in the brain of an insect were presented by Labhart (1988). He recorded intracellularly from polarization-opponent neurons in the optic lobe of crickets. Most recordings from the cricket optic lobe were from a

single anatomically identified type of neuron termed POL1 (Labhart, 1988). POL1 neurons are highly specialized analyzers of *E*-vector orientation. They have an extremely low threshold sensitivity, which theoretically would allow signaling of *E*-vector orientations at light levels of the moonless night sky (Labhart et al., 2001). In fact, the behavioral threshold for *E*-vector elicited behavior was determined in the same range (Herzmann & Labhart, 1989). POL1 neurons are practically insensitive to unpolarized light and receive monochromatic input from blue photoreceptors. The neurons exist as three individuals per brain hemisphere each of which is tuned to a different *E*-vector orientation. POL1 neurons have been discussed to possibly serve the role of three macro-analyzers within an instantaneous *E*-vector detection system (Labhart, 1988). Although POL1 neurons are the best studied polarization-sensitive interneurons, nothing is known about their connections to the central brain or to motor output areas.

The first in-depth study of polarization-sensitive interneurons in the locust brain focused on the central complex (Vitzthum et al., 2002). This is a midline-spanning neuropil in the center of the brain and consists of the upper and the lower divisions of the central body, the protocerebral bridge, and a pair of noduli. Neurons of the central complex are arranged in a matrix-like pattern of columns and layers (Williams, 1975). According to this structuring, polarization-sensitive neurons of the central complex can be divided into columnar neurons and tangential neurons. Most of these neurons have ramifications in small areas of the lateral accessory lobe, a paired neuropil that is closely connected to the central complex. Unlike POL1 neurons in crickets, neurons reported by Vitzthum et al. (2002) could not be categorized into classes of preferred *E*-vectors. Responses to unpolarized light that are absent in POL1 neurons of crickets, were observed in most of the central-complex neurons. Some of these neurons receive input from both eyes and have a receptive field that is centered with respect to the

zenith, where *E*-vector orientation is independent of solar elevation. Recent recordings from polarization-sensitive neurons of the protocerebral bridge, the dorsalmost part of the central complex, have revealed a first functional correlate of the columnar structure of the central complex. The preferred *E*-vector directions of the neurons gradually change from column to column, such that a polarotopic map is represented in the columns of the protocerebral bridge (S. Heinze and U. Homberg, in preparation).

In locusts, a combination of morphological studies and intracellular recordings allowed to trace the polarization vision pathway from the DRA of the compound eye to the central complex (Fig. 1, Homberg et al. 2003). Photoreceptors of the DRA terminate in dorsal rim areas of the lamina and the medulla. The dorsal rim area of the medulla is connected to the ventralmost layer of the anterior lobe of the lobula and to the lower unit of the anterior optic tubercle (AOTu), a small area anteriorly in the locust midbrain. The lower unit of the AOTu is connected by a small fiber tract, the tubercle-lateral lobe tract to small areas within the lateral accessory lobe: the lateral triangle and the median olive. These areas are the input site of polarization sensitive tangential neurons of the lower unit of the central body.

Most of the data describing the polarization-vision pathway (Homberg et al., 2003) originated from morphological studies. The primary aim of my Doctoral thesis project was to test through intracellular recordings the hypothesis that the lower unit of the AOTu participates in polarization vision. Four types of interneurons with ramifications in the lower unit of the AOTu were characterized in multiple recordings. All of these neurons were sensitive to polarized light, substantiating our hypothesis (Chapter I, → page 19). Two types of neuron, called lobula tubercle neuron (LoTu1) and tubercle tubercle neuron (TuTu1), were especially amenable to intracellular recordings, due to their large axon diameters. In the first set of experiments, we found that all polarization-sensitive neurons were also responsive to unpolarized light (Chapter I, →
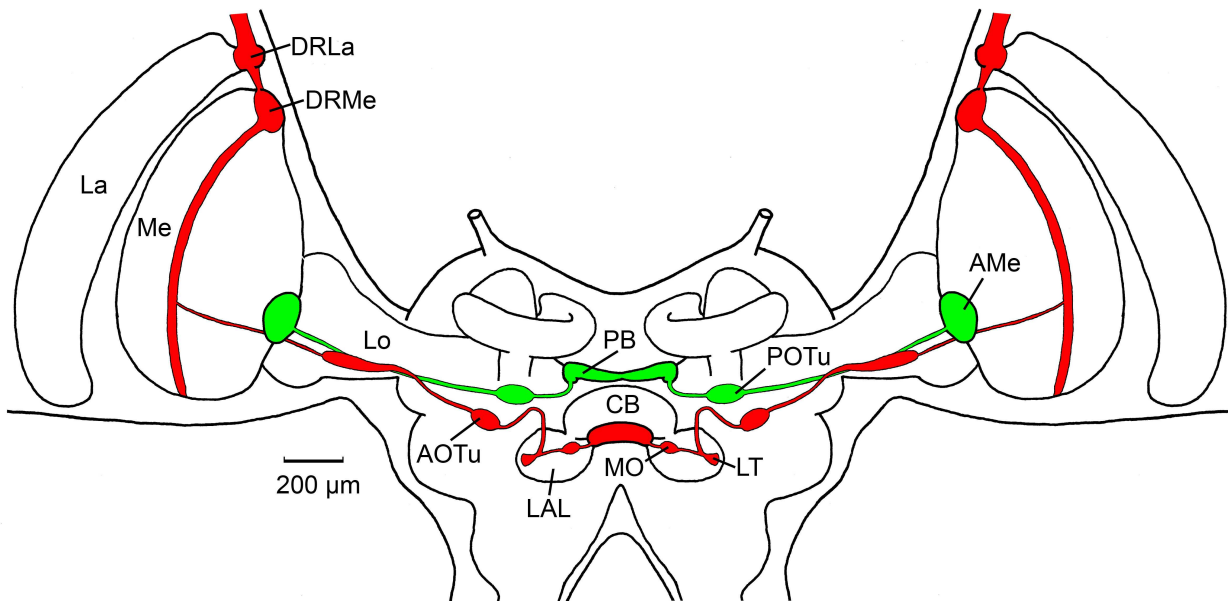
Figure 1: Neuronal pathways between the optic lobes and the central complex. The polarization vision pathway (red) connects the medulla (Me), via the lobula (Lo), the anterior optic tubercle (AOTu), and the lateral accessory lobe (LAL) to the central body. Neurons from the AOTu project to the lateral triangle (LT) and the median olive (MO) within the LAL. Input to this pathway is provided by polarization-sensitive photoreceptors that terminate within the dorsal rim areas of the lamina (DRLa) and the medulla (DRMe). A posterior fiber pathway (green) connects the accessory medulla (AMe) to the posterior optic tubercle (POTu) and the protocerebral bridge (PB). (Adapted from Homberg et al. 2003)

page 19). To investigate the significance of this finding, we extended the stimulation with unpolarized light in a second set of experiments. The responses of both LoTu1 and TuTu1 to UV and green light spots from different directions suggest that these neurons signal the horizontal direction of the sun (solar azimuth), by exploiting both intensity- and color-gradients as well as the sky-polarization pattern (Chapter II, $\rightarrow$ page 35). The use of both unpolarized and polarized light information to detect the solar azimuth can result in conflicting information provided by the different cues. One way to reduce this conflict of information is to exclude certain areas of polarized skylight from being analyzed by the polarization-vision system. By stimulating with different degrees of polarization *(d)*, we showed that the threshold for *E*-vector detection lies around *d*-values of 0.3. This means that an area of around 100° around the sun contains no visible *E*-vector information for these

neurons (Chapter III, $\rightarrow$ page 51). Recent behavioral experiments further confirmed that the pathway described above is vital for polarotaxis in locusts. Tethered locusts that are flown under a slowly rotating polarizer show periodic changes in yaw torque with a period of 180° (Mappes & Homberg, 2004). When the anterior optic tract is unilaterally transected, the locusts are still able to respond to the rotating *E*-vector in the same manner as intact animals. However, when the DRA that is contralateral to the transection site is occluded, the animals become disoriented (Mappes and Homberg, in revison).

Time compensation

To function properly, a sky-compass system usually needs to be time-compensated. The internal navigation system of an animal that wants to maintain a certain course during the day needs to constantly update the angle between

the sun and its target direction. Besides knowledge about the apparent motion of the sun, this requires the presence of an internal time signal. As to the current knowledge, neurons of the central complex do not exhibit time-compensated tuning to polarized light, but signal fixed directions of the E-vector orientation relative to the animal (S. Heinze and U. Homberg, in preparation). Therefore, time compensation might act at a processing stage following the central-complex network and should be present in descending neurons that project to motor control areas in the thoracic ganglia.

A neuronal pathway connects the protocerebral bridge of the central complex and the accessory medulla of the optic lobe via the posterior optic tubercle (Figure 1; Homberg, 2004). The biological significance of this connection is not known yet, but the involvement of the accessory medulla offers room for an attractive speculation: Lesion and transplantation experiments in cockroaches showed that the accessory medulla is the pacemaker of the circadian clock (Stengl & Homberg, 1994; Reischig et al., 2004). The accessory medulla in the locust brain closely resembles that of the cockroach (Homberg, 2004). Thus, the accessory medulla could provide the time-signal, which is required for a time-compensated sky-compass system. Whether the locust is capable of true compass navigation has not been shown yet. However, flying locust swarms and hopper bands are able to maintained constant migratory directions over hours, independent of wind direction (Kennedy, 1951, 1945; Baker et al., 1984). These observations strongly suggest that active spatial orientation involving a time-compensated sky compass underlies locust migrations.

References

Baker, P. S., Gewecke, M., & Cooter, R. J. (1984). Flight orientation of swarming Locusta migratoria. Physiol Entomol, 9, 247–252.

Baker, R. R. (1978). The Evolutionary Ecology of Animal Migration.

Brunner, D. & Labhart, T. (1987). Behavioural evidence for polarization vision in crickets. Physiol Entomol, 12, 1–10.

Coemans, M. A., Vos Hzn, J. J., & Nuboer, J. F. (1994). The relation between celestial colour gradients and the position of the sun, with regard to the sun compass. Vision Res, 34, 1461–70.

Croll, R. P. (2003). Complexities of a simple system: new lessons, old challenges and peripheral questions for the gill withdrawal reflex of Aplysia. Brain Res Rev, 43, 266–274.

Dacke, M., Byrne, M. J., Scholtz, C. H., & Warrant, E. J. (2004). Lunar orientation in a beetle. Proc Biol Sci, 271, 361–5.

Edrich, W., Neumeyer, C., & Helversen, O. (1979). "Anti-sun orientation" of bees with regard to a field of ultraviolet light. JournalComp Physiol, 134, 151–157.

Fent, K. (1985). Himmelsorientierung der Wüstenameise Cataglyphis bicolor: Bedeutung von Komplexaugen und Ocellen. Ph.D. thesis, Zürich.

Haidinger, W. K. (1844). Über das direkte Erkennen des polarisierten Lichts. Poggendorf Annalen, 63, 29–39.

Hansson, B. S. (1995). Olfaction in Lepidoptera. CMLS, 51, 1003–1027.

Herzmann, D. & Labhart, T. (1989). Spectral sensitivity and absolute threshold of polarization vision in crickets: a behavioral study. J Comp Physiol, 165, 315–319.

Homberg, U. (2004). In search of the sky compass in the insect brain. Naturwissenschaften, 91, 199–208.

Homberg, U., Hofer, S., Pfeiffer, K., & Gebhardt, S. (2003). Organization and neural connections of the anterior optic tubercle in the brain of the locust, Schistocerca gregaria. J Comp Neurol, 462, 415–30.

Homberg, U. & Paech, A. (2002). Ultrastructure and orientation of ommatidia in the dorsal rim area of the locust compound eye. Arthr Struct Develop, 30, 271–280.

Horváth, G., Gál, J., Labhart, T., & Wehner, R. (2002). Does reflection polarization by plants influence colour perception in insects? Polarimetric measurements applied to a polarization-sensitive model retina of Papilio butterflies. J Exp Biol, 205, 3281–98.

Horváth, G. & Varjú, D. (2004). Polarized Light in Animal Vision: Polarization Patterns in Nature. (Springer).

Kelber, A. (1999). Why 'false' colours are seen by butterflies. Nature, 402, 251.

Kennedy, J. S. (1945). Observations on the mass migration of desert locust hoppers. Trans R Entomol Soc Lond, 95, 247–262.

Kennedy, J. S. (1951). The Migration of the Desert Locust (Schistocerca gregaria Forsk.). I. The Behaviour of Swarms. II. A Theory of Long-Range Migrations. Phil Trans Roy Soc Lond B, 235, 163–290.

Labhart, T. (1988). Polarization-opponent interneurons in the insect visual system. Nature, 331, 435–437.

Labhart, T. & Meyer, E. P. (1999). Detectors for polarized skylight in insects: a survey of ommatidial specializations in the dorsal rim area of the compound eye. Microsc Res Tech, 47, 368–79.

Labhart, T., Petzold, J., & Helbling, H. (2001). Spatial integration in polarization-sensitive interneurones of crickets: a survey of evidence, mechanisms and benefits. J Exp Biol, 204, 2423–30.

Mappes, M. & Homberg, U. (2004). Behavioral analysis of polarization vision in tethered flying locusts. J Comp Physiol, 190, 61–8.

Papi, F. (1992). Animal homing. (Chapman Hall New York).

Pomozi, I., Horváth, G., & Wehner, R. (2001). How the clear-sky angle of polarization pattern continues underneath clouds: full-sky measurements and implications for animal orientation. J Exp Biol, 204, 2933–42.

Reischig, T., Petri, B., & Stengl, M. (2004). Pigment-dispersing hormone (PDH)-immunoreactive neurons form a direct coupling pathway between the bilaterally symmetric circadian pacemakers of the cockroach Leucophaea maderae. Cell Tissue Res, 318, 553–64.

Roberts, M. B. V. (1962). The Giant Fibre Reflex of the Earthworm, Lumbricus Terrestris L: I. The Rapid Response. J Exp Biol, 39, 227.

Rossel, S. & Wehner, R. (1984). Celestial orientation in bees: the use of spectral cues. J Comp Physiol, 155, 605–613.

Santschi, F. (1923). L' orientation sidérale des fourmis, et quelques considération sur leurs différéntes possibilités d' orientation. Mém Soc Vaudoise Sci Nat, 4, 137–175.

Schmidt-Koenig, K. (1958). Experimentelle Einfluß-nahme auf die 24-Stunden-Periodik bei Brieftauben und deren Auswirkungen unter besonderer Berücksichtigung des Heimfindevermögens. Zeitschr Tierpsych, 15, 301–331.

Schwind, R. (1984). The plunge reaction of the backswimmerNotonecta glauca. J Comp Physiol, 155, 319–321.

Schwind, R. (1991). Polarization vision in water insects and insects living on a moist substrate. J Comp Physiol, 169, 531–540.

Snyder, A. W. & Laughlin, B. (1975). Dichroism and absorption by photoreceptors. J Comp Physiol, 100, 101–116.

Stengl, M. & Homberg, U. (1994). Pigment-dispersing hormone-immunoreactive neurons in the cockroach Leucophaea maderae share properties with circadian pacemaker neurons. J Comp Physiol, 175, 203–13.

Strutt, J. W. (1871). On the light from the sky, its polarization and colour. Phil. Mag., 41, 274–279.

Sweeney, A., Jiggins, C., & Johnsen, S. (2003). Polarized light as a mating signal in a butterfly. Nature, 423, 31–32.

Vitzthum, H., Müller, M., & Homberg, U. (2002). Neurons of the central complex of the locust Schistocerca gregaria are sensitive to polarized light. J Neurosci, 22, 1114–25.

von Frisch, K. (1948). Gelöste und ungelöste Rätsel der Bienensprache. Naturwissenschaften, 35, 12–23.

von Frisch, K. (1949). Die Polarisation des Himmelslichtes als orientierender Faktor bei den Tänzen der Bienen. Experientia, 5, 142–148.

von Philipsborn, A. & Labhart, T. (1990). A behavioral study of polarization vision in the fly Musca domestica. J Comp Physiol, 167, 737–743.

Waterman, T. H. (1989). Animal navigation. (Scientific American Library).

Wehner, R. (1982). Himmelsnavigation bei Insekten. Neurophysiologie und Verhalten. Neujahrsbl Naturforsch Ges, 184, 1–132.

Wehner, R. (1997). The ant's celestial compass system: spectral and polarization channels. (Basel: Birkhäuser).

Wehner, R. & Strasser, S. (1985). The POL area of the honey bee's eye: behavioural evidence. Physiol Entomol, 10, 337–349.

Williams, J. L. D. (1975). Anatomical studies of the insect central nervous system: a ground-plan of the midbrain and an introduction to the central complex in the locust, Schistocerca gregaria (Orthoptera). J Zool (Lond), 176, 67–86.

Polarization-sensitive and light-sensitive neurons in two parallel pathways passing through the anterior optic tubercle in the locust brain

Polarization-Sensitive and Light-Sensitive Neurons in Two Parallel Pathways Passing Through the Anterior Optic Tubercle in the Locust Brain

Keram Pfeiffer,[1] Michiyo Kinoshita,[2] and Uwe Homberg[1]

[1]*Department of Biology, Animal Physiology, University of Marburg, Marburg, Germany; and* [2]*Graduate School of Integrated Science, Yokohama City University, Yokohama, Japan*

Pfeiffer, Keram, Michiyo Kinoshita, and Uwe Homberg. Polarization-sensitive and light-sensitive neurons in two parallel pathways passing through the anterior optic tubercle in the locust brain. *J Neurophysiol* 94: 3903–3915, 2005. First published July 27, 2005; doi:10.1152/jn.00276.2005. Many migrating animals use a sun compass for long-range navigation. One of the guiding cues used by insects is the polarization pattern of the blue sky. In the desert locust *Schistocerca gregaria,* neurons of the central complex, a neuropil in the center of the brain, are sensitive to polarized light and might serve a key role in compass navigation. Visual pathways to the central complex include signal processing in the upper and lower units of the anterior optic tubercle. To determine whether these pathways carry polarization-vision signals, we have recorded the responses of interneurons of the optic tubercle of the locust to visual stimuli including polarized light. All neurons of the lower unit but only one of five recorded neurons of the upper unit of the tubercle were sensitive to linearly polarized light presented in the dorsal visual field. These neurons showed polarization opponency, or a sinusoidal modulation of activity, during stimulation through a rotating polarizer. Two types of bilateral interneurons preferred particular *e*-vector orientations, reflecting the presence of bilateral pairs of these neurons in the brain. We show here for the first time neurons with projections to the lateral accessory lobe that are suited to provide polarization input to the central complex. All neurons of the tubercle, furthermore, responded to unpolarized light, mostly with tonic activity changes. These responses strongly depended on stimulus position and might reflect navigation-relevant signals such as direct sunlight or visual landmarks that are integrated with polarization responses in neurons of the lower unit.

INTRODUCTION

Animals moving through their environment are guided by a variety of sensory cues they exploit to control their direction of locomotion and to calculate distances. Spatial orientation in mammals is characterized by internal representations of the spatial relationship between the animal′s body and its surrounding space. "Place cells" and "head direction cells" are well studied examples of neurons encoding spatial properties in the brain of rats and other mammals (Best et al. 2001; Poucet et al. 2003; Taube and Bassett 2003). These neurons signal the location of the animal within familiar terrain and encode the azimuthal orientation of the animal's head irrespective of its location. Activity of these neurons is influenced by distal visual and nonvisual cues but also by motion-related, idiothetic information. Insects rely on a system for spatial orientation based on landmark orientation in familiar terrain and on vector

orientation based on a sky-compass in unfamiliar terrain or when landmarks are not available (Giurfa and Capaldi 1999; Wehner 2003).

Many insect species have evolved a specialized region in their compound eye, the dorsal rim area that is highly adapted to detect the polarization pattern of the blue sky (Homberg and Paech 2002; Labhart and Meyer 1999). Common characteristics of dorsal rim areas that favor polarization vision include precise alignment of microvilli in two orthogonal blocks in each ommatidium, enhanced cross-sectional area and reduced length of rhabdoms, and homochromacy of dorsal rim photoreceptors (UV receptors in bees and ants, blue receptors in crickets and locusts) (reviewed by Labhart and Meyer 1999). Behavioral experiments in honeybees, desert ants, crickets, flies, and locusts showed that the dorsal rim area is essential for polarotactic orientation and, in bees and ants, for compass orientation (Brunner and Labhart 1987; Mappes and Homberg 2004; von Philipsborn and Labhart 1990; Wehner 2003). Polarization-sensitive interneurons (POL neurons), found in several areas of the insect brain, are involved in signaling the orientation of the animal relative to the sky polarization pattern (Homberg 2004; Labhart and Meyer 2002; Wehner 2003). POL neurons were studied in peripheral visual neuropils of the optic lobe in cockroaches (Kelly and Mote 1990; Loesel and Homberg 2001), crickets (Labhart et al. 2001), and ants (Labhart 2000). More recently in the desert locust and cricket, POL neurons were discovered in the central complex (Sakura and Labhart 2005; Vitzthum et al. 2002), a neuropil in the median protocerebrum involved in spatial orientation, right-left maneuvering, and other aspects of motor control (reviewed by Homberg 2004; Strauss 2002). POL neurons of the central complex have receptive fields oriented toward the zenith and show broad distribution of their prefered *e*-vector orientations (Homberg 2004; Labhart and Meyer 2002; Wehner 2003). Although direct evidence is still lacking, these features render these neurons particularly well suited to provide the directional component of an internal compass signal.

A recent anatomical study in the locust suggests that a small area in the brain, the anterior optic tubercle (AOTu), is a relay station in the neural pathway from polarization-sensitive photoreceptors to the central complex (Homberg et al. 2003) (Fig. 1A). We showed that two parallel pathways originating in the medulla provide, via two subunits of the AOTu, visual input to two subunits of the central complex, the upper and lower divisions of the central body. To provide direct evidence for a
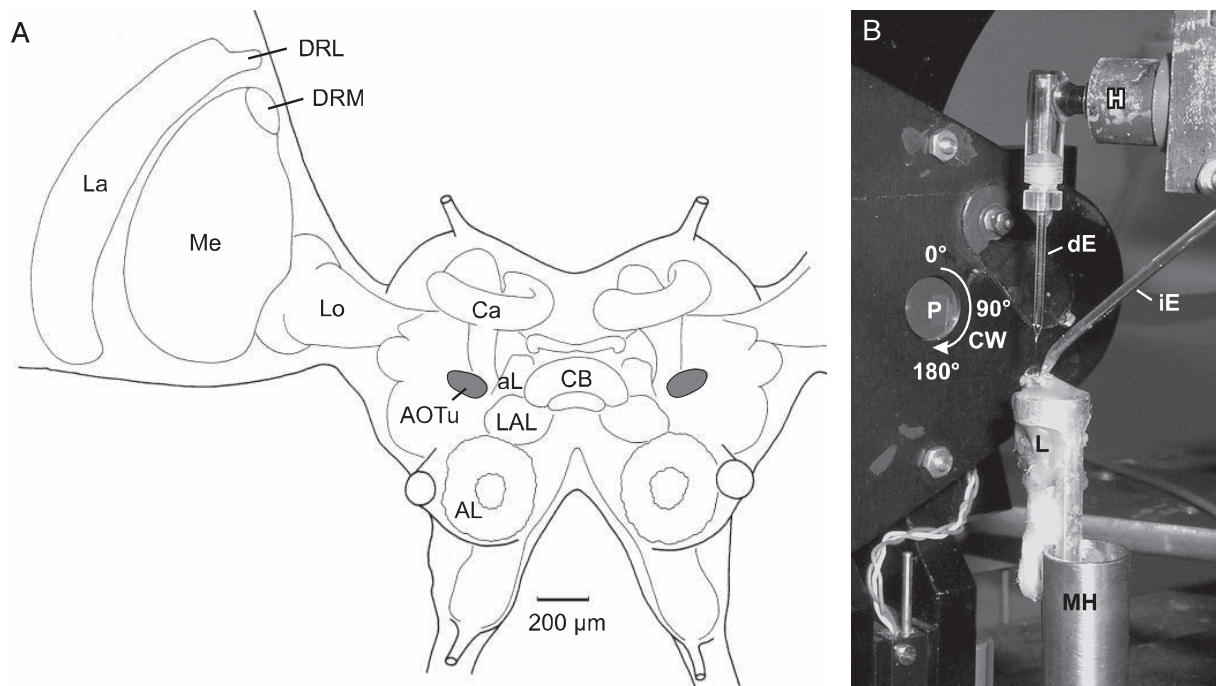
FIG. 1. Diagram of the locust brain and experimental setup for stimulation with polarized light. *A*: frontal reconstruction of the locust brain, showing the main neuropils. Visual information is primarily processed in the optic lobe, which is formed by the 3 visual neuropils lamina (La), medulla (Me), and lobula (Lo). The dorsal rim of the lamina (DRL) and medulla (DRM) receive input from polarization-sensitive photoreceptors of the dorsal rim area. Recordings were made from neurons in the anterior optic tubercle (AOTu, gray) of the median protocerebrum. AL, antennal lobe; aL, Ca, α-lobe and calyx of the mushroom body; CB, central body; LAL, lateral accessory lobe. *B*: ventrolateral view of a locust (L) during polarized-light stimulation. Arrow indicates clockwise (CW) rotation of the polarizer (P). dE, different electrode; iE, ground electrode; H, headstage; MH, metal holder.

role of the AOTu in polarization vision, we characterized the responses of AOTu neurons to visual signals, in particular polarized light. Our present study supports the hypothesis that the AOTu contributes prominently to the sky-compass system. The lower unit of the AOTu plays a role in interhemispheric exchange of polarized light information and acts as an input stage for POL neurons of the central complex. Both units of the AOTu, furthermore, show responses to unpolarized light stimuli that may directly mediate information about solar position and thus may also be relevant to navigational tasks.

METHODS

Preparation

Adult locusts (*Schistocerca gregaria*) were taken from crowded laboratory cultures at the University of Marburg, 1–3 wk after imaginal moult. Animals were anesthetized by cooling for 20–30 min. After removal of the legs, the locusts were waxed to a metal holder. The head capsule was opened frontally by cutting dorsally between frons and vertex, laterally along the inner boundaries of the lateral ocelli and the outer boundaries of the ocular sutures, and ventrally parallel to the epistomal suture. After cutting of the antennal nerves, the cuticle, tracheal air sacs, and fat body were removed to expose the brain. To minimize movements, all muscles in the head capsule were transected. The metal holder with the locust was mounted vertically into the experimental setup (Fig. 1*B*). A stainless steel platform was inserted between the esophageal connectives. It supported the brain from posterior and served as a ground electrode. In some preparations, the brain was additionally stabilized by slightly pushing a stainless steel ring against its frontal surface. If these measures did not suffice

to obtain stable recordings, the abdomen and the entire gut were removed, and the thorax was filled with cotton tissue and petroleum jelly (Vaseline) to prevent desiccation. To facilitate microelectrode penetration, we used forceps to remove the neural sheath above the target area. During the whole experiment, the brain was submersed in locust saline (Clements and May 1974).

Electrophysiology

Microelectrodes, with a resistance of 70–200 MΩ in the tissue, were drawn from omega-shaped borosilicate capillaries (0.75 mm ID, 1.5 mm OD; Hilgenberg, Malsfeld, Germany) with a Flaming/Brown puller (P-97, Sutter, Novato, CA). Their tips were either filled with a 5% aqueous solution of Lucifer yellow (Sigma, Deisenhofen, Germany) or with 4% Neurobiotin (Vector Laboratories, Burlingame, UK) in 1 M KCl. The shanks were filled with 0.1 M LiCl (Lucifer electrodes) or 1 M KCl (Neurobiotin electrodes). Intracellular signals were amplified and filtered (10×, 2 kHz low-pass) with a custom-built amplifier and monitored with an audiomonitor and a digital oscilloscope (Hameg HM 205–3; Hameg, Frankfurt/Main, Germany). After sampling at 25 kHz with a Digidata 1322A (Axon Instruments, Union City, CA), the data were stored on a personal computer, using pClamp 9 (Axon Instruments). To compensate for shifts in baseline, some recordings were digitally filtered (10 Hz high pass). After recording, the tracer was injected iontophoretically into the cell with constant hyperpolarizing current (3–5 nA, 1–7 min, Lucifer yellow) or constant depolarizing current (3 nA, 1–7 min, Neurobiotin).

Visual stimulation

Experiments were carried out in the dark with two experimental setups. On the first setup, light stimuli were provided by a xenon arc

(XBO 150 W) and filtered through an infrared short pass filter. Because locust polarization-sensitive photoreceptors are blue-sensitive (Eggers and Gewecke 1993), light was passed through a standard glass light guide (Schölly, Denzlingen, Germany; spectral range ~400–800 nm), connected to a perimeter. Either a linear polarizer (HN38S, Polaroid, Cambridge, MA) or a neutral density filter of equal transmission was moved into the light path. Stimuli were applied from the zenith and, for unpolarized light flashes, also from lateral to the right and left eye (0° elevation, in a few experiments, 30° elevation, duration of unpolarized light stimuli: 1.5–3 s). The angular extent of the stimulus at the locust's eye was 4.7°, its irradiance was 125 μW/cm^2. To test for polarization sensitivity, the polarizer was rotated through 180° (angular velocity: 12.9–34°/s) either clockwise (0–180°) or counterclockwise (180–0°) as seen by the animal (Fig. 1*B*). An orientation parallel to the longitudinal axis of the animal was defined as 0°.

At a second experimental setup, polarizer and neutral density filter were illuminated through a standard glass light guide that was connected to a 150 W halogen bulb (3200 K; irradiance at the locust head: 13 μW/cm^2, visual angle: 2.1°; spectral range: ~400–800 nm). Lateral light stimuli could be applied by additional light guides (standard glass), illuminated by 150 W halogen bulbs. These stimuli appeared at a visual angle of 3° and an irradiance of 2–4 μW/cm^2. After weak responses to unpolarized light were encountered in some neurons, the halogen light source was replaced by a stronger xenon arc (XBO 75 W) and quarz optics to increase the intensity of the stimuli and to expand the spectral range to UV (irradiance: 67 μW/cm^2, visual angle: 2.1°, spectral range: ~280–800 nm; polarizer HNP'B, Polaroid). Under both illuminations, the polarizer was rotated through 360° in either direction. Angular velocity was 20 or 21.8°/s.

Ocular dominance was tested in both experimental setups by shielding one eye from the light source with a handheld piece of cardboard. Additionally in some experiments, the ipsilateral eye was painted black (Marabu Decorlack matt, water based) during the recording to test for contralateral input.

Data analysis

Relative times of action potentials were evaluated by the threshold detection algorithm of pClamp 9. Mean background activities during darkness were obtained from counts of spikes in 1 s time intervals before each visual stimulus divided by the respective time. For single stimuli, tonic responses were scored as excitatory if the spiking activity during the last second of stimulation (A_{stim}) was higher than the mean background activity plus the SD and as inhibitory if A_{stim} was lower than the mean background activity minus the SD. For comparison of different recordings from the same cell type (TuTu1 and LoTu1 neurons), relative activity changes in response to unpolarized light stimuli were determined as A_{stim} divided by the number of spikes during one second immediately before stimulus onset (A_{pre}). The responses of these neurons to unpolarized light were statistically evaluated using the Wilcoxon test for paired samples (significance level $\alpha = 0.05$).

Neuronal responses to polarized light were analyzed using Oriana 2.02a (Kovach Computing Services, Anglesey, UK) for circular statistics and Origin 6.0 (Microcal, Northhampton, CA) for curve fitting. To investigate the presence of periodicity (= polarization sensitivity) in the neuronal responses to the rotating polarizer, we used the Rayleigh test (Batschelet 1981). We specifically tested whether the distribution of *e*-vector angles assigned to each spike in the recording trace showed directedness. Significant deviation from a random distribution indicating polarization sensitivity was set at a significance level of $\alpha = 0.01$. To obtain *e*-vector response plots of the polarization-sensitive neurons, means of spike frequencies ($\pm$SD) were determined during consecutive 10° bins from two to four revolutions of the polarizer. These were plotted against the bin centers as a function of *e*-vector angle. *e*-vector angles eliciting maximal spike activity (Φ_{max}) were determined by fitting $\sin^2$ functions to the data sets using the Origin 6.0 implementation of the nonlinear least-squares Levenberg-Marquardt algorithm. The match between the dataset and the fit is described by the coefficient of determination ($0 \leq R^2 \leq 1$). To test whether the distribution of Φ_{max} angles in multiple recordings from the same cell type (LoTu1 and TuTu1 neurons) was significantly different from randomness, Rao's spacing test was used (Batschelet 1981).

Histology

After recording and Neurobiotin/Lucifer injection, brains were dissected out of the head capsule and fixed for 1 h at room temperature or overnight at 4°C either in 4% paraformaldehyde in 0.1 M phosphate buffer (Lucifer preparations) or in fixative containing 4% paraformaldehyde, 0.25% glutaraldehyde, and 0.25% saturated picric acid in 0.1 M phosphate buffer (Neurobiotin preparations). Brains were then embedded in gelatin/albumin and fixed overnight in 8% formaldehyde in 0.1 M phosphate buffer. After sectioning at 35 μm with a vibrating blade microtome (VT 1000S, Leica, Wetzlar, Germany), the Neurobiotin preparations were incubated for 18 h with Streptavidin conjugated to horseradish-peroxidase (Amersham Buchler, Brunswick, Germany) at 1:200 in phosphate-buffered saline with 0.5% Triton X-100. The Lucifer yellow preparations were first incubated with rabbit anti-Lucifer yellow antiserum, then with goat-anti-rabbit antiserum and finally with a peroxidase-antiperoxidase conjugate (Homberg and Würden 1997). After incubation, Lucifer and Neurobiotin preparations were stained with 3,3'-diaminobenzidine tetrahydrochloride, hydrogen peroxide, and nickel ammonium sulfate as described by Vitzthum et al. (2002). Neurons were reconstructed from consecutive sections using a microscope with camera lucida attachment. Photomicrographs were made using a Zeiss Axioskop compound microscope equipped with a Polaroid DMC digital camera. All positional information refers to the body axis of the animal. The terms ipsi- and contralateral refer to the position of the cell body.

RESULTS

This study is based on 112 intracellular recordings obtained from neuronal processes in the AOTu. Dye injections were successfully completed in 92 neurons, which were categorized into seven morphological types. Twenty neurons that could not be stained were assigned to morphological types based on their physiological response properties. The unique combination of high background activity, polarization opponency, and reduction with brief total inhibition of spiking activity in the sinusoidal response to the rotating polarizer (see following text) allowed to assign 15 recordings from unstained neurons to TuTu1. Five unstained neurons were identified as LoTu1 based on characteristic combinations of low background activity and activation by all *e*-vector angles. The arborizations of the recorded cell types in the AOTu were restricted either to the upper or the lower subunit but never extended into both units. All neurons recorded from the lower unit, but only one neuron from the upper unit was polarization-sensitive. The neurons were termed after their main projection areas and enumerated if necessary. In some preparations, more than one cell was stained. In these cases, one of the neurons, interpreted as the recorded cell, was usually stained dark blue to black, whereas others appeared in shades of gray. Colabeling of certain cell types did not occur on a regular basis, and in all cases, the weakly labeled neurons had a major neurite in close proximity to the recording site. Therefore dye leakage through injuring of

neighboring cells rather than electrical coupling through gap junctions appears as the most likely reason for colabeling of neurons in our experiments. No systematic differences in polarization sensitivity (types of responsive neurons, polarization-opponency, ocular dominance, and *e*-vector tuning) were observed with the three types of polarized light stimulation, probably owing to the fact that locusts are sensitive to polarized light in the blue range (Eggers and Gewecke 1993). However, responses to unpolarized light flashes were clearly stronger and more robust with xenon arc stimulation (both with quarz and standard glass optics).

Neurons of the intertubercle tract

Three types of neuron, termed tubercle-tubercle neuron 1 (TuTu1) and lobula-tubercle neuron 1 and 2 (LoTu1, LoTu2), interconnected the AOTu of the right and left brain hemispheres via the intertubercle tract. Two of these neurons, LoTu1 and LoTu2, had additional bilateral ramifications in the anterior lobe of the lobula.

TuTu1 neurons

Stable recordings from TuTu1 neurons were obtained in 48 experiments. Their cell bodies are in the inferior lateral protocerebrum close to the antennal lobe. TuTu1 neurons have ramifications in the lower unit of the ipsilateral AOTu. An axonal fiber projects through the intertubercle tract and gives rise to a second tree of arborizations in the lower unit of the contralateral AOTu (Fig. 2*A*). Ipsilateral, presumably dendritic ramifications are smooth and are concentrated either in the outer or the inner hemisphere of the lower unit. These arborizations are less dense than the beaded contralateral terminals, which extend throughout the lower unit of the AOTu (Fig. 2*A*). Neurons with cell bodies in the right hemisphere were recorded 23 times, neurons with cell bodies in the left hemisphere 10 times, and 15 cells were not stained. Graded changes in membrane potential were not observed in any of the recordings, and, correspondingly, the soma and presumed dendritic input arborizations were always in the brain hemisphere contralateral to the recording site. Because all of the 15 unstained neurons were recorded in the right AOTu, their cell bodies had to be in the left brain hemisphere. In 13 recordings, two sibling TuTu1 neurons were stained. In eight cases, the somata were located on the same side. In two recordings, three TuTu1 neurons were stained, but in both cases only two cell bodies were in the same brain hemisphere, suggesting that TuTu1 neurons exist as two bilateral pairs of neurons.

TuTu1 neurons had a mean background activity of 31.6 ± 10.2 (SD) imp/s and a maximum activity of 63.0 ± 19.2 imp/s. The neurons responded to stimulation with unpolarized light depending on spatial position and type of light source. Lateral stimulation with halogen light (0° elevation) did not elicit a response in 12 of 13 experiments. Stimulation with xenon light led to tonic inhibitions when applied to both eyes from the zenith but had no significant effect when applied from lateral to the ipsi- or contralateral eye (Fig. 2*B*).

TuTu1 neurons showed polarization opponency, i.e., they were maximally excited by a particular *e*-vector (Φ_{max}) and were maximally inhibited by an *e*-vector perpendicular to Φ_{max} (Fig. 2*C*). Ocular dominance was tested in eight experiments.

When the ipsilateral eye was shielded and/or painted black, the amplitude of the POL-response (maximum activity–minimum activity) was strongly reduced in seven experiments, but some residual response remained (Fig. 2*D*). Shielding the contralateral eye had little or no effect on the polarization response (Fig. 2*D*).

The distribution of Φ_{max} angles was significantly different from randomness (Rao's spacing test, $P < 0.01$) and differed between TuTu1 neurons with somata in the left brain hemisphere (Fig. 2*E*) and those with somata in the right brain hemisphere (Fig. 2*F*). Recordings from TuTu1 with somata in the left hemisphere had a dominant peak of Φ_{max} orientations around 175° and a second, less prominent peak around 135° (Fig. 2*E*). Neurons with somata in the right hemisphere, in contrast, had a peak of Φ_{max} angles around 45° (Fig. 2*F*). In addition, four neurons had Φ_{max} angles between 140 and 180° (Fig. 2*F*). The mean of the coefficients of determination (R^2) for the $\sin^2$ fits was 0.92 ± 0.075 (±SD; binocular stimulation, $n = 48$).

LoTu1 neurons

Recordings from LoTu1 neurons were obtained in 55 experiments. The soma of LoTu1 is located in close proximity to those of the TuTu1 neurons in the inferior lateral protocerebrum and has a diameter of 25–30 μm. Ramifications in both brain hemispheres are in the ventralmost layer 1 of the anterior lobe of the lobula and, via fibers in the anterior optic tracts, in the lower unit of the AOTu. Ipsilateral arborizations have a smooth appearance, while ramifications in the contralateral AOTu and lobula are varicose (Fig. 3, *A* and *B*). Small, blebby sidebranches extend from the neurite in the contralateral anterior optic tract (Fig. 3*A*). The commissural axon of LoTu1 connects both lower units of the AOTu via the intertubercle tract and has a diameter of 6 μm. In 35 preparations, the cell bodies were located in the right, in 15 preparations, in the left brain hemisphere, and 5 neurons were not stained. In all preparations with two stained LoTu1 neurons, their cell bodies were on opposite sides ($n = 6$). More than two LoTu1 cells were never stained in one brain. Only one LoTu1 neuron was recorded from the soma-sided AOTu, and this recording was the only one showing graded potentials in addition to spikes.

LoTu1 neurons had a background activity of 8.1 ± 5.4 imp/s and a maximum activity of 43.3 ± 16.1 imp/s. In 39 of the 55 recordings, maximum activity was reached during stimulation with unpolarized light. Unpolarized halogen light from ipsi- or contralateral had no effect in 20 of 21 recordings. Unpolarized xenon light from ipsilateral caused phasic-tonic excitations, followed in some cases by off inhibitions (Fig. 3*F*). Zenithal stimulation led to tonic inhibition, in some cases with rebound excitation, and contralateral stimulation did not result in a significant response (Fig. 3*F*).

Zenithal stimulation with polarized light led to tonic excitation that was sinusoidally modulated in strength by the rotating *e*-vector; maximum and minimum activity occurred at perpendicular *e*-vectors (Fig. 3, *C* and *D*). Ocular dominance was tested in 12 experiments. When the contralateral eye was shielded from polarized light stimulation by a piece of cardboard, the *e*-vector response was similar to that of binocular stimulation but with a slightly reduced activation in some recordings (Fig. 3*D*). When the ipsilateral eye was shielded
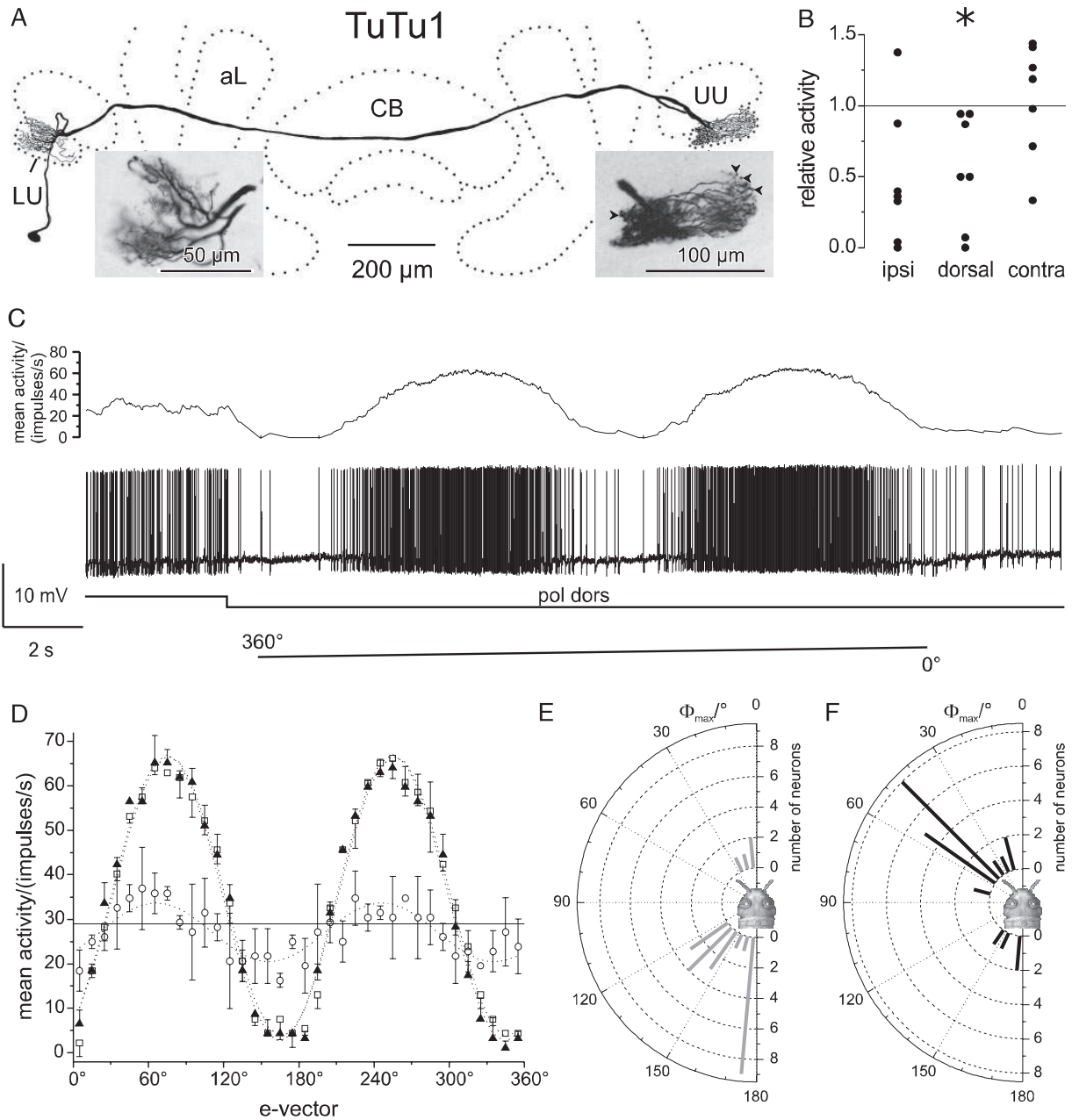
FIG. 2. Polarization-sensitive TuTu1 neurons. *A*: frontal reconstruction. Arborizations of TuTu1 are confined to the lower units of the AOTu (LU) in both hemispheres of the protocerebrum. The axon crosses the midline of the brain within the intertubercle tract. Contralateral terminals are varicose (arrowheads) and more dense than ipsilateral ones. aL, α-lobe of the mushroom body; CB, central body; UU, upper unit of the AOTu. *B*: relative tonic activity changes in TuTu1 in response to unpolarized light flashes (xenon arc, standard glass optics) from ipsilateral, dorsal, and contralateral ($n = 7$); solid line, background activity; asterisk indicates significant inhibition to dorsal stimulation (Wilcoxon test for paired samples, $P < 0.05$). *C*: mean activity and intracellular recording trace of a TuTu1 during stimulation with dorsally presented polarized light, rotating through 360° (halogen light source). Lights on is indicated by a step in the stimulus trace (pol dors). *D*: *e*-vector response plots for stimulation of the ipsilateral eye ($\square$), the contralateral eye ($\circ$), and both eyes ($\blacktriangle$), same recording as in *C*. Solid line, background activity. Each dataset shows means of spike frequencies from 2 counterclockwise revolutions of the polarizer. Neural activity under all stimulus conditions is significantly different from a uniform distribution (Rayleigh test, $P < 0.01$). Sin^2 fits (dotted line) revealed Φ_{max} orientations at 76° for ipsilateral stimulation ($\square$, $R^2 = 0.982$), at 66° for contralateral stimulation ($\circ$, $R^2 = 0.732$), and at 75° for binocular stimulation ($\blacktriangle$, $R^2 = 0.983$). *E* and *F*: distribution of Φ_{max} orientations from TuTu1 neurons with cell bodies in the left (*E*, $n = 25$) and right (*F*, $n = 22$) brain hemisphere. Only mean Φ_{max} angles from experiments with equal numbers (2–6) of clockwise and counterclockwise rotations are included.

and/or painted black, spiking activity remained at background level and was not significantly different from uniformity during *e*-vector rotation (Rayleigh test). This indicates that the response to polarized light is mediated exclusively by the ipsilateral eye (Fig. 3*D*).

Depending on the location of the cell body, Φ_{max} was at a mean *e*-vector of 41° (soma in the right hemisphere; $n = 26$, angular deviation: 21.4°) or at 134° (soma in the left hemisphere; $n = 20$, angular deviation: 21.9°; Fig. 3*E*, Rao's spacing test, $P < 0.01$). The mean of the coefficients of determination (R^2) for the $\sin^2$ fits was 0.795 ± 0.114 (binocular stimulation, $n = 55$).
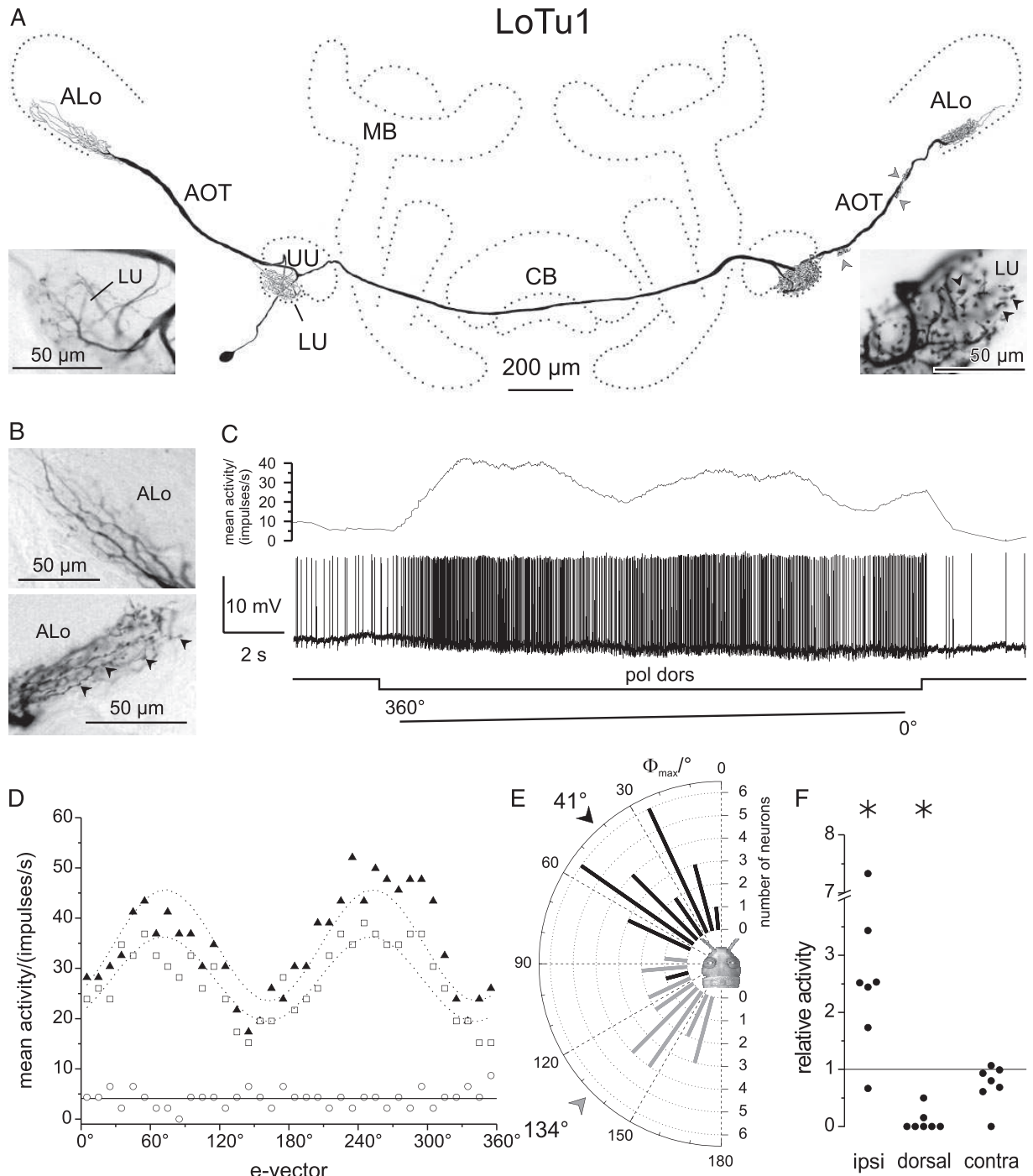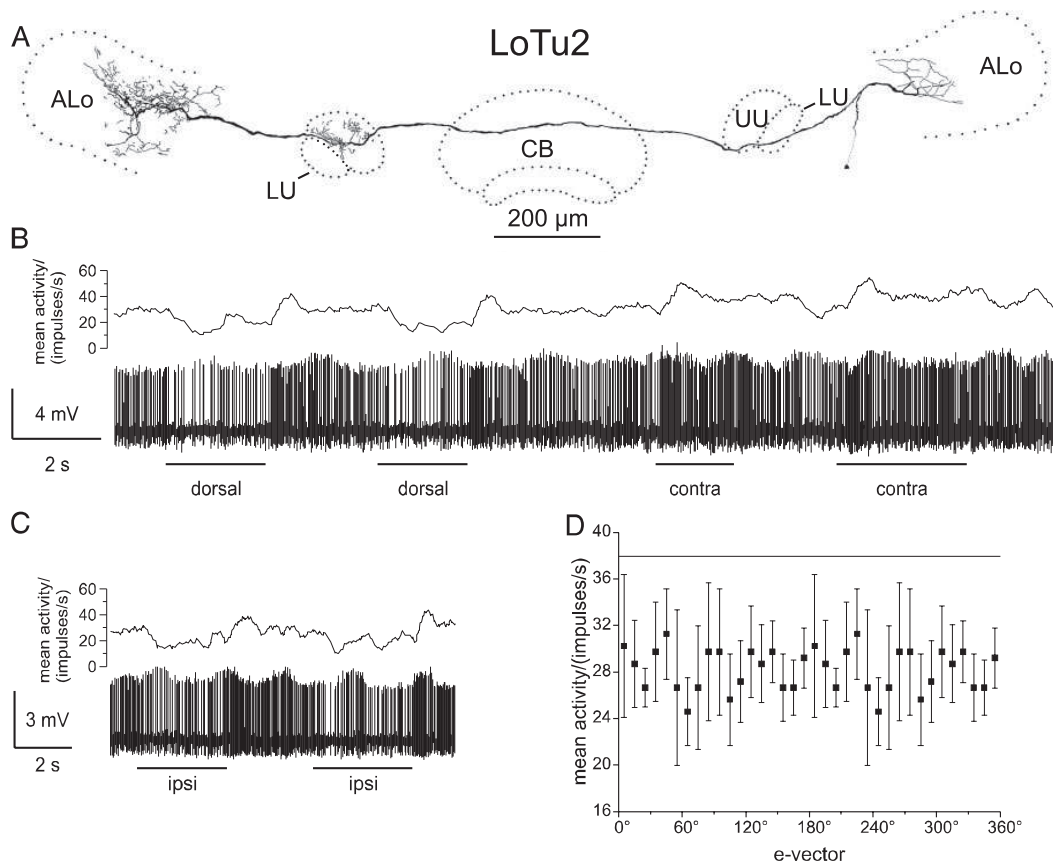
FIG. 4.   Anatomy and physiology of LoTu2 neurons. *A*: frontal reconstruction. The neuron connects the ALo of both optic lobes via the intertubercle tract and has beaded terminals in parts of the UU of the contralateral AOTu. *B* and *C*: intracellular recordings (10 Hz digitally high pass filtered) from a LoTu2. Whereas stimulation with unpolarized light from dorsal (*B,* xenon arc with standard glass optics) and ipsilateral (*C*) causes tonic inhibitions followed by phasic off-excitations, stimulation of the contralateral eye (*B*, contra) leads to excitation. *D*: *e*-vector response plot from 180° rotations (double-plotted, i.e., 180–360° identical with 0–180°, means ± SD, *n* = 4; xenon arc stimulation, standard glass optics). Polarized dorsal light inhibits LoTu2 independent of *e*-vector angle (Rayleigh test, *P* = 0.999). Solid line, background activity.

LoTu2 neurons

Recordings from LoTu2 neurons were obtained twice. Their cell bodies (diameter: 20–25 μm) are located in the inferior lateral protocerebrum more lateral than that of the LoTu1 neuron. Smooth ramifications extend through layer 2 of the anterior lobe of the lobula. The axon enters the median protocerebrum via the anterior optic tract, bypasses the ipsilateral

AOTu posteriorly, and crosses the brain midline within the intertubercle tract. Arborizations with small numbers of beaded terminals are present in the upper unit of the contralateral AOTu and widely in layer 2 of the anterior lobe of the contralateral lobula (Fig. 4A) (Homberg et al. 2003).

LoTu2 neurons had a background activity of ~35 imp/s. Unpolarized light led to weak tonic inhibition when presented from ipsilateral and dorsal but excited the cells when presented

FIG. 3.   Polarization-sensitive LoTu1 neurons. *A* and *B*: morphology LoTu1. *A*: frontal reconstruction and photomicrographs of ramifications in the right and left AOTu. The neuron ramifies in the LU of the AOTu and in the anterior lobe of the lobula (ALo) of both brain hemispheres. Terminals in the contralateral LU show varicosities (black arrowheads in photomicrograph). Additional varicose sidebranches arise from the neurite in the contralateral anterior optic tract (gray arrowheads). MB, mushroom body. *B*: photomicrographs of arborizations in the ipsilateral (*top*) and contralateral (*bottom*) ALo. Arrowheads indicate varicosities in the contralateral ALo. *C*: mean activity and intracellular recording showing the response of a LoTu1 to dorsally presented polarized light, rotating through 360° (halogen light). Lights on and off are indicated by steps in the stimulus trace (pol dors). *D*: *e*-vector response plots for stimulation of the ipsilateral eye (□), the contralateral eye (○), and both eyes (▲), same recording as in *C*. Solid line indicates background activity. Each dataset shows spike frequencies from a single counterclockwise revolution of the polarizer. Neural activity during stimulation of the ipsilateral eye and both eyes are significantly different from a uniform distribution (Rayleigh test, *P* < 0.01). Sin^2 fits (dotted lines) revealed Φ_{max} orientations at 71° for ipsilateral stimulation (open squares, R^2 = 0.714) and at 73° for binocular stimulation (solid triangles, R^2 = 0.690). *E*: *e*-vectors eliciting maximal spike frequencies (Φ_{max}) in 46 LoTu1 neurons with somata in the left (gray) or right brain hemisphere (black). Only mean Φ_{max} angles from experiments with equal numbers (2–6) of clockwise and counterclockwise rotations are included. Arrows show mean Φ_{max} angles of either group (Rao's spacing test, *P* < 0.01). *F*: relative tonic activity changes in LoTu1 in response to unpolarized light flashes from ipsilateral, dorsal, and contralateral (xenon arc stimulation, standard glass optics); solid line indicates background activity, asterisks indicate significant activity changes to ipsilateral and dorsal stimulation (Wilcoxon test for paired samples, *P* < 0.05).

from contralateral (Fig. 4, *B* and *C*; xenon arc stimulation with standard glass optics). Zenithal polarized light led to tonic reduction in activity, which was independent of *e*-vector angle in both recordings (Fig. 4*D*).

Neurons of the tubercle-accessory lobe tract

Three types of neuron connected the AOTu with the lateral accessory lobe through the tubercle-accessory lobe tract. One of these cell types had additional ramifications in the lobula.

TuLAL1a neurons

Colabeling of TuLAL1a neurons occurred in many recordings from LoTu1 or TuTu1 (*n* = 14). However, because of their small neurites, only two intracellular recordings were obtained. The somata of TuLAL1a neurons are located close to the anterior surface of the brain near the antennal lobe. Primary neurites enter the AOTu from median and give rise to dense ramifications that are concentrated in the inner, middle, or outer third of the lower unit of the AOTu. The arborizations of

the neuron presented in Fig. 5*A* are confined to the middle third of the lower unit, while the micrograph of Fig. 5*B* shows a TuLAL1a neuron with a dendritic field in the inner third of the lower unit (black arrowheads). Axonal fibers of TuLAL1a neurons leave the tubercle and project via the tubercle-accessory lobe tract to the lateral accessory lobe. Terminals were always confined to a certain subfield in the lateral accessory lobe, the lateral triangle, and were shaped as large, irregular bulges ($\leq$15 μm) with tiny filiform appendices (Fig. 5*C*).

The background activities of the two recorded TuLAL1a neurons ranged from 4 to 6.5 imp/s. Neuronal activity during *e*-vector-rotation was significantly different from a uniform distribution for both neurons (Rayleigh test, *P* < 0.01). Both TuLAL1a neurons showed polarization opponency with sinusoidal *e*-vector response curves, Φ_{max} at 40 and 117°, respectively, and total inhibition accompanied by membrane hyperpolarization around Φ_{min} (Fig. 5, *D* and *E*). Halogen light stimulation with unpolarized light from ventrofrontal led to excitation followed by an off-inhibition of $\leq$4 s duration in one recording, whereas it had no effect in the second recording. Ipsilateral unpolarized light had no influence on the spiking
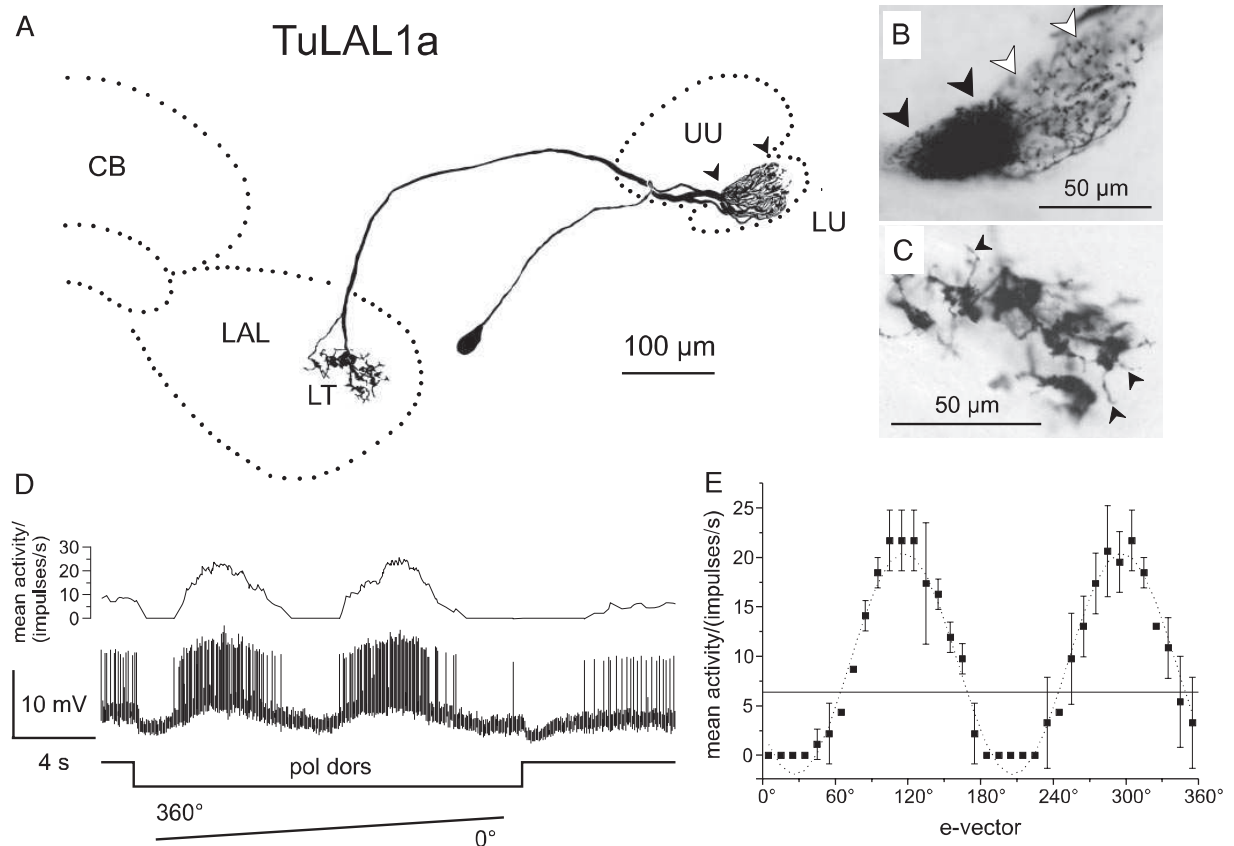
FIG. 5. Polarization-sensitive TuLAL1a neurons. *A*: frontal reconstruction of a TuLAL1a neuron. The neuron ramifies in the LU of the AOTu and projects to the lateral triangle (LT) of the lateral accessory lobe (LAL). *B*: arborizations of double-impaled LoTu1/TuLAL1a neurons. Unlike ramifications of LoTu1 (white arrowheads), those of TuLAL1a (black arrowheads) are restricted to the inner third of the lower unit of the AOTu. *C*: axon terminals within the lateral triangle form large irregularly shaped knobs that extend to tiny, filiform appendices (arrowheads). *D*: intracellular recording and mean spiking activity from TuLAL1a depicted in *A*. Membrane potential and spiking activity of the cell are sinusoidally modulated during a full revolution of the dorsally presented polarizer (pol dors; xenon arc stimulation, quarz optics). *E*: *e*-vector response plot (means $\pm$ SD from 1 clockwise and 1 counterclockwise turn through 360°). The occurence of spikes during *e*-vector rotation is significantly different from a uniform distribution (Rayleigh test, *P* < 0.01). The sin^2 fit (dotted line) revealed a Φ_{max} of 117° (R^2 = 0.969).

activity of the neurons, contralateral stimulation evoked activation in one recording. Dorsal unpolarized light, tested in one experiment, inhibited the neuron.

TuLAL1b neurons

Neurons of this type were co-stained in 21 preparations of LoTu1 and TuTu1 recordings, indicating a close spatial relationship between these cell types. Owing to the small axon diameter of TuLAL1b neurons, however, only two intracellular recordings were achieved (Fig. 6). TuLAL1b neurons comprise at least three morphological subtypes. All of them have their somata (15 μm diam) in the inferior protocerebrum together with the TuLAL1a cell bodies. Fine smooth processes in the lobula and in the lower unit of the AOTu are located in the same areas as those of LoTu1 neurons (Fig. 6B). From the lower unit of the tubercle, axonal fibers run via the tubercle-accessory lobe tract medially through the angle formed by the α-lobe and peduncle of the mushroom body and then ventrally into the lateral accessory lobe. The three subtypes of TuLAL1b project to different subcompartments of the lateral accessory lobe. The cells terminate in large knobs of $\sim$10 μm diameter either in the lateral triangle, in the median olive, or in both neuropils of the lateral accessory lobe (Fig. 6B).

Without stimulation one of the recorded TuLAL1b neuron remained silent (Fig. 6A), the other neuron spiked at 2.5 imp/s.

One of the two neurons was excited by contralateral but not by ipsilateral light (halogen light source, Fig. 6A), whereas the second cell was unresponsive to both stimuli. In both neurons spiking activity during *e*-vector rotation was significantly different from a uniform distribution (Rayleigh test, $P < 0.01$). Stimulation with polarized light resulted in an *e*-vector-dependent sinusoidal all-activation response with Φ_{max} at 79° in one neuron (Fig. 6C) and Φ_{max} at 15° in the second cell (not shown).

TuLAL2a neurons

Two recordings were obtained from TuLAL2a neurons. Their cell bodies are located in the inferior lateral protocerebrum close to the antennal lobe and have diameters from 18 to 20 μm. Arborizations in the upper unit of the AOTu have a fine granular structure (Fig. 7B). Axons project through the tubercle-accessory lobe tract and invade large areas of the lateral accessory lobe with varicose processes but spare the median olive and the lateral triangle (Fig. 7, *A* and *C*).

Both recordings showed action potentials as well as graded potentials (Figs. 7E) indicating that the recording sites were in or near the dendritic zones of the neurons. Although the recordings were stable, the activity of both neurons showed strong fluctuations both at background level and during stimulation. Background activity ranged from 10 to 20 imp/s in one
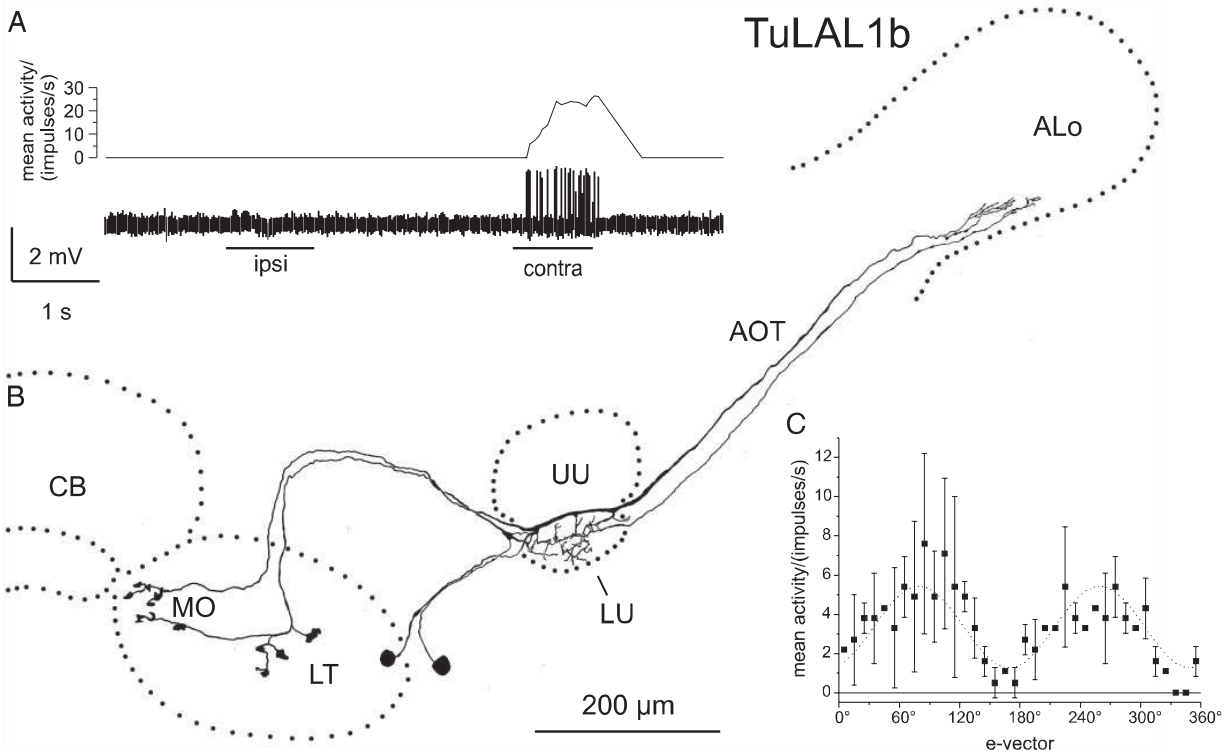
FIG. 6. Polarization-sensitive TuLAL1b neurons. *A*: intracellular recording (10 Hz digitally highpass-filtered) and mean activity of 1 of the TuLAL1b neurons shown in *B*. The neuron shows no background activity and remains silent when the animal is stimulated with unpolarized ipsilateral halogen light (ipsi). Contralateral stimulation with unpolarized light (contra; halogen light source) leads to tonic excitation. *B*: frontal reconstruction. Two TuLAL1b neurons were colabeled. Both neurons connect the most ventral layer of the ALo to the LU of the AOTu via the anterior optic tract (AOT). Continuing axons project to the lateral accessory lobe. The few, large terminals are confined to the LT and the median olive (MO) or to the MO alone. *C*: *e*-vector response plot (means ± SD from 2 clockwise and 2 counterclockwise turns through 360°; xenon arc stimulation, quarz optics). The occurence of spikes during *e*-vector rotation is significantly different from a uniform distribution (Rayleigh test, $P < 0.01$). The sin^2-fit (dotted line) revealed a Φ_{max} of 79° ($R^2 = 0.664$). Solid line, background activity.
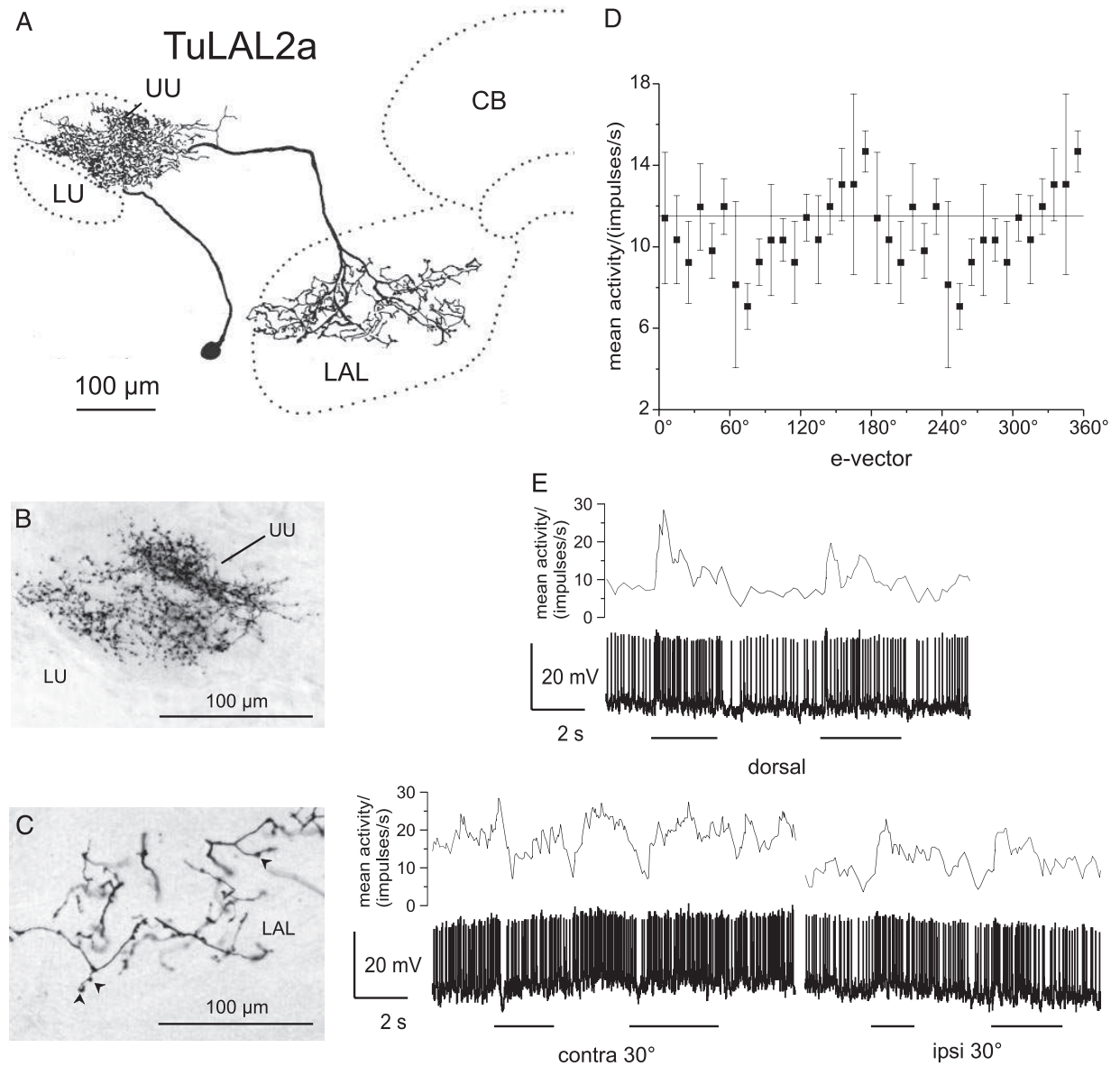
FIG. 7. TuLAL2a neuron from the UU of the AOTu. *A*: frontal reconstruction. The neuron connects the upper unit of the AOTu to large areas of the lateral accessory lobe (LAL). *B*: ramifications in the AOTu are of fine grainy appearance. *C*: projections in the LAL bear varicosities (arrowheads). *D*: *e*-vector response plot from 180°-rotations (double-plotted, i.e., 180–360° identical with 0–180°, means ± SD, *n* = 4; xenon arc stimulation, standard glass optics). Solid line, background activity. Spiking activity during *e*-vector rotation was not significantly different from uniformity (Rayleigh test, *P* = 0.123). *E*: mean activity and original recording trace during stimulation with unpolarized light from the zenith (dorsal), and at 30° elevation from ipsilateral (ipsi) and contralateral (contra; xenon arc stimulation, standard glass optics).

recording and between 50 and 60 imp/s in the second. During *e*-vector rotation, neuronal activity in one of the two neurons was not significantly different from a uniform distribution (Rayleigh test, *P* = 0.123; Fig. 7*D*, xenon arc stimulation, standard glass optics). The second neuron, of high background activity, was polarization-sensitive. The responses to different *e*-vector orientations were significantly different from a uniform distribution (Rayleigh test, *P* = 0.006). The neuron showed polarization opponency with Φ_{max} at 109° (halogen light source, R^2 = 0.64; not shown). Both neurons were

phasic-tonically excited by zenithal unpolarized light (Fig. 7*E*). One neuron stimulated with xenon light (standard glass optics), showed phasic on-inhibition to contralateral stimulation and phasic-tonic excitations to ipsilateral light (Fig. 7*E*), whereas the second neuron was unresponsive to lateral halogen stimulation.

Lobula loop neuron

This neuron was encountered only once. Its soma (20–25 μm diam) was in the superior lateral protocerebrum posterior
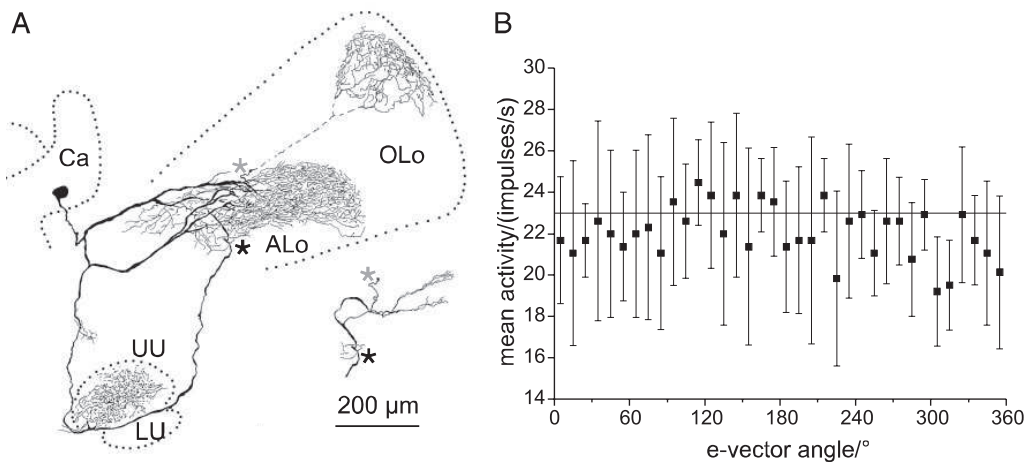
FIG. 8.   Neuron from the upper unit of the AOTu that loops from and to the lobula. *A*: frontal reconstruction. The neuron has extensive arborizations in the anterior lobe of the lobula (ALo) and projects to the UU of the AOTu. The axon projects back to the optic lobe and gives rise to another field of ramifications in the outer lobe of the lobula (OLo). *B*: *e*-vector response plot (means ± SD from 7 counterclockwise turns through 360°; xenon arc stimulation, quarz optics). Neuronal activity during *e*-vector rotation is not significantly different from uniformity (Rayleigh test, *P* = 0.762). Solid line, background activity.

to the calyx. Two collaterals extended from the primary neurite to the lobula and gave rise to a dense meshwork of ramifications in layer 2 of the anterior lobe of the lobula. Another fiber descended to the upper unit of the AOTu and gave rise to dense sidebranches in both lobes of the upper unit. The fiber continued into the anterior optic tract toward the lobula, contributed to the arborizations in layer 2 of the anterior lobe of the lobula, and continued to terminal ramifications in dorsal aspects of the outer lobe of the lobula (Fig. 8*A*). The processes in all three neuropils were of beaded shape with those in the AOTu being the most large and dense ones. The neuron had a background activity of 20–30 imp/s. When stimulated with dorsal polarized light, spiking activity was independent of *e*-vector angle (Rayleigh test, *P* = 0.762; Fig. 8*B*).

DISCUSSION

The upper and lower units of the AOTu in the locust brain are parts of two parallel pathways that connect peripheral visual neuropils to the central complex (Homberg et al. 2003). Overlapping branching patterns, especially between neurons from the lower unit of the AOTu and polarization-sensitive interneurons (POL neurons) from the central complex, suggested that the lower unit of the AOTu is part of the polarization vision pathway and feeds input into the central complex. Here we describe the morphology and physiological responses, especially to plane-polarized light, of neurons from the AOTu. All neurons from the lower unit of the AOTu were tuned to distinct *e*-vector orientations of dorsally presented plane-polarized light, substantiating our hypothesis that the AOTu is part of the locust's sky-compass navigation system. In contrast, only one of five recorded neurons from the upper unit was weakly polarization-sensitive. During the course of experiments, several combinations of light intensities and bandwidths were used, but all stimuli included blue light corresponding to the spectral sensitivity of locust polarization-sensitive photoreceptors (Eggers and Gewecke 1993). Accordingly, neither differences in intensity nor in spectral bandwidth of the stimuli

we used affected the properties of polarized-light responses (types of responsive neurons, polarization-opponency, ocular dominance, and *e*-vector tuning) in these neurons. All neurons, however, also showed responses to unpolarized light that strongly depended on the stimulus position within the visual field of the animal. These responses were more pronounced with high-intensity xenon arc stimulation.

Orientation to polarized light was first discovered in honeybees by Karl von Frisch over 50 years ago (von Frisch 1949). Subsequently polarization vision was demonstrated behaviorally in several other insect species, including the ant *Cataglyphis bicolor* (Wehner 1994), the cricket *Gryllus campestris* (Brunner and Labhart 1987), the fly *Musca domestica* (von Philipsborn and Labhart 1990), the locusts *Locusta migratoria* and *Schistocerca gregaria* (Eggers and Weber 1993; Mappes and Homberg 2004), the beetle *Scarabaeus zambesianus* (Dacke et al. 2003), and the butterfly *Danaus plexippus* (Reppert et al. 2004). The mechanisms in the CNS, however, that accomplish this fascinating skill are still poorly understood. So far, POL neurons have been recorded from the optic lobe (cricket: Labhart 1988; Labhart et al. 2001; desert ant: Labhart 2000; cockroach: Kelly and Mote 1990; Loesel and Homberg 2001; desert locust: Homberg and Würden 1997) and, in the locust and cricket, from an area in the midbrain, the central complex (Sakura and Labhart 2005; Vitzthum et al. 2002). To bridge the gap between both stages of polarized-light processing, we recorded from an intercalated neuropil that receives input from the optic lobe and sends output toward the central complex. While multiple recordings were archieved from bilateral interneurons of the AOTu and from projection neurons to the central complex, no recordings were obtained from the large number of medulla line tangentials with axonal terminals in the AOTu (Homberg et al. 2003). If these neurons, like LoTu1 and TuLAL1b, also provide polarization input to the AOTu, their *e*-vector tuning might largely account for the broad distribution of Φ_{max} orientations found in the central complex (Vitzthum et al. 2002).

Φ_{max} tuning

Polarization-sensitive interneurons in the medulla of crickets, termed POL1, exist as three physiological subtypes per brain hemisphere (Labhart and Petzold 1993), and each subtype is tuned to a different *e*-vector orientation (Labhart et al. 2001). In contrast, in the central complex of the locust and cricket, there is no evidence for the presence of only a few *e*-vector tuning types, but neurons are tuned to a large variety of *e*-vector orientations (Sakura and Labhart 2005; Vitzthum et al. 2002). The two types of bilateral POL neurons studied here, LoTu1 and TuTu1, did show distinct Φ_{max} orientations. In LoTu1, we found one tuning type per brain hemisphere (Fig. 3). This corresponds with Dextran injections into the AOTu (Homberg et al. 2003) that never revealed more than one LoTu1 neuron per brain hemisphere. The mean Φ_{max} orientations of the two neurons (LoTu1 of the right hemisphere: 41°, LoTu1 of the left hemisphere: 134°) are nearly perpendicular to each other and are mirror-symmetric with respect to the longitudinal axis of the animal (Fig. 3*E*). These properties correspond well with the general bilateral symmetry in the organization of insect brain functions.

In TuTu1 neurons, four classes of Φ_{max} orientations appear to be present. Neurons with somata in the left hemisphere show peaks in Φ_{max} tuning around 175° and around 135° (Fig. 2*E*). Most neurons with somata in the right hemisphere, in contrast, are tuned to a Φ_{max} around 45°, but a small group of four cells with Φ_{max} orientations between 140 and 180° deviate considerably from this population and suggest a second peak in this range. The presence of two Φ_{max} classes per hemisphere in TuTu1 neurons fits well with anatomical data. Impalements of pairs of TuTu1 neurons per hemisphere were occasionally encountered in this study, but more than two TuTu1 neurons per hemisphere were never found, even in mass dye injections into the AOTu (U. Homberg and S. Hofer, unpublished data). As expected from bilateral symmetry of brain functions, two classes of Φ_{max} orientations (135° in right TuTu1 and 45° in left TuTu1) are orthogonal to each other, whereas the two other tuning types (near 175°) may deviate only slightly from each other.

Due to earth rotation, a sky compass to function properly requires constant time compensation. Neurons that use the solar azimuth to signal directions, therefore, have to shift their Φ_{max} tuning as the sun moves across the sky during the day. All experiments in this study were performed between 9:00 AM and 10:30 PM. Because LoTu1 and TuTu1 neurons showed distinct classes of Φ_{max} independent of daytime, they appear to signal the orientation of the animal relative to the sky and irrespective of daytime. We therefore assume that time compensation is performed at higer stages of the polarization vision system, possibly in the central complex.

Ocular dominance

Ocular dominance for polarized-light sensitivity was tested in LoTu1 and TuTu1 neurons. The responses to ipsilateral and bilateral stimulation were identical in TuTu1 neurons (Fig. 2*D*), and they were similar in LoTu1 cells (Fig. 3*D*). When the ipsilateral eye was occluded, visual responses were abolished in LoTu1, indicating that the neuron receives polarization input only through the ipsilateral eye. In TuTu1, polarization sensi-

tivity was strongly reduced but not completely abolished after occlusion of the ipsilateral eye. This indicates that polarization input is dominated but not exclusively mediated by the ipsilateral eye. Both in TuTu1 and LoTu1, smooth fiber specializations are present on arborizations in the ipsilateral hemisphere, commonly interpreted as synaptic input sites, and beaded or varicose processes on contralateral terminals, generally interpreted as synaptic output sites. This suggests that both neurons receive input largely or exclusively in the ipsilateral lobula and AOTu and provide polarized light input to the contralateral brain hemisphere.

Polarization sensitivity with and without opponency

POL neurons of the locust central complex show polarization opponency and thus receive antagonistic input from orthogonally oriented polarization analyzers (Vitzthum et al. 2002). While TuTu1 and TuLAL1a neurons are of the opponency type (Figs. 2 and 5), LoTu1 and TuLAL1b are excited by all *e*-vector orientations, i.e., they show sinusoidal modulation of spiking activity during *e*-vector rotation but no inhibitory component (Figs. 3 and 6). This indicates that LoTu1 and TuLAL1b neurons may receive excitatory input from only one tuning-type of polarization analyzers. Alternatively, they might receive a polarization-opponent input together with a polarization-insensitive excitatory input to light, perhaps through different photoreceptors as suggested by their strong tonic responses to unpolarized light.

Sensitivity to unpolarized light

In contrast to POL neurons in the cricket optic lobe (Labhart and Petzold 1993), all neurons of the AOTu responded to unpolarized light stimuli, largely with tonic activity changes. Responses were generally stronger and more robust with quarz optics and xenon arc stimulation, which was ∼1 log unit below the irradiance of direct sunlight under clear sky conditions in Marburg (personal measurements). Responses were strongly dependent on stimulus position, and the occurence of inhibitory and excitatory responses in the same neuron (e.g., LoTu1, Fig. 3*F*) indicates complex receptive field properties with inhibitory and excitatory subfields. In certain POL neurons like TuTu1, weak tonic responses to unpolarized light might reflect an imbalance in the polarization-opponent inputs, whereas the strong responses in others, especially LoTu1, argue for the integration of spatially separate polarization and nonpolarization inputs. The differences in neuronal responses to halogen- versus xenon-lamp stimulation are likely to reflect both wavelength-dependency of the response and intensity differences between the light stimuli of the two experimental setups. Preliminary data on the chromatic properties of the LoTu1 and TuTu1 neurons, indeed, revealed eye-region dependent sensitivity to unpolarized UV and green light, in addition to polarization sensitivity mediated by blue receptors of the drosal rim area (unpublished results).

Behavioral studies, especially in ants and honeybees, showed that, in addition to the sky polarization pattern, intensity and spectral gradients in the sky, solar azimuth, and landmarks are exploited for spatial orientation (Giurfa and Capaldi 1999; Wehner 1997, 2003). How and where in the brain these features are integrated with polarization information is unclear at present.

Some aspects of the sky, like solar azimuth and intensity gradients are tightly linked to the sky polarization pattern and might possibly be encoded in the response profiles of neurons of the lower unit of the AOTu. Other aspects like landmarks are more independent from celestial cues and might be funnelled to brain areas supervising spatial orientation through an independent pathway, perhaps via the upper unit of the tubercle. While the biological role of visual projections through the two units of the AOTu is still speculative, it offers some attractive possibilities for further experimentation. If responses to unpolarized light in POL neurons of the AOTu do, indeed, reflect solar azimuth, maximum response to unpolarized light should occur at a meridian orthogonal to Φ_{max} orientation in the zenith, reflecting the situation in the sky. First experiments indeed, showed a spatial relationship of ~90° between the azimuthal position of the receptive field for unpolarized light and Φ_{max} orientation in LoTu1 neurons (Pfeiffer et al. 2005) and thus support this hypothesis. Such response profiles may serve to distinguish between the solar and the antisolar azimuth, which is not possible based on the analysis of *e*-vector orientation alone.

REFERENCES

Batschelet E. *Circular Statistics in Biology.* London: Academic, 1981.

Best PJ, White AM, and Minai A. Spatial processing in the brain: the activity of hippocampal place cells. *Annu Rev Neurosci* 24: 459–486, 2001.

Brunner D and Labhart T. Behavioral evidence for polarization vision in crickets. *Physiol Entomol* 12: 1–10, 1987.

Clements AN and May TE. Studies on locust neuromuscular physiology in relation to glutamic acid. *J Exp Biol* 60: 673–705, 1974.

Dacke M, Nilsson DE, Scholtz CH, Byrne M, and Warrant EJ. Animal behaviour: insect orientation to polarized moonlight. *Nature* 424: 33, 2003.

Eggers A and Gewecke M. The dorsal rim area of the compound eye and polarization vision in the desert locust (*Schistocerca gregaria*). In: *Sensory Systems of Arthropods,* edited by Wiese K, Gribakin FG, Popov AV, and Renninger G. Basel: Birkhäuser, 1993, p. 101–109.

Eggers A and Weber T. Behavioral evidence for polarization vision in locusts. In: *Gene-Brain-Behaviour,* edited by Elsner N and Heisenberg M. Stuttgart: Thieme, 1993, p. 336.

Giurfa M and Capaldi EA. Vectors, routes and maps: new discoveries about navigation in insects. *Trends Neurosci* 22: 237–242, 1999.

Homberg U. In search of the sky compass in the insect brain. *Naturwissenschaften* 91: 199–208, 2004.

Homberg U and Würden S. Movement-sensitive, polarization-sensitive, and light-sensitive neurons of the medulla and accessory medulla of the locust, *Schistocerca gregaria. J Comp Neurol* 386: 329–346, 1997.

Homberg U and Paech A. Ultrastructure and orientation of ommatidia in the dorsal rim area of the locust compound eye. *Arthropod Struct Dev* 30: 271–280, 2002.

Homberg U, Hofer S, Pfeiffer K, and Gebhardt S. Organization and neural connections of the anterior optic tubercle in the brain of the locust, *Schistocerca gregaria. J Comp Neurol* 462: 415–430, 2003.

Kelly KM and Mote MI. Electrophysiology and anatomy of medulla interneurons in the optic lobe of the cockroach, *Periplaneta americana. J Comp Physiol [A]* 167: 745–756, 1990.

Labhart T. Polarization-opponent interneurons in the insect visual system. *Nature* 331: 435–437, 1988.

Labhart T. Polarization-sensitive interneurons in the optic lobe of the desert ant *Cataglyphis bicolor. Naturwissenschaften* 87: 133–136, 2000.

Labhart T and Petzold J. Processing of polarized light information in the visual system of crickets. In: *Sensory Systems of Arthropods,* edited by Wiese K, Gribakin F, Popov A, and Renninger G. Basel: Birkhäuser, 1993, p. 158–168.

Labhart T and Meyer EP. Detectors for polarized skylight in insects: a survey of ommatidial specializations in the dorsal rim area of the compound eye. *Microsc Res Tech* 47: 368–379, 1999.

Labhart T and Meyer EP. Neural mechanisms in insect navigation: polarization compass and odometer. *Curr Opin Neurobiol* 12: 707–714, 2002.

Labhart T, Petzold J, and Helbling H. Spatial integration in polarization-sensitive interneurones of crickets: a survey of evidence, mechanisms and benefits. *J Exp Biol* 204: 2423–2430, 2001.

Loesel R and Homberg U. Anatomy and physiology of neurons with processes in the accessory medulla of the cockroach *Leucophaea maderae. J Comp Neurol* 439: 193–207, 2001.

Mappes M and Homberg U. Behavioral analysis of polarization vision in tethered flying locusts. *J Comp Physiol [A]* 190: 61–68, 2004.

Pfeiffer K, Kinoshita M, and Homberg U. Integration of celestial orientation cues in an identified neuron in the brain of the desert locust, *Schistocerca gregaria.* In: *Neuroforum 2005 Suppl.*, edited by Krieglstein K and Zimmermann H. Heidelberg: Spektrum, 2005, p. 29B.

Poucet B, Lenck-Santini P-P, Paz-Villagrán V, and Save E. Place cells, neocortex and spatial navigation: a short review. *J Physiol Paris* 97: 537–546, 2003.

Reppert SM, Zhu H, and White RH. Polarized light helps monarch butterflies navigate. *Curr Biol* 14: 155–158, 2004.

Sakura M and Labhart T. Polarization-sensitive neurons in the central complex of the cricket, *Gryllus bimaculatus.* In: *Neuroforum 2005 Suppl.*, edited by Krieglstein K and Zimmermann H. Heidelberg: Spektrum, 2005, p. 154B.

Strauss R. The central complex and the genetic dissection of locomotor behaviour. *Curr Opin Neurobiol* 12: 633–638, 2002.

Taube JS and Bassett JP. Persistent neural activity in head direction cells. *Cereb Cortex* 13: 1162–1172, 2003.

Vitzthum H, Müller M, and Homberg U. Neurons of the central complex of the locust *Schistocerca gregaria* are sensitive to polarized light. *J Neurosci* 22: 1114–1125, 2002.

von Frisch K. Die Polarisation des Himmelslichtes als orientierender Faktor bei den Tänzen der Bienen. *Experientia* 5: 142–148, 1949.

von Philipsborn A and Labhart T. A behavioral study of polarization vision in the fly, *Musca domestica. J Comp Physiol [A]* 167: 737–743, 1990.

Wehner R. The polarization-vision project: championing organismic biology. In: *Neural Basis of Behavioural Adaptations,* edited by Schildberger K and Elsner N. Stuttgart: Gustav Fischer, 1994, p. 103–143.

Wehner R. The ant's celestial compass system: spectral and polarization channels. In: *Orientation and Communication in Arthropods,* edited by Lehrer M. Basel: Birkhäuser, 1997, p. 145–185.

Wehner R. Desert ant navigation: how miniature brains solve complex tasks. *J Comp Physiol [A]* 189: 579–588, 2003.

Coding of spatial directions via time-compensated combination of celestial compass cues

Coding of spatial directions via time-compensated combination of celestial compass cues

Keram Pfeiffer and Uwe Homberg

Department of Biology, Animal Physiology, University of Marburg, Marburg, Germany
*Correspondence should be addressed to U.H. (Homberg@staff.uni-marburg.de)*

Many animals use the sun as a reference for spatial orientation. In addition to direct sunlight, the sky provides two other sources of directional information, a colour gradient and a pattern of polarization. Relying on sky polarization poses two fundamental problems: *E*-vector orientations in the sky do not allow to distinguish between the solar and antisolar hemispheres and the polarization pattern changes with changing solar elevation during the day. Here we present neurons in the brain of a locust that overcome both problems by combining all three sources of information and by compensating for diurnal changes in *E*-vector orientations.

Spatial orientation is a key requirement for animals that move far from their nests or migrate to new favorable areas. One of the tasks involved is to maintain a particular navigational direction. This is often accomplished by adjusting the direction of movement relative to the horizontal component of the sun´s direction, the solar azimuth (sun compass). In addition to direct view of the sun, the scattered light from the blue sky also bears directional information: it is polarized and its spectral composition depends on the angular distance from the sun. *E*-vectors of polarized sky-light are oriented in concentric circles around the sun (Fig. 1a) and the degree of polarization increases from 0% (direct sunlight) to approximately 75% at an angular distance of 90° from the sun (Brines & Gould, 1982). The ratio in light intensity between long wavelength (460-700 nm) and short wavelength (300-460 nm) light is largest in the vicinity of the sun (red side of the sky) and lowest at the opposite side (blue side of the sky, Coemans et al. (1994)). Bees and ants were shown to use spectral cues for celestial compass navigation, if their polarization-sensitive eye regions are painted over (Rossel & Wehner, 1984; Wehner, 1997).Two-choice experiments, likewise, revealed that the color vision system of homing pigeons is suited to exploit the chromatic gradient of the sky as a navigational cue (Coemans et al., 1994).

While progress has been made on the neuronal basis of the polarization compass, especially in crickets and locusts (for reviews see: (Labhart & Meyer, 2002; Labhart et al., 2001; Homberg, 2004), neural correlates of a sun compass or a chromatic compass have not been discovered in any animal species. Here we show that identified neurons in the locust brain respond to a combination of visual stimuli in a way that enables them to concurrently signal sun compass, chromatic compass, and polarization compass information. We suggest that by combining these three sources of information a shortcoming of polarization vision is overcome: by analyzing *E*-vector orientations alone, it is not possible to distinguish between the solar azimuth and the antisolar azimuth. The neurons reported here were originally identified as polarization-sensitive interneurons (POL-neurons) of the an-

a

b
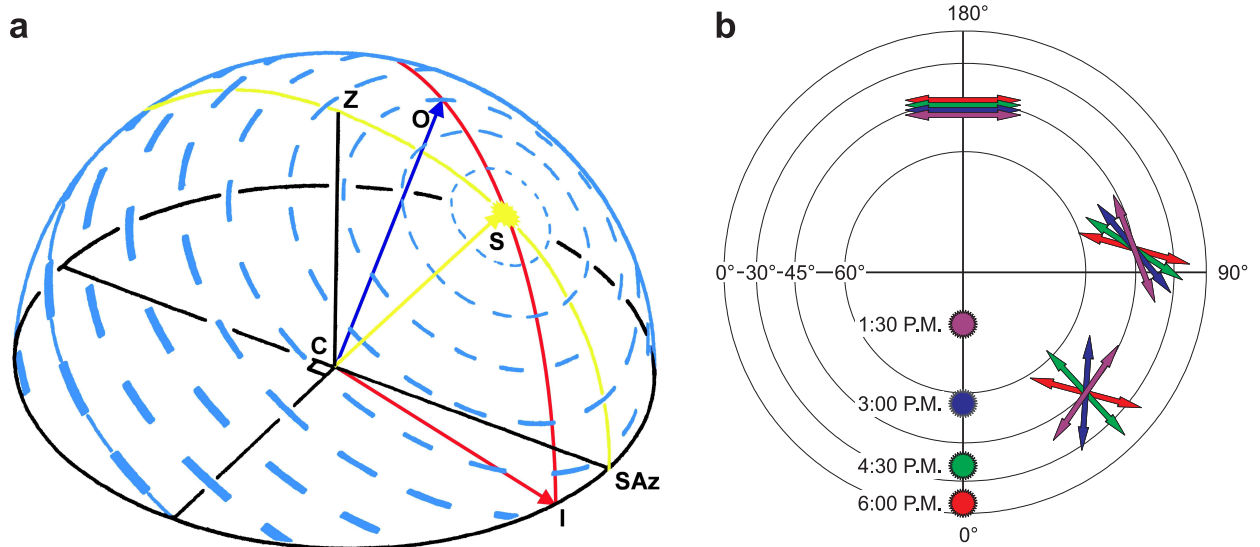
Figure 1: Polarization pattern of the blue sky. (a) Orientation and thickness of the bars indicate *E*-vector orientation and degree of polarization as seen by an observer in the center (C) of the sphere. *E*-vector orientation is always perpendicular to a great circle (red) through the observed point (O) and the sun (S). Along the solar meridian (yellow line through the sun) and in the zenith (Z), the azimuth of the sun (SAz) is directly readable from the *E*-vector orientation irrespective of the elevation of the sun. For all other points in the sky, the intersection point (I) between the horizon and the great circle through O and S differs from (SAz) by the angle between I, C and SAz. Adapted from Wehner (1982). (b) Zenithal projection of solar elevation and *E*-vector orientation for four times of June 24, 23.4° N, 6.5° E. Circles: elevation, straight lines: azimuth. In the course of the day *E*-vectors that do not lie on the solar meridian (0°-180° line) change their orientations. In the solar half of the sky (see *E*-vectors at 45° azimuth), the variability is higher than in the antisolar half of the sky (*E*-vectors at 99° azimuth). Close to the sun, the relation between solar elevation and *E*-vector orientation is highly nonlinear.

terior optic tubercle in the locust brain, a major target of visual interneurons from the primary visual brain centers (Pfeiffer et al., 2005; Homberg et al., 2003). In addition, they exhibit UV/green-opponency to unpolarized light stimuli (M. Kinoshita, KP, UH).

RESULTS

In the present study, we analyzed the azimuthal tuning of neurons from the anterior optic tubercle of the locust brain to green (530 nm) and UV (350 nm) light spots and compared these data to their tuning to dorsally presented polarized light (blue, 450 nm). Experiments were performed on animals raised in a green house with open view to the sky. For each recording we compared the preferred *E*-vector orientation (POL) to the preferred azimuth angle of a green light spot (Φ_{max}green). We recorded intracellularly from three types of POL-neuron of the anterior optic tubercle (LoTu1: n=15, TuTu1: n=23, TuLAL1b: n=7). Forty two (93%) of these neurons showed significant responses to a green light spot (see Methods for details on stimulation, Pfeiffer et al., 2005, for neuron morphology). In 30 of these experiments, we also tested the responses to UV light, which showed significant directedness in 27 neurons (90%).

LoTu1 neurons

LoTu1 neurons exhibited a background activity of 8.9±5.6 impulses/s in darkness. Dorsally presented polarized blue light elicited tonic excitation that was sinusoidally modulated in strength by the rotating *E*-vector (Fig. 2a). A green, unpolarized light spot moving around the head
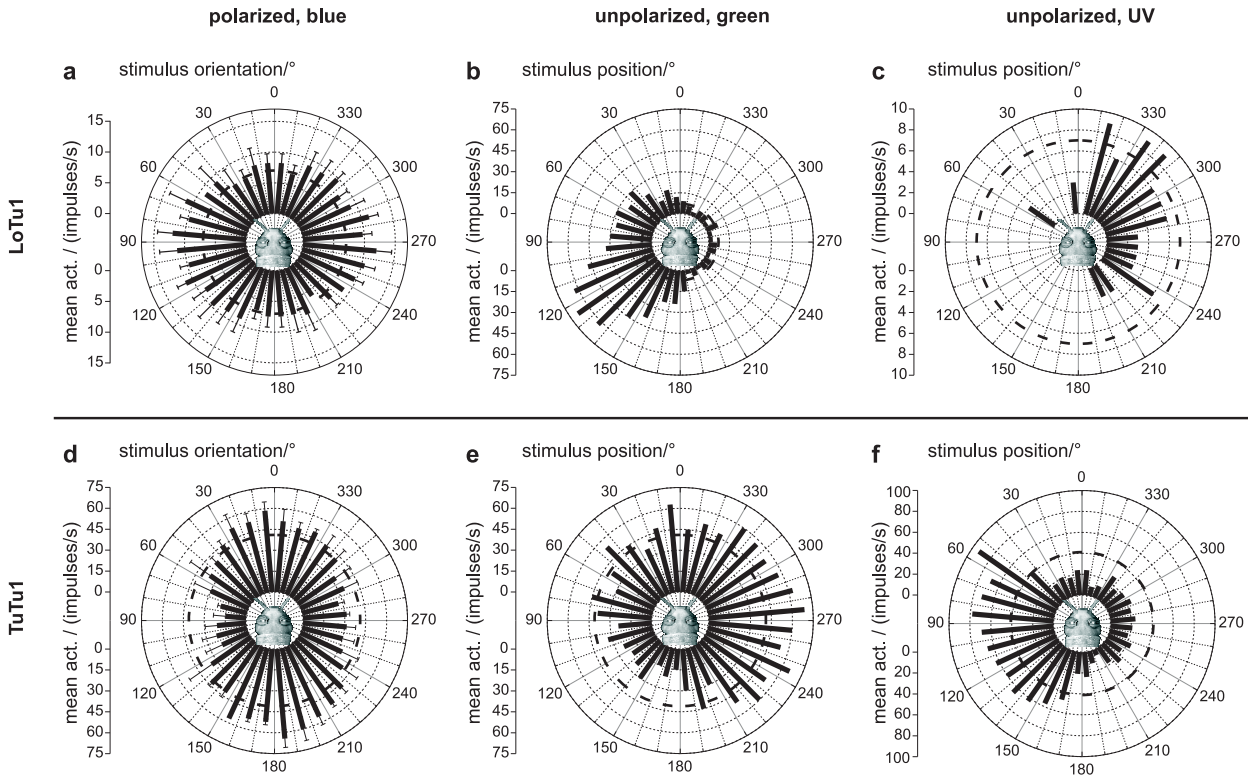
Figure 2: Response characteristics of a LoTu1 and a TuTu1 neuron to three different stimulation regimes. (a) The LoTu1 neuron is activated by all E-vector orientations but shows maximum response (Φ_{max}) at an E-vector orientation of $95°/275°$ (Rayleigh Test, p = 0.014). Thick, dashed lines in this and all other graphs indicate background activity. Error bars indicate s.d. (b, c) Depending on wavelength, ipsilateral, unpolarized light leads to strong excitation (b, green, $\Phi_{max} = 111°$, $p < 10^{-12}$) or to inhibition (c, UV, $\Phi_{max} = 313°$, $p = 2.13 \cdot 10^{-7}$). Contralateral stimulation with either color has no effect. (d-f) The TuTu1 neuron shows polarization opponency (polarized light excites or inhibits the cell depending on E-vector orientation, (d), $\Phi_{max} = 4°/184°$, $p = 10^{-12}$), color opponency (green and UV lead to opposite effects on spiking rate), (e, f), and spatial opponency (different positions of the same stimulus lead to opposite effects on the spiking rate, (e), $\Phi_{max} = 303°$, $9.4 \cdot 10^{-11}$, f, $\Phi_{max} = 101°$, $p < 10^{-12}$). Inhibition by contralateral UV light (as in f) was seen in 7 of 13 recordings.

of the animal at an elevation of 45° resulted in strong excitation of the neuron when presented in the ipsilateral (soma-sided) visual field, but had no effect on the contralateral side (Fig. 2b). When the unpolarized light was switched from green to UV, LoTu1 neurons were inhibited when the stimulus was in the ipsilateral visual field.

TuTu1 neurons

TuTu1 neurons had a higher background activity of 30.2 ± 11.1 impulses/s. The responses to all stimuli were more complex than those in LoTu1

neurons. In contrast to LoTu1 neurons, TuTu1 cells showed polarization opponency, i.e. they were maximally excited by a certain E-vector orientation (Φ_{max}) and were maximally inhibited by an E-vector orientation perpendicular to Φ_{max} (Fig. 2d). Moving an unpolarized, green light spot around the animal's head led to inhibition when presented in the ipsilateral field of view, and to excitation when presented contralaterally (Fig. 2e). An unpolarized UV light spot caused strong excitations in the ipsilateral field of view and, in 7 of 13 recordings (54%), inhbitions when presented contralaterally (Fig.
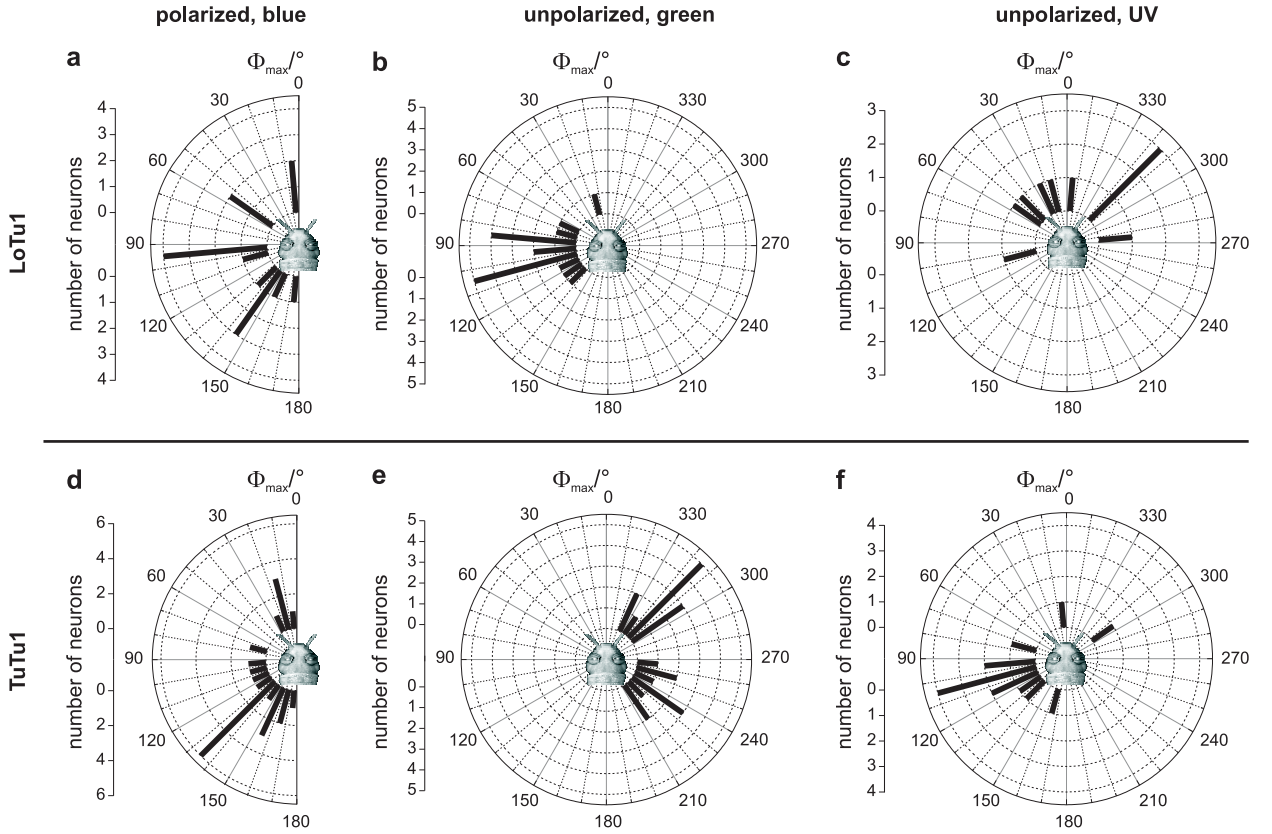
Figure 3: Distribution of Φ_{max} values in LoTu1 and TuTu1 neurons. The distribution of E-vector tunings of LoTu1 neurons is not significantly different from randomness (a, Rayleigh test, p = 0.734, length of mean vector r = 0.252, n = 15), but the distributions of Φ_{max} values in response to unpolarized light differ significantly from randomness (b, green, p = $5.01 \cdot 10^{-5}$, r = 0.882, n = 15, c, UV, p = 0.048, r = 0.579, n = 9). All distributions of Φ_{max} values from TuTu1 neurons (d through f) differ significantly from randomness (d, polarized blue light, p = 0.002, r = 0.531, n = 21, e, green, p = $1.4 \cdot 10^{-5}$, r = 0.751, n = 21, f, UV, p < 10^{-12}, r = 0.646, n = 13). While the green response shows two preferred directions (237°and 316°), there is only one peak in the distribution of Φ_{max} values for UV (107°± 54°).

2f). Thus, TuTu1 neurons exhibit color opponency combined with spatial opponency.

Distribution of tuning types

LoTu1 neurons The distribution of the preferred E-vector orientations of LoTu1 neurons did not differ significantly from randomness (Fig. 3a, Rayleigh test, p=0.394, length of mean vector r=0.252) and thus shows that the 15 LoTu1 neurons did not have a common preference for a certain E-vector orientation. This is different from our previous results from laboratory raised animals (Pfeiffer et al., 2005)

that revealed a common mean E-vector tuning for LoTu1 neurons at 41° (soma in right hemisphere), resp. 134° (soma in left hemisphere). In contrast to E-vector tuning, the preferred azimuth position of the green unpolarized light spot showed highly significant directedness (Rayleigh test, p = $8.92 \cdot 10^{-7}$, r = 0.882) with a mean angle of 94°± 29°. The distribution of the Φ_{max} UV angles had a mean at 355°, however, with a much larger angular deviation of± 61° (Rayleigh test, p = 0.048, r = 0.579). This results from the fact that the low background activity of LoTu1 neurons in combination with the inhibitory response to the UV stimulus provides
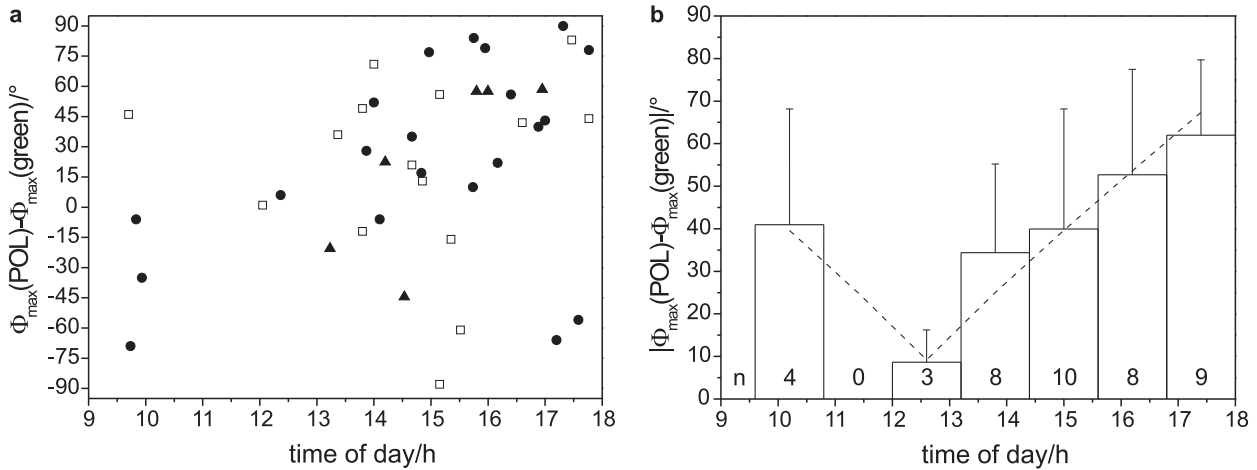
Figure 4: Daytime dependence of the angular distance between the preferred E-vector and the preferred green light direction. (a) Open squares: LoTu1 neurons, solid circles: TuTu1 neurons, solid triangles: TuLAL1b neurons. (b) Absolute values of the data in a were binned into 72 min bins. Mean angles and mean angular deviations were plotted against the bin center. A model that predicts the angular distance between the green Φ_{max} and the POL Φ_{max} was fitted to the data (dashed line, see Methods section). Fitting results: azimuthal angle between sun and viewing direction = 99.16°, elevation of viewing direction = 45.42°, date = June 24, longitude = 6.53°, latitude = 23.40°, $R^2 = 0.97213$.

a signal with considerably more noise than the high spiking rates during stimulation with green light (compare Figs. 2b and 2c).

TuTu1 neurons In TuTu1 neurons, the angular distributions for Φ_{max}POL, Φ_{max}green, and Φ_{max}UV differ significantly from randomness (Fig. 3d-f, Rayleigh test, POL: p = 0.012, green: p = $1.12 \cdot 10^{-6}$, UV: p = 0.003). Like in LoTu1 neurons the variability (indirectly measured by the length of the mean vector r) is largest for polarized light (r = 0.451), followed by unpolarized UV (r = 0.646) and is lowest for green unpolarized light (r = 0.751). The angular distribution for green light shows a bimodal distribution with the two mean angles at 237°±17° and 316°± 9°, possibly resulting from the fact that there are two TuTu1 neurons per brain hemisphere in the locust brain (Pfeiffer et al., 2005).

Diurnal attenuation of tuning

To investigate a possible adjustment of the neurons during the course of the day, we calculated for each recording the angle between the preferred E-vector orientation and the preferred direction of a green light spot (representing the sun). These difference-angles were plotted against the time of day of the recording (Fig. 4a). They were smallest around noon and became larger in the afternoon and evening (Fig. 4a).

To determine whether this temporal relation might reflect changes in celestial E-vector orientation in the course of the day (Fig. 1b), we binned the absolute values of the difference-angles, calculated the means and fitted a set of functions to the data (Fig. 4b). In the first set of functions we calculated the elevation of the sun and used the date, time of day, and geographical coordinates as parameters. In the second set we calculated the E-vector orientation of an observed point in the sky with the solar elevation and the elevation and azimuth as parameters (see Supplementary Information for formulas). The results of the fit are: azimuthal angle between sun and viewing direction = 99.16°, elevation of viewing direction = 45.42°, date = June 24, longitude = 6.53°, latitude = 23.40°, coefficienct of determination for the fit: R^2 =

0.97213. The fitting parameter "azimuthal angle between sun and viewing direction" becomes 99.16°. This means that at an azimuthal angle of 99.16° from the sun, E-vector orientation changes during the course of the day in the same way as the difference between Φ_{max}POL and Φ_{max}green of the neurons.

DISCUSSION

We show, that neurons of the anterior optic tubercle of the locust brain signal E-vector orientation of polarized light as well as direction of green and UV light spots. The tuning angles between the responses to polarized light and to unpolarized green light change in the course of the day in the same way as the E-vector orientation in certain parts of the sky.

The natural canopy can be divided into two halves: a solar half that is dominated by light of long wavelengths and an anti-solar half, dominated by short-wavelength light. They are referred to as the red and the blue half of the sky (Coemans et al., 1994). The colour opponency of both LoTu1 and TuTu1 neurons to green and UV light are well suited to discriminate between the solar and the antisolar half of the sky on the basis of the UV/green contrast. In addition, both neurons detect the solar azimuth as the brightest part in the red side of the sky. Do these cells extract the same information (solar azimuth) from the chromatic and intensity cues as from the sky polarization pattern? The angle between the solar azimuth and an E-vector in the sky (E-vector orientation) is 90° only along the solar meridian, e.g. in the zenith (see Fig. 1, Supplementary Fig. 2, Supplementary Fig. 3). As we showed previously, LoTu1 and TuTu1 receive polarization input only from the ipsilateral eye (Pfeiffer et al., 2005). The dorsal rim area of the compound eye that provides this input, points to the contralateral side of the sky resulting in a receptive field that is eccentric with respect to the zenith. The E-vector orientations perceived by this eccentric visual field depend on two parameters: 1. on the position of the sun

and 2. on the direction of view. In other words it depends on the orientation of the locust's head relative to the sun and on the elevation of the sun above the horizon and hence the time of day.

Judged by the axis of the dorsal rim area photoreceptors (Homberg & Paech, 2002), the receptive fields of the neurons lie in the contralateral field of view and thus the external changing rate (of an observed E-vector, Supplementary Fig. 3) and the internal changing rate (of the neurons sensitivity, Fig. 4) would match when the sun is behind the animal. The fitting parameter "longitude" that determines time of day of the solar culmination converges to 6.53° which is close to the actual 8.8° of Marburg. The parameter "elevation of viewing direction" becomes 45.42°. We do not have physiological data on the elevation of the receptive fields for polarization sensitivity of these neurons, but from the optical axes of the dorsal rim photoreceptors we would expect a somewhat higher elevation of around 60°. The course of the apparent motion of the sun during the day (solar ephemeris function) depends on the date and on the geographical latitude of the observer. Thus the parameters "date" and "latitude" influence the shape of our fitting function. The resulting fit (Fig. 4b) consists of two quasilinear functions. One is falling until noon and the other one is rising from noon to dusk. The linearity of the fit results from the linearity of the rising velocity of the sun (Supplementary Fig. 1), caused by the values that are determined for the parameters "date" and "latitude": June 24 (summer solstice = June 21) and 23.4° N (the tropic of cancer = 23.26° N). We conclude that instead of having detailed knowledge about the solar ephemeris function, it is sufficient for the locust to assume a linear relationship between time of day and solar elevation. The compensation of the neurons is carried out in such a way that celestial E-vector information is only relevant when the sun is behind the animal. This is in accordance with the finding that the strongest reactions to the green light spot occur when it is presented left or right from the animal.

Our results provide new insight into how sky compass signals are computed at neuronal levels. A major finding is that instead of using redundant systems for the different sources of directional information (polarization pattern, sun, spectral composition of skylight) all three parameters of the sky are integrated in a meaningful way within the same neurons. The main reason why the system has evolved in this way might be the obvious saving of space and energy by reducing the number of neurons to the necessary minimum. However, the combination of different cues might also originate from a shortcoming of polarized light information. The orientations of E-vectors range from 0° to 180° and thus cannot unambiguously signal the solar azimuth which covers a range of 360°. This can be overcome by adding other sources of directional information, like the color of the sky or the direct sunlight.

A disadvantage of processing these different signals with the same set of neurons is that the different systems do not always read the same reference direction from their input sources. The most prominent and reliable source of directional information is the sun itself. The low variability in the responses to the green light spot (distribution of Φ_{max}green, Fig. 3 b and d) strongly suggests that the sun is the major cue for the neurons reported here. Under what situations does the animal have to rely on other cues than direct sunlight? One scenario is the sky around dusk and dawn, when the sun is either below the horizon or hidden by obstacles. At low solar elevations, the polarization pattern provides rather accurate information on the solar azimuth, independent of viewing direction (see Supplementary Fig. 2). Under these situations the animals can rely on the canopy light without making large navigational errors. Our second major finding, the diurnal adaptation of the neurons' tuning, in the course of the day, shows that polarization information is also relevant during daytime. The direction perpendicular to the orientation of celestial E-vectors coincides with the solar azimuth (or antisolar azimuth) only along the solar meridian (Fig. 1). For all other celestial points, this direction can diverge up to± 90° from the solar azimuth, depending on the viewing direction. Since the E-vector orientation for those parts of the sky is not invariantly linked to the solar azimuth but changes in a predictable manner, the neurons can be tuned to correctly signal solar azimuth as extracted from E-vector orientation only for a single viewing direction. Our fitting results suggest that this is condition is fulfilled, when the sun is behind the animal. To minimize the influence of potentially misleading polarized light information on the neuron's activity when the sun is laterally, LoTu1 and TuTu1 neurons employ different mechanisms. In LoTu1 neurons the response to green unpolarized light is considerably stronger than the response to polarized light (scales in Fig. 2a and b). In a natural situation when the TuTu1 neuron has its highest activity (contralateral sunlight), the polarization-sensitive photoreceptors of the dorsal rim area face the solar half of the sky, which provides little input due to the small degree of polarization. In both types of neuron, the relative weight of input contributed by polarized light at Φ_{max}green is considerably reduced and thus may not influence the neurons' activity in a way that leads to miscalculation of the solar azimuth.

For both LoTu1 and TuTu1 neurons we did not find consistent Φ_{max}POL tunings across different recordings, in contrast to our previously reported results with laboratory raised animals that had never seen the natural canopy (Pfeiffer et al., 2005). This finding suggests that a basic tuning to polarized light is genetically determined, but that the diurnal changes in tuning are learned by the animals during developmental experience of the natural sky.

METHODS

Electrophysiology

Experiments were performed on adult, gregarious locusts *(Schistocerca gregaria)* from our laboratory colonies. Animals were raised in a greenhouse with clear glass that transmitted the natu-

ral polarization pattern of the sky. We recorded intracellularly with sharp microelectrodes from neuronal processes in the vicinity of the anterior optic tubercle. Some of the cells were injected with Neurobiotin (Vector Laboratories, Burlingame, UK) and later stained with Cy3 conjugated to Streptavidin (Amersham Buchler, Brunswick, Germany) in wholemount preparations. The three cell types were discriminated either by their morphology or by their spiking patterns and response properties. LoTu1 neurons could be distinguished from the other two types by their low background activity and response to polarized light that does not contain an inhibitory part. TuTu1 and TuLaL1b neurons were discriminated by their spiking patterns. We calculated inter-spike interval (ISI) histograms for the response to one revolution of the polarizer. TuLAL1b neurons spiked regularly at both low and high frequencies resulting in ISI histograms with a distribution that was rather symmetric around the maximum. TuTu1 neurons exhibited a bursty spiking behavior especially at high discharge rates which results in higher numbers of short ISIs than long ones. Thus the histogram shows a steep initial slope and a peak that is considerably shifted to the left with respect to the mean of all occurring ISIs.

All but one LoTu1 and one TuTu1 neuron had their perikarya in the left brain hemisphere as judged either by their morphology or by the absence of EPSPs (Pfeiffer et al., 2005). To integrate the data of the two neurons with their soma in the right hemisphere into Fig. 3, we mirrored their Φ_{max} values at the midline. Thus for the LoTu1 neuron, Φ_{max}POL became 151° (originally 29°) and Φ_{max}green became 80° (originally 280°). For the TuTu1 neuron Φ_{max}POL became 142° (originally 38°) and Φ_{max}green became 316° (originally 44°). For details on preparation and electrophysiology see (Pfeiffer et al., 2005).

Stimulation

Polarized light stimuli were presented dorsally, by passing the light of a blue LED (Luxeon LED emitter, LXHL-BB01, 1 W, 470 nm, Philips Lumileds Lighting Company, San Jose, California, USA) through a polarizer (HN38S, Polaroid, Cambridge, MA, USA) rotating at 30°/s. The angular size of the stimulus was 6.6° with an irradiance of 12 µW/cm^2.

Unpolarized green (530 nm) and UV (350 nm) light stimuli of equal photon flux (9.2 · 10^{13} photons·cm^{-2}·s^{-1}) were produced by passing light from a xenon arc lamp (XBO 150 W) through interference filters, a neutral density wedge and a quartz lightguide. The stimuli appeared to the animal as discs of 16.3° diameter that moved in a circular path (30°/s) around the center of the head at an elevation of 45°.

Data evaluation

Spike trains were digitzed with a CED 1401 plus (Cambridge Electronic Design Limited, Cambridge, Great Britain) at 25 kHz and processed using a spike2 script. Spike times were evaluated via threshold detection and converted to angles according to the position of the stimulus at the time of each spike. The preference angle (Φ_{max}) was found by calculating the mean of the angles during one to six revolutions of the stimulation device, using the trigonometric functions methods (Batschelet, 1981). Neurons were regarded sensitive to a stimulus if the distribution of angles differed significantly from randomness (Rayleigh test, α=0.05, using Oriana 2.02b, Kovach Computing Services, Anglesey, UK).

For each recording, the angular distance between the Φ_{max} value obtained from stimulation with polarized light and the Φ_{max} value obtained from stimulation with unpolarized, green light was calculated and plotted against the time of day of the recording. Data were binned into 72 min bins and the means of the absolute angles within each bin were plotted against the bin centers. To fit these data, we used two sets of formulas. The first describes the solar ephemeris

function and depends on geographical coordinates and the date. The second calculates the angle between the solar azimuth and a great circle through an observed point and the sun (see Fig. 1). The latter set of formulas depends on the coordinates of the sun and the observed point. The solar azimuth was set to 0°, hence the azimuth of the observed point is equal to the angle between the solar and the visual azimuth.

Statistics

The Rayleigh test of uniformity is a circular statistics test (Batschelet, 1981). It is used calculate the probability of the null-hypothesis that a given sample of angles is distributed in a uniform manner. When the null-hypothesis is rejected, the distribution of angles shows significant directedness.

Competing interests statement The authors declare that they have no competing financial interests.

References

Batschelet, E. (1981). Circular Statistics in Biology. Academic Press, 111 Fifth Ave., New York, NY 10003, 1981, 388.

Brines, M. L. & Gould, J. L. (1982). Skylight Polarization patterns and Animal Orientation. J Exp Bio, 96, 69.

Coemans, M. A., Vos Hzn, J. J., & Nuboer, J. F. (1994). The relation between celestial colour gradients and the position of the sun, with regard to the sun compass. Vision Res, 34, 1461–70.

Homberg, U. (2004). In search of the sky compass in the insect brain. Naturwissenschaften, 91, 199–208.

Homberg, U., Hofer, S., Pfeiffer, K., & Gebhardt, S. (2003). Organization and neural connections of the anterior optic tubercle in the brain of the locust, Schistocerca gregaria. J Comp Neurol, 462, 415–30.

Homberg, U. & Paech, A. (2002). Ultrastructure and orientation of ommatidia in the dorsal rim area of the locust compound eye. Arthr Struct Develop, 30, 271–280.

Labhart, T. & Meyer, E. P. (2002). Neural mechanisms in insect navigation: polarization compass and odometer. Curr Opin Neurobiol, 12, 707–14.

Labhart, T., Petzold, J., & Helbling, H. (2001). Spatial integration in polarization-sensitive interneurones of crickets: a survey of evidence, mechanisms and benefits. J Exp Biol, 204, 2423–30.

Pfeiffer, K., Kinoshita, M., & Homberg, U. (2005). Polarization-sensitive and light-sensitive neurons in two parallel pathways passing through the anterior optic tubercle in the locust brain. J Neurophysiol, 94, 3903–15.

Rossel, S. & Wehner, R. (1984). Celestial orientation in bees: the use of spectral cues. J Comp Physiol, 155, 605–613.

Wehner, R. (1982). Himmelsnavigation bei Insekten. Neurophysiologie und Verhalten. Neujahrsbl Naturforsch Ges, 184, 1–132.

Wehner, R. (1997). The ant's celestial compass system: spectral and polarization channels. (Basel: Birkhäuser).

SUPPORTING ONLINE MATERIAL

Calculations

Symbols and abbreviations (in order of appearance)

- **EOT**: Equation of time

- **B**: a coefficient within the EOT

- **n**: daynumber (January 1st =1, January 2nd =2 ...)

- **LAT**: local apparent time

- **LT**: local time (expressed as a fraction of one day)

- **λ**: longitude (geographical)

- **HA**: hour angle

- **α_s**: elevation of the sun

- **φ**: latitude (geographical)

- **φ_s**: azimuth of the sun

- **α_o**: elevation of an observed point in the sky

- **φ**: azimuth of an observed point in the sky

Calculation of the solar elevation   To calculate the solar elevation, we first calculated the equation of time (EOT). The EOT is the difference between local apparent time (that can be determined by a sundial) and local time (time determined by a clock). The equation of time results from the obliquity of the earth' s axis and from the elipticity of its orbit around the sun.

$$EOT = 229.2 \cdot ((0.000075 + (0.001868 \cdot cos(B)) - (0.032077 \cdot$$
$$\cdot sin(B)) - (0.014615 \cdot cos(2B)) - 0.04089 \cdot sin(2B))) \tag{1}$$

with
$$B = ((n - 1) \cdot (360/365)) \tag{2}$$

Next the local apparent time (LAT) is calculated. In the following equation, LAT is calulated for the timezone of Marburg (GMT + 1h).

$$LAT = (LT + (4 \cdot (\lambda - 15) + EOT)/24/60) \cdot 24 \tag{3}$$

The declination δ is the angle between the plane of the earth equator and the sun at local noon. It can be calculated as:

$$\delta = 23.45 \cdot sin(360 \cdot (284 + n)/365) \tag{4}$$

The hour angle (HA) is the angular distance between the sun and the local meridian.

$$HA = -1 \cdot (180 - LAT \cdot 15) \tag{5}$$

With the results from the above equations, we can calculate the elevation of the sun (α_s) as:

$$\alpha_s = \arcsin(\sin(\delta) \cdot \sin(\varphi) + \cos(HA) \cdot \cos(\delta) \cdot \cos(\varphi)) \tag{6}$$

The above equations were taken from Duffie & Beckman (1987). To control the accuracy of our calculations, we compared our results to data from the U.S. naval Observatory homepage (aa.usno.navy.mil). For the given parameters (June 24, 23.4° N, 6.53° E) no difference is visible (Supplementary Fig. 1).
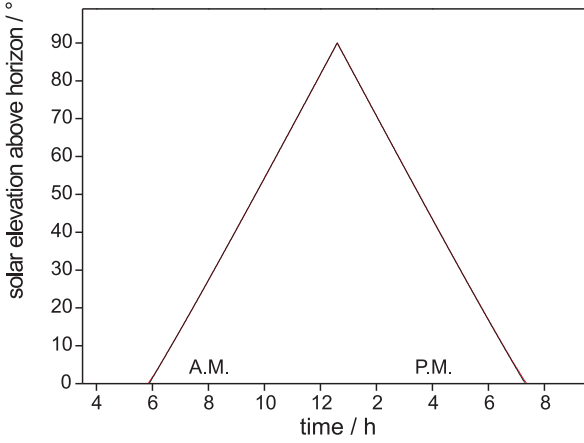
Supplementary Figure 1: Course of solar elevation during June 24 at 23.4° N, 6.53° E. Data calculated with the formulae given above (black) and obtained from the U.S. naval Observatory homepage (aa.usno.navy.mil, red) are plotted on top of each other.

Calculation of the E-vector orientation (Φ) Let α_s be the elevation of the sun and φ_s be the azimuth of the sun.

Then we can calculate the vector $\vec{s}$ of the solar direction as

$$\vec{s} = \begin{pmatrix} s_1 \\ s_2 \\ s_3 \end{pmatrix} = \begin{pmatrix} \sin(90° - \alpha_s) \cdot \cos(\varphi_s) \\ \sin(90° - \alpha_s) \cdot \sin(\varphi_s) \\ \cos(90° - \alpha_s) \end{pmatrix} \tag{7}$$

Let (α_o and φ_o) be the elevation and the azimuth of an observed point in the sky. Then analogous to 7, we get for the vector $\vec{o}$ of the observed point:

$$\vec{o} = \begin{pmatrix} o_1 \\ o_2 \\ o_3 \end{pmatrix} = \begin{pmatrix} \sin(90° - \alpha_o) \cdot \cos(\varphi_o) \\ \sin(90° - \alpha_o) \cdot \sin(\varphi_o) \\ \cos(90° - \alpha_o) \end{pmatrix} \tag{8}$$

According to the single scattering Rayleigh model, the E-vector $\vec{e}$ is perpendicular to the direction of the sun and to the direction of the observed point. Thus it can be calculated as the vector product of $\vec{s}$ and $\vec{o}$:

$$\vec{e} = \vec{s} \times \vec{o} \tag{9}$$

$$\begin{pmatrix} e_1 \\ e_2 \\ e_3 \end{pmatrix} = \begin{pmatrix} s_1 \\ s_2 \\ s_3 \end{pmatrix} \times \begin{pmatrix} o_1 \\ o_2 \\ o_3 \end{pmatrix} = \begin{pmatrix} s_2 \cdot o_3 - s_3 \cdot o_2 \\ s_3 \cdot o_1 - s_1 \cdot o_3 \\ s_1 \cdot o_2 - s_2 \cdot o_1 \end{pmatrix} \tag{10}$$

By backtransformation from the vector coordinates, the E-vector orientation Φ can be calculated as:

$$\Phi = \arctan\left(\frac{e_2}{e_1}\right) \tag{11}$$
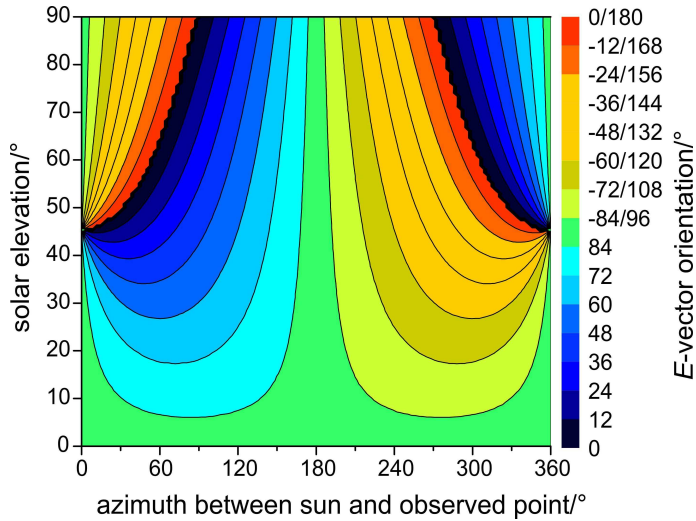
Supplementary Figure 2: *E*-vector orientation (colour coded) as a function of horizontal viewing direction (x-axis) and solar elevation (y-axis), calculated for 45.4° elevation of the viewing direction. At low elevations of the sun and around the antisolar azimuth (180°) *E*-vectors are oriented approximately perpendicular to the solar azimuth (green).

Linearity of E-vector changing rates At different angular distances from the sun, changes in E-vector orientation in the course of the day differ considerably (Fig. 1b main article, Supplementary Fig. 3a). In the vicinity of the sun, the changing rates are highly nonlinear. At 90° from the sun, the linearity of the changing rate is highest (Supplementary Fig. 3b). The slope of linear fits through the functions in Supplementary Fig. 3b (not shown) decreases with increasing distance from the sun. Obviously an adjustment of the neurons that eliminates a mismatch between sun information and E-vector information is only possible for one azimuthal angle to the sun.
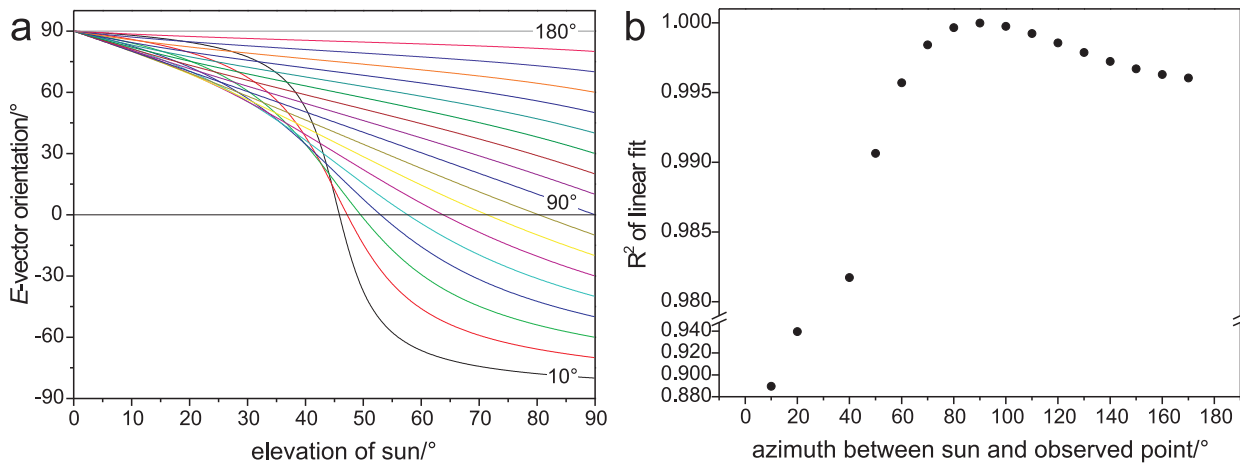
Supplementary Figure 3: a *E*-vector orientation as a function of solar elevation, calculated for 45.4° elevation of the viewing direction. Each graph shows the *E*-vector orientations for a certain azimuth between the sun and the observed point (10° to 180°). In the vicinity of the sun changes in *E*-vector orientation are highly nonlinear in relation to the solar elevation. **b** R^2 (coefficient of determination) for linear fits through the graphs shown in **a** (fitlines not shown). At a viewing angle of 90° from the sun, the *E*-vector orientation changes as a linear function of solar elevation.

References

Duffie, J. A. & Beckman, W. A. (1987). Sonnenenergie: Thermische Prozesse. (Bauverlag, Gütersloh).

Performance of polarization-sensitive interneurons of the anterior optic tubercle in the locust brain at different degrees of polarization

Performance of polarization-sensitive interneurons of the anterior optic tubercle in the locust brain at different degrees of polarization

Keram Pfeiffer and Uwe Homberg

Department of Biology, Animal Physiology, University of Marburg, Marburg, Germany

Correspondence should be addressed to U.H. (Homberg@staff.uni-marburg.de)

In the natural sky, light is partly polarized with *E*-vectors arranged in concentric circles around the sun. Organisms that perceive this pattern are able to use it as a reference for spatial orientation. Intracellular recordings have analyzed polarization-sensitive neurons in several insect species. In most of these studies, however, the stimulation was carried out using nearly totally polarized light with the degree *(d)* of polarization close to 1. In contrast, *d* in the natural sky is usually well below 0.75. To study polarization-sensitive interneurons under more natural conditions, we investigated the influence of *d* on the responses of two identified neurons from the locust brain. Both neurons, termed LoTu1 and TuTu1 interconnect the anterior optic tubercles in the midbrain. We show that both neurons signal *E*-vector directions down to *d*-values of 0.3. With decreasing *d*, the neurons were increasingly inhibited by the unpolarized light component of the stimulus. We conclude that even under optimal sky-light conditions, a circular area of about 100° in diameter around the sun does not provide useful *E*-vector information to the neurons. We suggest that these restrictions serve to exclude the procesing of *E*-vector information by the neurons that is in conflict with direct sunlight information.

During its way from the sun to the earth, light is scattered by gas molecules and particles in the atmosphere and thus becomes partly polarized. As a result of this scattering, the sunlit sky shows a pattern of polarization, that can be described in approximation by the single scattering Rayleigh model (Strutt, 1871). According to Rayleigh scattering, *E*-vectors are oriented tangentially to concentric circles around a point light source. The degree of polarization, i.e. the percentage of light that is linearly polarized, increases from the unpolarized light source (degree of polarization, *d*=0) to a maximum of totally linearly polarized light at an angle of 90° away from the light source (*d*=1). The sky-light polarization pattern differs in several respects from the pattern described by the Rayleigh model and depends critically on meteorological conditions. The closest approximation between the Rayleigh model and the natural sky occurs on cloudless days, especially at low solar elevations. Under these conditions the degree of polarization can be up to *d*=0.75 (Brines & Gould, 1982). *E*-vector orientation is reasonably well described by the Rayleigh model, while the degree of polarization is heavily reduced by clouds (Pomozi et al., 2001; Suhai & Horváth, 2004).

Many insect species have evolved the ability to perceive the sky polarization pattern (reviewed by Horváth & Varjú 2004). Behavioral exper-

iments have demonstrated the ability of bees, ants, flies, crickets, locusts, and dung beetles to orient themselves using polarized light information (von Frisch, 1949; Wehner, 2003; von Philipsborn & Labhart, 1990; Brunner & Labhart, 1987; Mappes & Homberg, 2004; Dacke et al., 2004). All of these species possess a specialized dorsal part of the compound eye, the dorsal rim area, that is highly adapted for the perception of polarized light (Labhart & Meyer, 1999; Homberg & Paech, 2002; Dacke et al., 2003). In bees, ants, crickets and locusts it was also shown that the dorsal rim area is necessary for the E-vector-dependent behavior (Wehner, 1982; Wehner & Strasser, 1985; Fent, 1985; Brunner & Labhart, 1987; Mappes & Homberg, 2004).

Intracellular recordings from the brain of several insect species (cricket: Labhart (1988); ant: Labhart (2000); cockroach: Loesel & Homberg (2001); locust: Homberg (2004)) have demonstrated neurons that respond to stimulation with linearly polarized light. The POL1 neurons from the medulla of crickets are the best-studied of these polarization-sensitive interneurons. POL1 neurons are largely insensitive to stimuli other that polarized light and thus are pure analyzers of E-vector orientation. The cells are capable of signaling E-vector orientation down to d-values of 0.05 (Labhart, 1996).

In the anterior optic tubercle of desert locusts, two neurons have been analyzed that can be termed solar azimuth analyzers (Homberg et al. (2003); Pfeiffer et al. (2005); KP, UH, in preparation). The lobula-tubercle neuron (LoTu1) and the tubercle-tubercle neuron (TuTu1) are sensitive to the position and wavelength of an unpolarized light spot and concurrently to the E-vector orientation of a polarized light stimulus. The response properties of these neurons suggest that they extract the solar azimuth from the UV/green contrast, the intensity of the skylight, and, in adddition, from its pattern of polarized light (M. Kinoshita, KP, UH, in preparation; KP, UH, in preparation).

The angle between E-vector orientation and solar azimuth is only constant along the solar meridian, the great circle through the sun and the zenith. At other points in the sky it depends on solar elevation and on the azimuth between the observed point and the sun. In the vicinity of the sun, E-vector orientations exhibit the highest variability and thus might provide ambiguous information. In the present study, we have investigated the influence of the degree of polarization of a polarized-light stimulus on the spiking activity of LoTu1 and TuTu1 neurons in the locust. We show that both neurons signal E-vector orientations down to degrees of polarization of $d=0.3$. In addition, the data provide further evidence for specific interactions of polarization-sensitive and -insensitive input channels to both cell types.

RESULTS

This study is based on 20 intracellular recordings from neurons with ramifications in the anterior optic tubercle. Most of the data were obtained from the neuron types LoTu1 (n=9) and TuTu1 (n=8). These neurons have large neurites of up to 6 μm in diameter. Neurons of the AOTu-LAL tract that connects the anterior optic tubercle (AOTu) with the lateral accessory lobe (LAL) have much smaller fiber diameters and were only encountered three times (TuLAL1a: n=1, TuLAL1b, n=2). These neurons showed similar responses to varying d-values as the other two types, but were not analyzed further due to the small number of observations. All cell types have been characterized before and could be distinguished on the basis of their physiology (Pfeiffer et al. (2005); KP, UH, in preparation). The neurons are part of the anterior polarization vision pathway that connects the polarized-light sensitive photoreceptors of the dorsal rim area of the compound eye with the central complex in the locust midbrain (Homberg et al., 2003). LoTu1 and TuTu1 neurons cross the midline of the brain and interconnect both anterior optic tubercles. LoTu1 has additional ramifications in the anterior lobe of both lobulae. The degree of polarization (d-value) used for stimula-
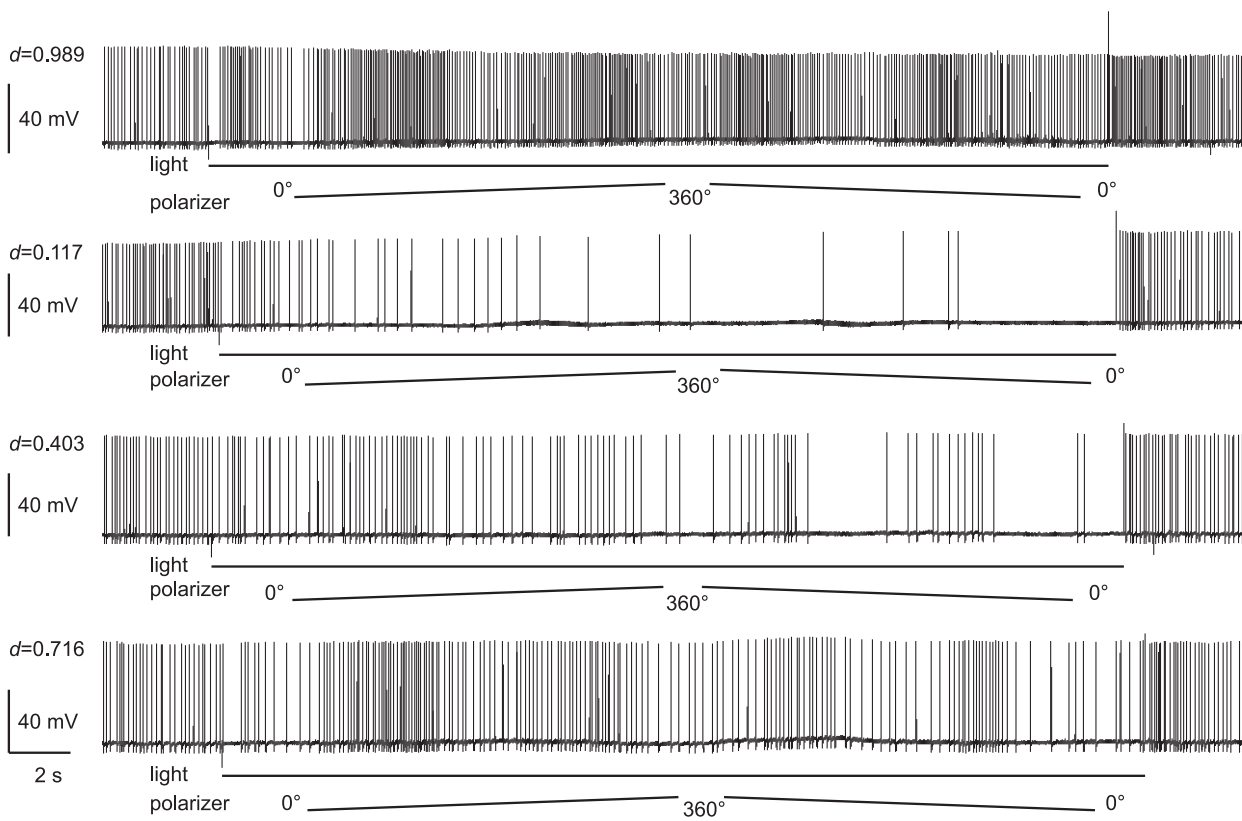
Figure 1: Responses of a LoTu1 neuron to four different degrees of polarization. The duration of the polarized light stimulus *(light)* is indicated by a bar. The rotation of the polarizer *(polarizer)* is indicated by ramps. Angles *(0°, 360°)* indicate the orientation of the polarizer rather than *E*-vector orientation which is shifted due to the retarder (see Methods). The modulation of the neuron's activity strongly depends on the degree of polarization. At low *d*-values, the neuron is inhibited irrespective of *E*-vector orientation. Negative and positive artifacts at light on and off result from voltage peaks that occured during switching of the LED. Recording traces appear in chronological order.

tion ranged from 0.06 to 0.991. In half of the preparations we were able to stimulate the same neurons with at least four different degrees of polarization.

General observations

In both LoTu1 and TuTu1 neurons, we observed two effects of the degree of polarization on spiking behavior. First, at high *d*-values, the amplitude of spike activity modulation was higher than at low *d*-values (Figs. 1, 2) and second, the mean spiking activity during stimulation was higher at high *d*-values (Fig. 3). In LoTu1 neurons, the mean spiking rate gradually decreased

with falling *d*-values (Fig. 3A) and dropped below background level at the lowest degrees of polarization. In TuTu1 neurons the mean spiking rate remained rather constant between *d*=0.06 and *d*=0.68, but strongly increased at the highest *d*-values (Fig. 3B).

Quantification of the response strength

To quantify the response strength, we used the response value *R* that was introduced by (Labhart, 1996). To calculate *R*, spikes were counted within 18 subsequent bins of 20° width during a 360° rotation of the polarizer. Then the mean number of spikes throughout the 18 bins was calculated. *R* is the sum of differences between
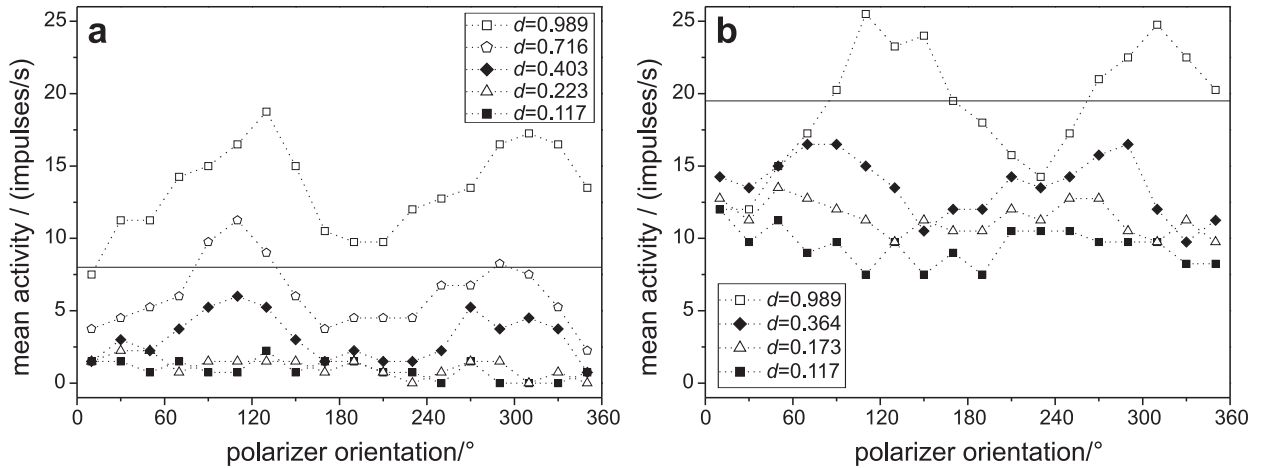
Figure 2: *E*-vector response curves from the recordings of the LoTu1 neuron shown in Fig. 1 and from a TuTu1 neuron. Data points show mean activity within 20° bins. Different symbols denote different degrees of polarization *(d)*. Solid lines indicate background activity in darkness. Both the response amplitude and the overall activity depend on the degree of polarization. (a) LoTu1 neuron. At *d*=0.989, the cell is excited above background level at all *E*-vector orientations. With falling *d*-values, the cell is increasingly inhibited even at the preferred *E*-vector orientation. (b) TuTu1 neuron. At *d*=0.989 the activity of the neuron is modulated around the background level. Similar to LoTu1, the overall activity of TuTu1 becomes lower at low degrees of polarization, but remains higher than that of LoTu1 at all levels of *d*.
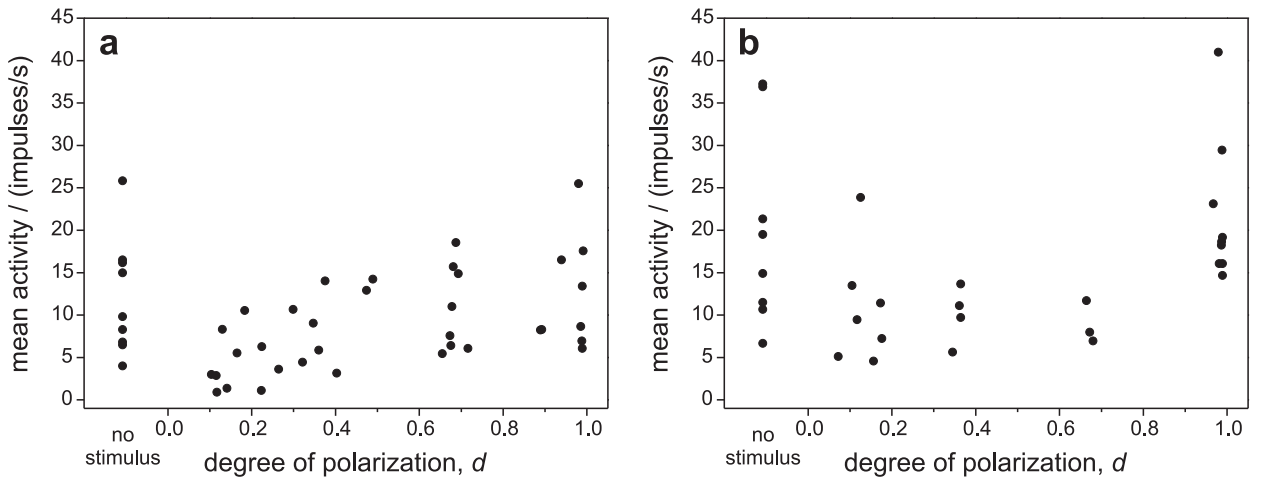
Figure 3: Mean spiking activity of LoTu1 and TuTu1 neurons at different degrees of polarization. Spikes during stimulation were counted and divided by the stimulus duration. Data points at no stimulus show mean spiking activity during 12 s of darkness. (a) LoTu1 neurons are inhibited by low degrees of polarization and gradually increase their spiking activity above background level with increasing degree of polarization. (b) TuTu1 neurons maintain rather constant spiking activity throughout a wide range of *d*-values. At the highest degree of polarization, however, spiking activity increased considerably.

the mean spike counts and the individual spike counts within the bins. Hence, R is a measure of the amplitude of spike frequency modulation.

In all recordings R depended on the degree of polarization. With increasing degree of polar-
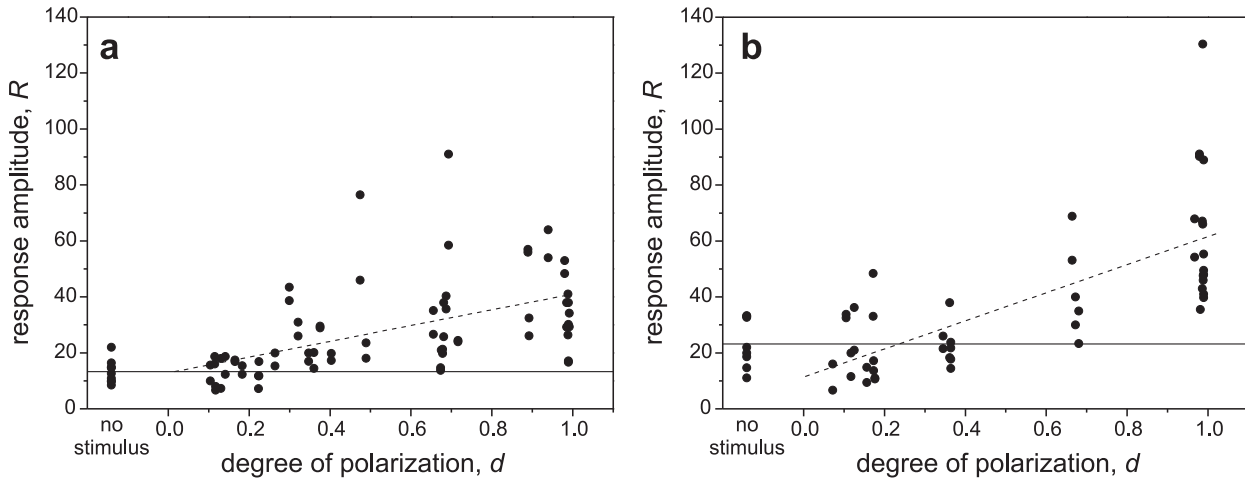
Figure 4: Response amplitude R (see text for definition) as a function of the degree of polarization. Data points are from single 360° rotations of the polarizer. At no stimulus, data points show activity during 12 s of darkness. Solid lines: mean background activity at darkness (no stimulus). Dotted lines: linear regressions through the stimulus data. In both LoTu1 neurons (a) and TuTu1 neurons (b) the response amplitude R is linearly dependent on the degree of polarization. The slopes of the fitting lines indicate that TuTu1 neurons (b), ($R = 50.2 \cdot d + 11.3$, $R^2 = 0.521$ are more sensitive to changes in the degree of polarization than LoTu1 neurons (a), ($R = 28.1 \cdot d + 12.9$, $R^2 = 0.279$).

ization, the response amplitude of the neurons, and thus R, became larger (Fig. 4). For recordings, in which at least four degrees of polarization were tested, we fitted straight lines through the d/R plots (not shown). In all cases we found a high degree of linearity. The mean of the coefficients of determination (R^2) from the linear fits was 0.891 (n=10, SD=0.114). Though all recordings exhibited a linear relation between the degree of polarization *(d)* and the response value R, the slope of the fitting lines differed considerably between individuals, which partly explains the scatter in Fig. 4. Another factor contributing to scatter is inter-individual differences in overall response strength (i.e., the y-intercept of the fitting lines). To investigate possible differences in the responsiveness of LoTu1 and TuTu1 neurons, we calculated linear regressions through all response values of the respective types of neuron (Fig. 4, see figure legend for equation of the fits). The slopes of both fits differed considerably, indicating that TuTu1 neurons (slope of fit = 50.2) were more sensitive to changes in d than LoTu1 neurons (slope of fit = 28.1). As indicated by the different slopes of

the fitting lines, the dependency between d and R is significantly different in LoTu1 and TuTu1 (ANCOVA, $F_{1,112}$=6.30, p=0.014).

The response value R is a measure of spike frequency modulation. It does not provide information about the directedness of the response i.e. whether the frequency modulation is correlated with the stimulus orientation. This information is provided by the length of the mean vector r (see methods for details on R and r). It is a measure of the concentration of angles around the mean E-vector tuning angle Φ_{max}. If spiking frequency fluctuates randomly, r is small, but if spiking modulation is elicited by the rotating E-vector, and thus depends on its orientation, r is larger. Fig. 5 shows the length of the mean vector r, calculated from subsequent right and left 360°-rotations, as a function of d. Like the response value R, the length of the mean vector r depends on the degree of polarization (linear fit, $R^2 = 0.264$, ANOVA $F_{1,58}$=20.5, p<0.0001). Comparison of the r-values of LoTu1 and TuTu1 neurons revealed no significant difference between the two groups (ANCOVA, $F_{1,64}$ = 0.023, p=0.881).

Threshold

To determine the degree of polarization that is necessary to obtain a spike response that shows significantly more directedness than the control (spiking activity during 12 s of darkness), we grouped the r-values obtained during stimulation into five groups of d-values (group 1: 0.72 - 0.183, group 2: 0.223 - 0.347, group 3: 0.360 - 0.489, group 4: 0.655 - 0.716, group 5: 0.889 - 0.991, Fig. 5). In an ANOVA the groups were compared pairwise (Tukey's Post Hoc test, α=0.05). Groups three to five differed significantly from the control group. Therefore, the threshold sensitivity lies between d=0.285 and d=0.425 (centers of groups 2 and 3). Due to the grouping of values, this calculation provides only a gross estimate of threshold.

A more precise estimate of threshold sensitivity is provided by comparing the mean vector length r obtained during stimulation, with the upper 95% confidence limit of r obtained without stimulation (Fig. 5). For d-values above 0.3, all r-values exceed the upper 95% confidence limit of the dark control. This indicates the ability of the neurons to discriminate E-vector orientations down to d-values of 0.3.

Coding reliability

To test how consistent E-vector signaling is between repetitions of the same stimulus, we calculated Φ_{max} values (see methods for definition) for the two subsequent 180° rotations during a 360° revolution of the polarizer. For clockwise rotations the difference angle $\Delta\Phi_{max}$ was calculated as $\Phi_{max}(180°$ to $360°)$-$\Phi_{max}(0°$ to $180°)$. For counterclockwise rotations $\Delta\Phi_{max}$ was calculated as $\Phi_{max}(360°$ to $180°)$-$\Phi_{max}(180°$ to $0°)$. As expected, the angular deviation (Fig. 6) of $\Delta\Phi_{max}$ varies with the degree of polarization. At small d-values below 0.2, $\Delta\Phi_{max}$ covers nearly the whole possible range between - 90° and 90°. As indicated in Fig. 6, we classified the $\Delta\Phi_{max}$ values into five groups. To test which of the distributions of $\Delta\Phi_{max}$ angles are significantly different, we used the Mardia-

Watson-Wheeler Test (Mardia & Jupp, 2000). This is a non-parametric test that determines whether two or more distributions of angles are identical. The control group 5 (d=0.889 to 0.991) differed significantly from the two groups of low polarization (group 1: d=0.72 to 0.183, W=11.634, p=0.003, group 2: d= 0.223 to 0.347, W=9.909, p=0.003). The distribution of $\Delta\Phi_{max}$ values within groups 3 (d=0.36 to 0.489) and 4 (d=0.655 to 0.716) did not differ significantly from that of group 5. Thus, the accuracy of E-vector coding does not change significantly down to d-values around 0.425 (center of group 3).

Theoretical considerations

Given a sensitivity threshold for polarized light around $d = 0.3$, it is possible to estimate the minimum angular distance of a patch of sky from the sun that is required to provide detectable polarization information for the neurons studied here. According to the single scattering Rayleigh model (Coulson, 1988), the dependency between the angular distance θ from a light source and the degree of polarization (d) is:

$$d = \frac{1 - \cos^2 \cdot \theta}{1 + \cos^2 \cdot \theta}$$

The d-values calculated with this term lie between 0 and 1. The highest degrees of sky-light polarization measured in a polarimetry study, however, did not exceed d-values of 0.75 (Brines & Gould, 1982). To account for this we multiplied the term with 0.75. The resulting graph is shown in Fig. 7. The gray rectangle under the curve describes the area around the sun at which LoTu1 and TuTu1 neurons are not able to discriminate E-vector orientations. With an estimated threshold of $d = 0.3$, the angular extent of the E-vector blind area around the sun can be calculated by resolving the equation

$$0.3 = 0.75 \cdot \frac{1 - \cos^2 \cdot \theta}{1 + \cos^2 \cdot \theta}$$

The angle θ then becomes 49.1. This means that a circular area of approximately 100° in diameter
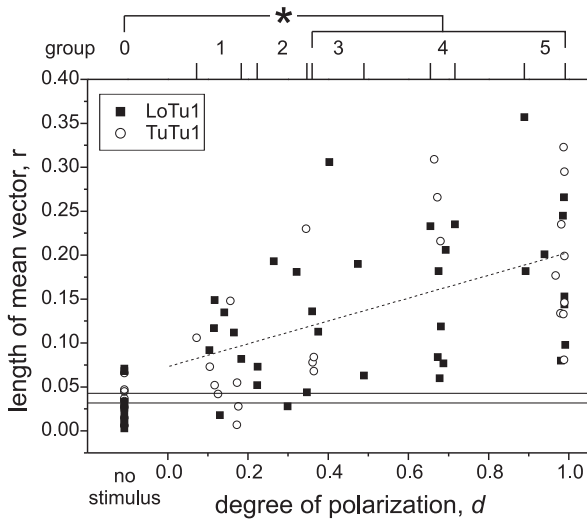
Figure 5: Directedness of the neuronal responses measured by the length of the mean vector r (see text for details). Directedness increases in both types of neuron with increasing degree of polarization. Data points were obtained by calculating the mean vector of the angles of the polarizer at which spikes occurred during a right and a left rotation. Data at no stimulus were calculated identically for 12 s of darkness. Solid lines indicate the mean and the upper 95% confidence limit of the no stimulus data. Dotted line shows the linear regression through the stimulus data ($r = 0.13 \cdot d + 0.07$, $R^2 = 0.264$). Groups of d-values used for statistics are indicated on top of the plot. Groups three to five differed significantly from the no stimulus group (ANOVA, Tukey's Post Hoc test, $\alpha = 0.05$).
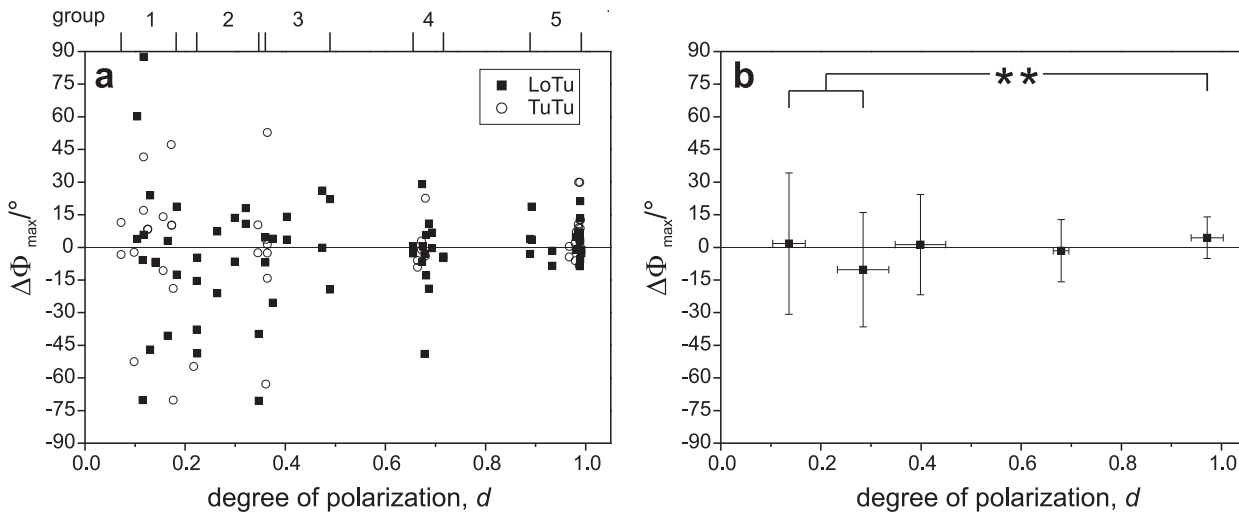
Figure 6: Reliability of E-vector coding. Difference of the preferred E-vector angle ($\Delta\Phi_{max}$) in two subsequent 180° rotations of the polarizer. (a) Raw data. Each symbol indicates one $\Delta\Phi_{max}$ value. Five ranges that have been used to calculate the data in (b) are indicated on top of the plot. (b) Means and standard deviations of the data points within each group (group ranges indicated on top of a). The distribution of angles in group 5 differed significantly from those in groups 1 (p=0.003) and 2 (p=0.007) but not from those in groups 3 (p=0.569) and 4 (p=0.191, Mardia-Watson-Wheeler test).

around the sun does not provide useful E-vector information to the neurons.

DISCUSSION

We investigated the response properties of two identified neurons of the anterior optic tubercle in the locust brain at different degrees of polarization (d). Like most polarization-sensitive interneurons, LoTu1 and TuTu1 neurons show a sinusoidal modulation of spike frequency with a periodicity of 180° when stimulated with linearly polarized light with rotating E-vector. Two major effects on this response pattern were observed when d was reduced: (i) The amplitude of the polarization response decreases linearly
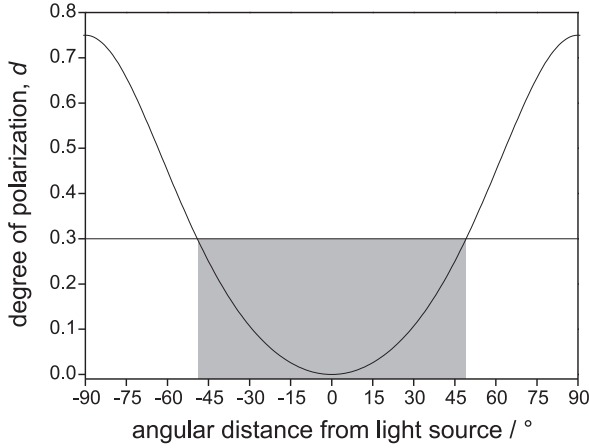
Figure 7: Theoretical distribution of the degree of polarization as a function of distance from a light source, calculated using the single scattering Rayleigh model (adjusted by a factor of 0.75, see results). The horizontal line indicates the threshold for E-vector signaling in LoTu1 and TuTu1 neurons. The gray rectangle shows the theoretical area around the sun at which these neurons are not able to extract E-vector information from the skylight. The E-vector-blind area is a circle of approximately $100°$ in diameter around the sun.

with decreasing d-values and shows a threshold around $d = 0.3$, and (ii) with decreasing d-values, an increasing tonic inhbition becomes apparent during stimulation. These results suggest that LoTu1 und TuTu1 neurons integrate two kinds of visual input. A set of orthogonal E-vector analyzers leads to the sinusoidal modulation of the response, while an apparently polarization-insensitive visual input provides a tonic inhibition.

Quantification of the response strength

The response value R was introduced by Labhart (1996) to quantify the response strength of POL1 neurons in crickets to polarized light. The POL1 neurons studied by Labhart showed high spiking rates of up to 100 impulses/s at Φ_{max} and total inhibition around Φ_{min} resulting in R-values of up to 200 and above, when the degree of polarization was $d=1$. In the recordings presented in this study, we found maximum spiking rates between 25 and 50 impulses/s and no total inhibition around Φ_{min}, i.e. smaller modulations of spike frequency. The maximum R-value we observed was 130 but usually, it ranged around 60 in TuTu1 and 40 in LoTu1 for d-values close to 1. Two problems become apparent when using the R-value for threshold detection: (i) Its maximal possible value (R_{max}) depends on the number of bins (n) and on the mean activity (A_{mean}), since $R_{max} = 2 \cdot A_{mean} \cdot (n - 1)$,

and (ii) R is sensitive to spontaneous fluctuations in spiking activity. These two features of R render it unsuited to determine the response threshold of the neurons presented here. However, the R-value is well suited to describe the influence of the degree of polarization on spike frequency modulation. Both the LoTu1 and TuTu1 neurons exhibit less activity during stimulation with low d-values than in darkness. Spiking activity in darkness is not very regular. At low d-values, the response R can, therefore, be lower than in the dark control, despite obvious polarization sensitivity, i.e. spike frequency modulations with a $180°$ periodicity.

The length of the mean vector r is sensitive to the distribution of angles (i.e. spike times) and always covers the same range between 0 and 1. Thus it is well suited to compare spike activity during darkness and stimulation. While spontaneous fluctuations in spike frequency have minor influence on r as long as they occur randomly, E-vector-coupled variations in spike frequency with a $180°$ periodicity will lead to larger r-values. Thus r can be used as a measure of directedness of a neuronal response to a periodic stimulus. It is especially suited to compare the undirected background spiking activity with the directed responses to a stimulus.

Coding reliability

Coding reliability is comparable between the different degrees of polarization, but not between different stimulus conditions. The accuracy by which Φ_{max} can be calculated, not only depends on the actual accuracy of neural signaling, but also on the number of action potentials that occur during the rotation of the polarizer. Thus the overall activity of the neuron matters as well as the velocity of polarizer rotation. The former depends on the individual neuron, but the latter can be influenced by the experimenter. Due to the limited time during intracellular recordings, we had to find a compromise between the number of different stimuli (d-values) we tested in a recording and the accuracy at which we could measure the responses. Therefore, we rotated the polarizer at $30°$/s which allowed us to stimulate at five different d-values within a recording period of four minutes. The coding reliability we measured under these circumstances was given by the deviation of Φ_{max} in two subsequent $180°$ rotations of the polarizer. At the highest degrees of polarization we found a mean angular deviation of $\pm\ 9.5°$. This was taken as the best possible performance and compared to four other groups of lower d-values, which resulted in the same threshold as the measurements discussed below.

The coding reliability of LoTu1 and TuTu1 under the above stimulus conditions is rather poor. The system as a whole might compensate this by two mechanisms. As discussed later, LoTu1 and TuTu1 neurons employ various sky-light cues to detect the solar azimuth. This co-processing of sky-light color and intensity and the associated increase in fidelity might greatly improve the performance under natural conditions, compared to the artificial stimulation regime of polarized light alone. In addition, the signal to noise ratio might be improved by population coding at later stages, presumably in the central complex.

Natural sky-light polarization

The single scattering Rayleigh model describes the polarization pattern in an ideal atmosphere in which all particles are smaller than the wavelength of the light and in which each ray of light (emitted by a point source) is only scattered once. As a result, E-vectors would be oriented perpendicular to a great circle through the observed point in the sky, the sun and the observer and the degree of polarization would increase from 0 (direct light) to 1 at $90°$ from the sun. Since neither of the prerequisites of the Rayleigh model is truly fulfilled for the sky-polarization pattern, it differs considerably from theory. While the orientation of E-vectors in the sky is rather well described by the Rayleigh model (Suhai & Horváth, 2004), the degree of polarization lies usually below 0.75 (Brines & Gould, 1982) and its distribution can differ considerably when disturbed by clouds (Pomozi et al., 2001). This makes it an unreliable source of information and experiments in honeybees have, indeed, shown that E-vector orientation rather than degree of polarization is the relevant cue for the animal (Brines & Gould, 1979; Rossel & Wehner, 1984). However, sensitivity to different degrees of polarization might be important to exclude parts of the sky from influencing the calculation of solar azimuth (as discussed below).

Response threshold

We determined the threshold d-value for the polarization response of the neurons in two different ways. The statistical method (ANOVA, Tukey's Post Hoc test) is objective but due to the grouping of the data results in a large range rather than a single threshold value. The second method (estimation from the confidence limit) does not provide statistical evidence but is not restricted to the data groups. Both methods estimated the response threshold in the range between $d=0.285$ and $d=0.425$. This is also the range in which E-vector coding becomes significantly less reliable than at d-values close to 1

(Fig. 6). In comparison with the threshold determined here for single neurons, the behavioral threshold could be even lower, by pooling the responses of a number of neurons and, thus, reduction of noise. Behavioral experiments with tethered flying locusts as described by Mappes & Homberg (2004) using various degrees of polarization are suited to clarify this point. In crickets walking on a Kramer-treadmill, the behavioral response threshold ($d=0.13$, Henze & Labhart (2005)) lies slightly above the physiological response threshold of single POL1 neurons ($d=0.05$, Labhart (1996)). Some individuals, however, even showed oriented behavior at d-values of 0.04.

Sensitivity to unpolarized light

The neurons reported here are sensitive to both unpolarized and polarized dorsally presented light. Both responses are mediated by blue-sensitive photoreceptors (M. Kinoshita, KP, UH, in preparation). When stimulated with dorsally presented linearly polarized light with rotating E-vector at $d=1$, the activity of LoTu1 neurons shows sinusoidal modulation, but is always above background. With the same stimulation, TuTu1 neurons exhibit polarization opponency, i.e. they are maximally excited by a certain E-vector orientation and maximally inhibited by the perpendicular E-vector orientation (Pfeiffer et al., 2005). Intensity response plots showed that LoTu1 neurons are about two log units more sensitive to polarized blue light than to unpolarized blue light (M. Kinoshita, KP, UH, in preparation). The intensities we used in this study were in the operating range for both the polarized and the unpolarized light response. Therefore, the partially polarized light elicited a mixture of responses to both polarized and unpolarized light. In future experiments both the degree of polarization and light intensity should be varied to clearly disentangle the effects of both stimuli. It is possible, that the absolute threshold sensitivity of the neurons lies below $d=0.3$ if measured at light levels that are subthreshold for the unpolarized light response. For the biology of the locust, however, a low absolute threshold for d might be irrelevant, because under natural lighting conditions, low degrees of polarization are usually coupled to high light intensities. This eventually means that even under optimal atmospheric conditions (blue cloudless sky) the E-vector orientations within a circular area of 100° diameter around the sun would not provide directional information to LoTu1 and TuTu1 neurons, as illustrated in Fig.7.

Previous experiments with unpolarized light stimuli that were moved around the head of the animal on a circular path suggested that LoTu1 and TuTu1 neurons signal solar azimuth, rather than E-vector orientations. Information about the solar azimuth can be extracted from the direct view of the sun, as well as from the UV/green contrast of the sky and for some constellations from the E-vector orientation in the sky. The latter, however, is not always a reliable source and can provide information that conflicts with the actual position of the sun. This is especially problematic in the solar hemisphere, where the orientation of E-vector rapidly changes with the azimuthal distance of the sun. With a threshold for the detection of polarized light that lies above the degree of polarization within this "turbulent" area, the E-vector orientation in this part of the sky becomes invisible to the neurons and cannot interfere with the detection of the solar azimuth.

Comparison with cricket POL1 neurons

POL1 neurons with ramifications in the medulla and accessory medulla of the field cricket have been studied particularly well. They receive antagonistic input from orthogonally oriented polarization analyzers and, like LoTu1 and TuTu1 neurons, are polarization-sensitive within the blue range of light (Labhart 1988; M. Kinoshita, KP, UH, in preparation). All three types of neuron receive monocular input only (POL1, LoTu1) or mainly (TuTu1) (Petzold, 2001; Pfeiffer et al., 2005) and, thus, have a receptive field

that is tilted toward the contralateral side of the sky (Labhart et al. 2001; Pfeiffer, unpublished results).

Besides these similarities, there are a number of obvious physiological differences. While both LoTu1 and TuTu1 show complex responses to unpolarized light stimuli that strongly depend on position, wavelength and intensity of the stimulus (KP, UH, in preparation), the cricket POL1 neurons show weak or no responses to unpolarized light (Labhart, 1988). Cricket POL1 neurons have a very low light intensity threshold. They can still signal E-vector orientations at $3.5 \cdot 10^7$ photons $\cdot$ cm$^{-2} \cdot$ s^{-1} which corresponds to light levels of a clear moonless night-sky (Labhart et al., 2001). In contrast, the threshold sensitivity of LoTu1 and TuTu1 neurons lies two (LoTu1) respectively three (TuTu1) log units higher (M. Kinoshita, KP, UH, in preparation).

The differences listed above show that the two systems have evolved into different directions. POL1 neurons of crickets are highly specialized detectors of E-vector orientation. All physiological properties of these neurons are adjusted to gain maximum directional information even from weak signals. LoTu1 and TuTu1 neurons, on the other hand, are solar azimuth detectors that exploit all sources of directional information provided by the sky: color, brightness and E-vector orientation. The differences in threshold for the degree of polarization fit well into this picture. Cricket POL1 neurons show robust E-vector responses down to d-values of 0.05. The relation between the degree of polarization and the response amplitude R is highly nonlinear due to the total inhibition of the neurons around Φ_{min} at d-values ≥ 0.2. The initial slope of the d/R plot is very steep ($R = 632.9 \cdot d + 1.5$) in the range between d=0.05 and 0.1 and expresses extreme sensitivity to changes in d-values within this range (Labhart, 1996). The low threshold allows the system to signal E-vector orientations reliably even under partly clouded skies, where the degree of polarization might be substantially reduced (Pomozi et al., 2001). The steep initial slope of the d/R relation and the sharp responses of the neurons that include areas of total inhi-

bition around Φ_{min} illustrate the extreme sensitivity of this system to polarized light.

The locust neurons presented here, in contrast, signal the horizontal position of the sun and, in addition, are sensitive to polarized light. In such a system, it might not be the goal to approximate the threshold sensitivity to the physical limits. As discussed above, the relatively high threshold of d=0.3 might rather reflect the attempt to exclude misleading sky-light areas from being analyzed than a lack of performance.

A possible reason for the differences we observed between cricket POL1 neurons and locust LoTu1 and TuTu1 neurons could be different adaptations of the two species to their respective habitat and ecology. A small animal like the cricket that forages through a meadow or field during dusk will rarely catch a direct view of the sun, while a patch of blue sky is usually visible. Gregarious locusts, on the other hand, are active throughout the day (high solar elevations), and during their flights at least the animals in the upper strata of a swarm will most likely see the sun. However, neither LoTu1/TuTu1 homologues in crickets nor POL1 neuron homologues in locust have been investigated or shown to exist yet. Therefore, the question whether the physiological differences described here reflect evolutionary divergence of the polarization-vision system under different evolutionary pressures or the coexistence of a pure polarization-compass together with a sky-compass in either animal remains to be answered.

METHODS

Animals

Experiments were performed on adult gregarious locusts *(Schistocerca gregaria)* of both sexes. Animals were obtained from crowded laboratory colonies at the University of Marburg and were kept at 28°C with a photoperiod of 12 h light and 12 h dark.

Preparation and Electrophysiology

Animals were cooled at 4°C for at least 20 min. Wings, legs, abdomen, and the entire guts were removed to minimize movements. Locusts were waxed to a metal holder using beeswax/rosin. The head capsule was opened frontally, and air sacs and fat tissue were removed to expose the brain. The neural sheath above the target area was removed with forceps. During the preparation and later during the experiment, the brain was submersed in locust saline (Clements & May, 1974). Sharp microelectrodes with resistances between 80 and 150 MΩ in the tissue were drawn from omega-shaped borosilicate glass (Hilgenberg, Malsfeld, Germany) using a Sutter P-97 puller (Sutter Instruments, Novato, CA). The tips of the electrodes were filled with 10 mM Alexa488 in 200 mM KCl, the shanks were filled with 1 M KCl. Neuronal activity was amplified and filtered (lowpass 2 kHz) with a custom built filter/amplifier. Spike trains were observed visually with a digital storage oscilloscope (HM 205-2, Hameg, Frankfurt/Main, Germany) and acoustically with a custom built audiomonitor. The amplified and filtered signal was digitized at 25 kHz with a CED 1401 plus (Cambridge Electronic Design, Cambridge, England) and stored on a personal computer using an automated script (spike2 software, version 4.12, Cambridge Electronic Design). Some of the neurons were iontophoretically injected by applying hyperpolarizing current of up to 5 nA for approximately 3 min. Dye-injected brains were dissected out of the head capsule and examinated with a Zeiss Axioskop fluorescence microscope (Zeiss, Göttingen, Germany). Owing to the superficial location of the recorded neurons in the anterior optic tubercle, Alexa488-injected neurons could be identified without further histochemical processing of the brains.

Stimulation

Unpolarized light from a blue LED (Luxeon LED emitter, LXHL-BB01, 1 W, peak wavelength 470 nm, spectral half width 25 nm, Philips Lumileds Lighting Company, San Jose, California, USA) was linearly polarized by passing through a high quality dichroic polarizer sheet (HNP' B, Polaroid, Cambridge, MA, USA) and then elliptically polarized by passing through a transparency (Copier/Laser Transparencies, P/N 003R96019, Xerox) that served as an optical retarder. By varying the angle between the E-vector orientation of the linear polarizer and the principal axis of the transparency, the ellipticity of the light could be varied between 0.06 (0 would be circularly polarized light) and 0.991 (1 would be linearly polarized light). In addition to varying the degree of polarization, rotation of the retarder also changes E-vector orientation. Thus the initial E-vector orientation of each stimulus differed with the degree of polarization. At the highest degree of polarization, the initial E-vector orientation was parallel to the longitudinal axis of the animal. To monitor the state of polarization, a polarimeter based on an integrated photodiode/transimpedance amplifier (OPT101, Texas Instruments, Dallas, USA) with a HNP' B polarizer on top was positioned close to the animal's head. The output voltage of the OPT101 (V) is linearly correlated with light intensity and thus changes during the rotation of the stimulus polarizer in a sinusoidal way. Ellipticity of the polarized light was calculated as:

$$d = \frac{V_{max} - V_{min}}{V_{max} + V_{min}}$$

To a photoreceptor (and to our polarimeter), elliptically polarized light and partially polarized light as occurring in the blue sky appear identical if they have the same d value (Labhart, 1996). At each degree of polarization we stimulated with a clockwise and a counterclockwise 360° revolution of the polarizer at 30°/s. The angular extent of the stimuli at the locust's eye was 20°, stimulus intensity was 52.6 µW/cm^2.

Data analysis

Spike trains were analyzed using a semiautomatic *spike2* script. Action potentials were

identified with the *spike2* threshhold function. Evaluation was carried out as described by (Labhart, 1996). In brief, action potentials during rotation of the polarizer were counted in 18 consecutive bins (each 20° wide). The response value R was calculated as

$$R = \sum_{i=1}^{i=18} |n_i - \bar{n}|$$

with n_i being the number of spikes in bin i, and $\bar{n}$ being the mean number of spikes during the 360° rotation. Thus R is the sum of absolute differences between E-vector specific spike counts and mean spike counts and hence expresses the amplitude of spike frequency modulation during stimulation. To calculate the preferred E-vector orientation of a neuron (Φ_{max}), we calculated the angle between the E-vector orientation and the longitudinal axis of the animal at the moment of each action potential that occurred during stimulation. From these angles, the mean was calculated using *Oriana 2.02c* (Kovach Computing Services, Anglesey, UK). The mean of a set of angles is a vector and thus is described by its direction and length. The length of a mean vector (r) lies between 0 and 1 and describes how concentrated the observed angles are around the mean angle (Batschelet, 1981, p.31, Chapter 2.1).

References

Batschelet, E. (1981). Circular Statistics in Biology. Academic Press, 111 Fifth Ave., New York, NY 10003, 1981, 388.

Brines, M. L. & Gould, J. L. (1979). Bees Have Rules. Science, 206, 571–573.

Brines, M. L. & Gould, J. L. (1982). Skylight Polarization patterns and Animal Orientation. J Exp Bio, 96, 69.

Brunner, D. & Labhart, T. (1987). Behavioural evidence for polarization vision in crickets. Physiol Entomol, 12, 1–10.

Clements, A. N. & May, T. E. (1974). Studies on Locust Neuromuscular Physiology in Relation to Glutamic Acid. J Exp Biol, 60, 673.

Coulson, K. L. (1988). Polarization and Intensity of Light in the Atmosphere. (A. Deepak Pub).

Dacke, M., Byrne, M. J., Scholtz, C. H., & Warrant, E. J. (2004). Lunar orientation in a beetle. Proc Biol Sci, 271, 361–5.

Dacke, M., Nordstrom, P., & Scholtz, C. H. (2003). Twilight orientation to polarised light in the crepuscular dung beetle Scarabaeus zambesianus. J Exp Biol, 206, 1535–43.

Fent, K. (1985). Himmelsorientierung der Wüstenameise Cataglyphis bicolor: Bedeutung von Komplexaugen und Ocellen. Ph.D. thesis, Zürich.

Henze, M. J. & Labhart, T. (2005). Cricket polarization vision under difficult stimulus conditions. vol. Neuroforum 2005 Suppl, p. 145B.

Homberg, U. (2004). In search of the sky compass in the insect brain. Naturwissenschaften, 91, 199–208.

Homberg, U., Hofer, S., Pfeiffer, K., & Gebhardt, S. (2003). Organization and neural connections of the anterior optic tubercle in the brain of the locust, Schistocerca gregaria. J Comp Neurol, 462, 415–30.

Homberg, U. & Paech, A. (2002). Ultrastructure and orientation of ommatidia in the dorsal rim area of the locust compound eye. Arthr Struct Develop, 30, 271–280.

Horváth, G. & Varjú, D. (2004). Polarized Light in Animal Vision: Polarization Patterns in Nature. (Springer).

Labhart, T. (1988). Polarization-opponent interneurons in the insect visual system. Nature, 331, 435–437.

Labhart, T. (1996). How polarization-sensitive interneurones of crickets perform at low degrees of polarization. J Exp Biol, 199, 1467–75.

Labhart, T. (2000). Polarization-sensitive interneurons in the optic lobe of the desert ant Cataglyphis bicolor. Naturwissenschaften, 87, 133–6.

Labhart, T. & Meyer, E. P. (1999). Detectors for polarized skylight in insects: a survey of ommatidial specializations in the dorsal rim area of the compound eye. Microsc Res Tech, 47, 368–79.

Labhart, T., Petzold, J., & Helbling, H. (2001). Spatial integration in polarization-sensitive interneurones of crickets: a survey of evidence, mechanisms and benefits. J Exp Biol, 204, 2423–30.

Loesel, R. & Homberg, U. (2001). Anatomy and physiology of neurons with processes in the accessory medulla of the cockroach Leucophaea maderae. J Comp Neurol, 439, 193–207.

Mappes, M. & Homberg, U. (2004). Behavioral analysis of polarization vision in tethered flying locusts. J Comp Physiol, 190, 61–8.

Mardia, K. V. & Jupp, P. E. (2000). Directional statistics. (Wiley New York).

Petzold, J. (2001). Polarisationsempfindliche Neuronen im Sehsystem der Feldgrille, Gryllus campestris: Elektrophysiologie, Anatomie und Modellrechnungen. Ph.D. thesis, Zürich.

Pfeiffer, K., Kinoshita, M., & Homberg, U. (2005). Polarization-sensitive and light-sensitive neurons in two parallel pathways passing through the anterior optic tubercle in the locust brain. J Neurophysiol, 94, 3903–15.

Pomozi, I., Horváth, G., & Wehner, R. (2001). How the clear-sky angle of polarization pattern continues underneath clouds: full-sky measurements and implications for animal orientation. J Exp Biol, 204, 2933–42.

Rossel, S. & Wehner, R. (1984). How bees analyse the polarization patterns in the sky. J Comp Physiol, 154, 607–615.

Strutt, J. W. (1871). On the light from the sky, its polarization and colour. Phil. Mag., 41, 274–279.

Suhai, B. & Horváth, G. (2004). How well does the Rayleigh model describe the E-vector distribution of skylight in clear and cloudy conditions? A full-sky polarimetric study. J Opt Soc Am A Opt Image Sci Vis, 21, 1669–76.

von Frisch, K. (1949). Die Polarisation des Himmelslichtes als orientierender Faktor bei den Tänzen der Bienen. Experientia, 5, 142–148.

von Philipsborn, A. & Labhart, T. (1990). A behavioral study of polarization vision in the fly Musca domestica. J Comp Physiol, 167, 737–743.

Wehner, R. (1982). Himmelsnavigation bei Insekten. Neurophysiologie und Verhalten. Neujahrsbl Naturforsch Ges, 184, 1–132.

Wehner, R. (2003). Desert ant navigation: how miniature brains solve complex tasks. J Comp Physiol, 189, 579–88.

Wehner, R. & Strasser, S. (1985). The POL area of the honey bee's eye: behavioural evidence. Physiol Entomol, 10, 337–349.

Spike2 scripts for data acquisition, data evaluation and model calculations

General remarks on spike2 scripts

Capabilities of the spike2 script language

The program spike2 (Cambridge Electronic Design, Cambridge, England) is an electrophysiology data acquisition and evaluation software. Besides its graphical user interface it offers a powerful script language. This language allows to automatize sequences of analysis and thus speed up work with electrophysiological data enormously. Besides this simple macro functionality it provides features of high level programming languages such as loops, branches and calls to user-defined and built-in functions. It allows designing of interactive dialogues as well as automatic online evaluation of data.

Glossary

In the following sections I will describe the functionality and usage of some scripts I have developed within the past two years. For an easier understanding of these manuals I will first explain some terms that are frequently used.

Tool bar   The tool bar is an area located below the menu within spike2, that can hold script-defined buttons. These buttons are usually associated with user-defined functions or sequences of built-in functions.

Script bar   The script bar is similar to the tool bar, but the buttons it holds are associated with scripts rather than with script functions. Thus it is especially suited for small scripts that are frequently used. Some functions of the script IntraCell are available as standalone scripts to be used within the script bar.

Front view/current view   The front view is the window that is on top of all other windows. The current view is the active window. It does not have to be visible, but it can be manipulated by the script.

.smr files   The file extension of the native spike2 data file format is smr.

.abf files   The file extenstion of data files created by Clampex, which is part of the pClamp program suite (Molecular Devices, Sunnyvale, CA) is .abf.

Message box   A message box is a small window that contains some informational text and an *OK* button. When the *OK* button is klicked, the message box disappears.

Text mark   Text marks allow to store text within a spike2 data file, which is associated with a point in time. A text mark appears as a colored rectangle within the recording in a separate channel. When you move the mouse pointer over the marker you can read the associated text. Both IntraCell ($\rightarrow$ page 70) and Record ($\rightarrow$ page 80) use text marks to store text information in the data files.

Instantaneous frequency   The instantaneous frequency of an event is the reciprocal value of the time that has passed between this event and the previous (inter event interval). Instantaneous frequency display is especially suited to observe spiking patterns, e.g. very regular spiking leads to bands in the instantaneous frequency.

Memory Channel   Memory channels are temporary channels that are created by spike2 during runtime. In the scripts described here, they are used to hold event times. Memory channels are deleted, when a spike2 file is closed. To save them, right-click on the channel and choose: *Write to channel.*

IntraCell

Version

The current version number of the script is 0.8.0.

Purpose

The script IntraCell is intended to facilitate and speed up electrophysiological data evaluation. It was especially developed for the evaluation of intracellular recordings from polarization-sensitive interneurons, but some of the functions provided may also be helpful for a variety of other applications.

Main tool bars

Due to the increasing number of functions, the buttons did no longer fit within one tool bar from version 0.8.0 on. Therefore IntraCell now works in three modes each with its own tool bar. At startup the main tool bar is shown. The tool bar functions can either be assessed by mouse or by keyboard. Underlines in the function names indicate the letter that is used as a keyboard shortcut for each function. The tool bar buttons of the main tool bar (from right to left) are:

button name	full name	page
quit		71
close		71
open		72
toggle dots	toggle dotsize	75
change dots	change dotsize	75
retrig	retrigger	75
chancom	channel commands	75
evaluate		75

Table 1: Buttons of the main toolbar.

The functions associated with these buttons allow basic file operations and settings. The last two buttons are used to change into different modes of the script. The *chancom* button switches to the channel commands tool bar, which provides the following buttons (from right to left):

button name	full name	page
done		
chan<u>d</u>elete	delete channel	76
chan<u>w</u>eight	channel weight	76
chan<u>h</u>ide	hide channel	76
all <u>on</u>	show all channels	76

Table 2: Buttons of the channel commands tool bar.

In the main tool bar, the *evaluate* button brings you to the evaluate tool bar that provides access to the functions for data evaluation. This tool bar contains the following buttons:

button name	full name	page
done		
<u>y</u> optim	y-axes optimize	76
<u>x</u> full	x-axis full scale	76
<u>g</u>etcurs	get cursors	76
<u>d</u>t	Δt	77
z<u>o</u>omcurs	zoom between cursors)	77
<u>p</u>himax	Φ_{max}	77
poldeg<u>r</u>ee	degree of polarization	78
PS<u>T</u>H	peri-stimulus time histogram	78
<u>m</u>anPSTH	manual peri-stimulus time histogram	79
<u>I</u>NTH	interval histogram	79
<u>u</u>npoleval	evaluate responses to unpolarized light	80

Table 3: Buttons of the evaluation tool bar.

Functions

Quit

To leave the script, you have to select quit. A dialogue entitled *Do you want to leave the script?* appears. Click *OK* to quit the script or cancel to stay within the script. You can decide to leave all data files opened by checking the checkbox *Quit but leave files open.* Otherwise the script will close all data files. For data files that have been converted from .abf files the script asks for permission to delete the .smr file.

Close

This button closes the front view. For data files that have been converted from .abf files the script asks for permission to delete the .smr file. If you have finished evaluating the file, I recommend to remove the .smr file to save space. If you plan to go on with the evaluation in a different session, keep the .smr file to save the time that is needed for conversion from .abf to .smr.

This function works properly for local files. However I do not take any responsibility for the loss of data. Be sure that the original .abf file exists if you select to delete the .smr file.

Open

This button allows you to open data files. You can also do this via the standard spike2 menu, but if you want to evaluate the data using IntraCell, I recommend you use the *open* button of Intracell. At first you are asked which file type you want to open. You can chose between smr and abf. These files have to be converted to spike2 data files files before opening. The resulting smr file has the same name as the abf file and is stored in the same directory.

The settings dialogue

When the data file is loaded, the settings dialogue appears. The following paragraphs explain the settings you have to make in the sequence they appear in the dialogue.
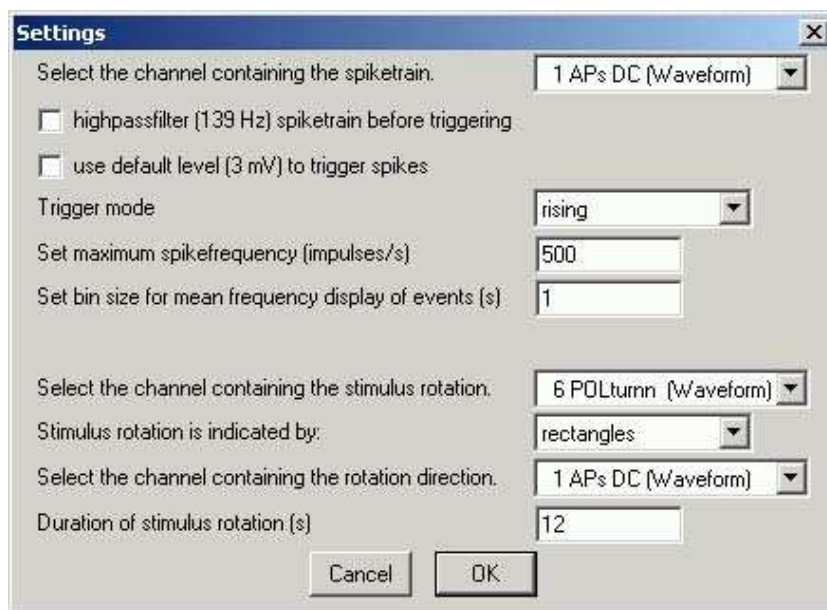
Figure 1: Settings dialogue of IntraCell.

Spike channel   First you have to tell IntraCell which channel contains your electrophysiological data. A drop-down menu holds all available channels and allows you to select one.

Highpass filter   Baseline drift or fluctuations in your data channel can be removed automatically by checking this checkbox. If you do so, a new dialogue will appear after you clicked *OK* on the settings dialogue. You have to decide in which channel the filtered data should be stored. Default is the first free channel, which is normally a good choice. You can select wether you want to filter the entire trace or only part of it. Since filtering takes time and the new channel requires disk space I recommend partial filtering. The range which should be filtered can be selected by two cursors.
When the data is filtered it is written to a new channel named *APs HP139* which is attached to the data file. This channel is then used to trigger the spike times. Please be aware that this channel **should only be used to trigger spike times.** The filtering procedure seriously damages the

waveform of the data. This feature has only been tested for data files sampled at 25 kHz. Possibly this filter does not work for lower sampling rates.

If this is the case and you need to filter your signal to be able to trigger events, you can choose *Channel process → DC Remove* from the *Analysis* menu. Then choose *retrigger* (→ page 75) from the main toolbar.

Default level If your data has a good signal-to-noise ratio and the background noise is in the range of maximally 2 mV, you can check this checkbox. IntraCell will then put the threshhold for spike triggering to 3 mV and omit the manual threshold setting (→ page 74).

Trigger mode Here you can select how events should be recognized by the trigger algorithm. Available modes are: *peak, trough, rising, falling.* When you chose *peak* or *trough*, events are extracted based on the time of a peak or trough in the waveform, after the threshold level has been crossed. The modes *rising* and *falling* extract events based on the time when the waveform crosses the threshold level in either rising or falling direction. For intracellular recordings I recommend *rising.* With noisy signals, the *peak* mode frequently extracts artifacts as events.

Maximum frequency This flag sets the maximum frequency that will be accepted upon extraction of events from the spike channel. In other words, it sets the minimum time that has to lie between two events. The trigger algorithm will ignore threshold-crossings in between. This is useful if you have high-frequency artifacts in your spike channel, e.g. from "buzzing". They will not be detected and upon automatic scaling of the y-axis, the scale of the event channels are scaled in a sensible range.

Of course you have to **make sure that the value you enter here is higher than the maximum event rate** of your electrophysiological data.

Bin size The events that are extracted from the spike channel are displayed in two memory channels. One displays dots that indicate instantaneous frequency, the other displays a line that indicates mean frequency. The mean frequency is calculated as a gliding average over a specified time window, the width of which is the bin size you have to enter here. Larger values result in smoother lines, but also increase the phase shift between the activity trace and the actual activity which results from gliding average method. For spike rates from approximately 10 impulses/s onwards, a setting of 0.5 - 1 s should be O.K.

POL rotation channel From this drop-down menu you have to select the channel that indicates rotation of the stimulus device which is used to apply polarized and unpolarized light stimuli. If the stimulus device outputs the voltage steps that are sent to a stepping motor, you should select the corresponding channel.

Filter rotation indicated by Depending on the stimulus device you are using you can select three values here: *rectangles, ramps (180°)* and *ramps (360°).* For later calculation of Φ_{max} -values **it is important what you chose here.** If you select *rectangles,* than IntraCell assumes that you are also providing a channel that indicates the direction of rotation. During the calculation of Φ_{max} (→ page 77) you will then not be asked for the direction of rotation. If you choose either *ramps (180°)* or *ramps (360°)* you will be asked for the direction of rotation each time you calculate

a Φ_{max} -value. The result of the conversion from spike times to angles ($\rightarrow$ page 77) depends on whether you chose *180°* or *360°*.

Direction channel   Some stimulus devices output the direction of rotation as a TTL signal. TTL high (+5 V) indicates right rotation (i.e. clockwise, as seen by the animal), TTL low (0 V) indicates left rotation (i.e. counterclockwise, as seen by the animal). When this is the case and the correct channel is selected here, the script automatically distinguishes between right and left rotations based on the voltage level within this channel. It evaluates whether the voltage of this channel is below or above 2.5 V during the rotation of the stimulus device. If your stimulus device does not provide such a channel (which is likely) this setting can simply be ignored. To use this feature, **it is required that you also select:** stimulus rotation is indicated by *rectangles.*

Duration of rotation   Here you have to enter the duration of one rotation of the stimulus device. It is **very important** that this setting is correct, since it is used for several types of data evaluation. A wrong setting here will for example lead to wrong Φ_{max} values.
If you are not sure about the duration of rotation when you are opening a file, you can click *OK*. Then you can measure the duration with the Δt function ($\rightarrow$ page 77) and go back to the *settings* dialogue by clicking *retrig* ($\rightarrow$ page 75) to set the correct value.

Threshold setting

If you did not check the checkbox entitled *Use default level (3 mV) to trigger spikes* you have to set the threshold for spike triggering manually. Thus, after you click *OK* in the settings dialogue, the spike channel is maximized and a horizontal cursor allows you to set the threshold. The tool bar changes and holds now some buttons that facilitate scaling and cursor operations.

Smart yoptim (smart y-axis optimize)   Automatical scaling of the y-axis is problematic, when the trace contains large artifacts or other data points that lie far outside the range of the physiological data. In intracellular recordings this is usually the case when an iontophoretical dye injection is conducted. Scaling between the largest and smallest sample point in such cases usually means that the spike amplitude becomes very small. This function calculates the mean ($\bar{x}$) and the standard deviation (sd) of all data points within the visible x-range and then the y-axis is scaled between $\bar{x} - sd$ and $\bar{x} + 3 \cdot sd$. This is in most cases a reasonable range which allows for trigger setting.

Y optim (y-axis optimize)   This is the same function as provided by the main tool bar ($\rightarrow$ page 76).

X full (full scale x-axis)   This is the same function as provided by the main tool bar ($\rightarrow$ page 76).

Numeric threshold   If you need to use an exact threshold level, then this button is for you. You can enter a numeric value at which the horizontal cursor is then positioned. The value can be a real number such as 3.14159.

Get hcursor   If the horizontal cursor is outside the visible range, click this button to bring it back. The cursor is then positioned within the visible y-range.

OK Once you have properly set the threshold you can click *OK* to proceed.

Event channels

After completion of the initial settings, IntraCell sets up two new memory channels that hold the events which have been extracted from the spike channel. An event is the time of occurrence of a spike within the recording. Within spike2 events can be displayed in different ways. By default, IntraCell displays mean frequency ($\rightarrow$ page 73) and instantaneous frequency.
In addition to the two event channels, a third one named POLstim is created. It holds the starting times of the stimulus rotation. They are displayed as vertical lines.
All three channels created by IntraCell are memory channels, which means that they are not permanent. To make a memory channel permanent, right-click on the channel and choose *Write to channel*.

Toggle dots

The instantaneous frequency of the events is plotted as dots. Depending on overall activity, x axis scaling or printer model you use, you might want bigger or smaller dots. With this button, you can toggle the dot size of the front view between small and large dots, the size of which can be set by the *change dots* function.

Change dots

Here you can set the size of small and large dots for the front view. You can choose a value between 0 (tiny) and 9 (huge) for both dot types. For each data file that is open, these sizes are separately stored in the registry. When the file is closed, the values are deleted. Defaults are 0 for small and 2 for large dots.

Retrig (retrigger)

This button brings back the *settings* dialogue ($\rightarrow$ page 72), that appears when you open a file using the "open" button. Use this to alter any of the settings for the front view. This will also force you, to retrigger the events, because the old memory channels will be deleted. Write them to permanent channels before you click *retrig* if you want to keep them. This can be done by right-clicking on a memory channel and selecting *Write to channel*

Chancom (channel commands)

This button switches to the channel commands toolbar. To get back to the main toolbar you have to click *done* in the channel commands toolbar.

Evaluate

To start the evaluation of your data file click this button. The main tool bar disappears and the evaluation toolbar is displayed. To get back to the main toolbar you have to click *done* in the evaluation toolbar.

Chandelete (delete channel)

This button can be used to delete unused channels in your data file. You can select a channel by clicking on its channel number. Hold down Ctrl (Strg on german keyboards) while clicking to select more than one channel. **Use this feature with extreme caution! Deleted channels can not be restored!**

Chweight (channel weight)

You can alter the vertical space a channel uses by altering its channel weight. When opening a new data file, all channels have the weight 1. To change the weight of a channel, you have to select it by clicking on the channel number. Hold down Ctrl (Strg on german keyboards) while clicking to select more than one channel. Now choose the *chweight* button. A dialogue appears that asks you to set a weight factor between 0.01 and 100. The default value is always 2. Click *OK* to change the weight of the selected channels or *Cancel* to leave it untouched.

Chanhide (hide channel)

If you have many channels within your data file you might want to hide those that are currently not of importance. As with the other channel commands, you have to select one or (by holding Ctrl while clicking) more channels by clicking on their channel number. If you then click *chanhide*, the channels will be hidden.

All on

Click this button to make all channels of your data file visible.

Y optim (optimize y-axis)

Y optimize scales the y axes of all channels (including hidden ones) between the smallest and largest sample point within the visible x-range.

X full (full scale x-axis)

Press this button to display the full x-range of a data file.

Getcurs (get cursors)

If there are no cursors in the data file, or they are outside the visible time range, select this function. Then cursors 1 and 2 will appear equally spaced within the visible time range. Attention: If you work with more than two cursors this function is not suitable for you. It first deletes all cursors and then brings up two new ones.

Dt ($\triangle$t)

This function calculates the time between cursors 1 and 2 and prints the result to a message box. The output format depends on the duration and can range from days to ns. If cursor 1 or 2 do not exist, the function deletes all cursors and brings up two cursors within the visible time range. Then the user is asked to set them around the region of interest. Clicking *OK* then performs the calculation.

Zoomcurs

Use this to scale the front view from cursor 1 to cursor 2 and optimize all y axes.

Phimax (Φ_{max})

Theory This function calculates the Φ_{max}-angle of the neuronal response to polarization- or azimuth stimulation. The Φ_{max} is the angle between the E-vector orientation or stimulus direction and the longitudinal axis of the animal, at which the neuron exhibits its highest activity. The calculation is performed as follows: First, each spike that occurs during the rotation of the stimulus is assigned the angle of the stimulus at that time. Than the mean, of these angles (Φ_{max}) and the length of the mean-vector (r) is calculated using the trigonometric functions method (Batschelet, 1981). The angular deviation (*angdev*) in degrees is calculated using the formula

$$angdev = \sqrt{-2 * Ln(r)} \cdot \frac{180}{\pi}$$

To check for the significance of the neuronal response, the Rayleigh test of uniformity is performed. This test calculates the probability (p) that the following null hypothesis is true: "The data are distributed in a uniform manner." The statistical test value (Z) is calculated as:

$$Z = n \cdot r^2,$$

where n is the number of observations (action potentials in our case). From Z, the probability is calculated as:

$$p = e^{-Z}$$

For small numbers of observations ($n < 50$), the formula has to be corrected. The probability p then is:

$$p = e^{-Z} \cdot \frac{1 + \frac{2 \cdot Z - Z^2}{4 \cdot n} - 24 \cdot Z - 132 \cdot r \cdot Z + 76 \cdot Z^3 - 9 \cdot Z^4}{288 \cdot n^2}$$

When the null hypothesis is rejected, the data are not distributed uniformly and thus show directedness.

Usage To obtain correct results, make sure the settings for *Stimulus rotation is indicated by: rectangles/ramps (180˚)/ramps (360˚)* ($\rightarrow$ page 73) and *duration of stimulus rotation (s)* ($\rightarrow$ page 74) are properly chosen. If you select *ramps*, then the field *Select the channel containing the rotation direction* must also show the correct channel.

To determine the beginning of the stimulus, you are asked to set cursor 1 accordingly. When you click *OK*, cursor 2 appears at the end of the stimulus rotation. This is a visual control for you to

make sure that the duration of rotation is set correctly. In case the direction of rotation is not recognized automatically *(ramps (180°)* and *(ramps (360°))* you are asked to select the direction of rotation. Now the script calculates the Φ_{max} and performs the Rayleigh test, as described above. This is done twice, treating the data either as axial (180° periodicity) or circular (360° periodicity). The results are printed to a message box and to the log window. They include the filename of the data file with the full path, the region that was analyzed, the number of events, the mean activity within that region and the angular deviation. For processing in other programs, the list of angles that were calculated from the spike times is copied to the clipboard and saved as an ASCII file. The ASCII file is saved to the same folder the original data file was opened from. It is named *datafile*_EVENTS_degrees_from_*starttime*_to_*endtime_directionof rotation*_for_phimax.txt

Poldegree

This function is used to calculate the degree of polarization from a channel that contains the data from a polarimeter.

Theory   The degree of polarization *(d)* can by measured with a photoradiometer that is equipped with a polarizer in front of its detector diode. Such a device is called polarimeter. When a polarizer, that produces linearly polarized light of different degrees of polarization (or elliptically polarized light of different ellipticities), is rotated in front of a polarimeter, a sinusoidal curve is measured. The amplitude of this curve indicates the degree of polarization of plane-polarized light or the ellipticity of elliptically polarized light, respectively. When V_{max} is the maximum and V_{min} the minimum output voltage of the polarimeter during a 180° rotation of the polarizer, *(d)* is defined as:

$$d = \frac{V_{max} - V_{min}}{V_{max} + V_{min}}$$

For some photoradiometers, the output voltage in darkness is different from 0 V. In this case the formula has to be corrected for this dark voltage *(dv)*:

$$d = \frac{(V_{max} - dv) - (V_{min} - dv)}{(V_{max} - dv) + (V_{min} - dv)} = \frac{V_{max} - V_{min}}{V_{max} + V_{min} - 2 \cdot dv}$$

Usage   When you click the *poldegree* button, you are asked to select the appropriate channel. After you click *OK*, this channel is maximized and provided with three horizontal and one vertical cursors. The tool bar then contains the buttons *x full* and *y optim*, that have the same functions as in the evaluate tool bar ($\rightarrow$ page 76) and several functions to bring the cursors into the visible range. Position the horizontal cursors at the dark value, the maximum and the minimum output voltage of the polarimeter. The cursors are renumbered during the evaluation so the sequence of the cursors does not matter. When you click *OK*, you are asked to set cursor 1. The degree of polarization that is calculated from the horizontal cursor positions is saved in a new channel, named POLdeg as a text mark ($\rightarrow$ page 69) at the position of this cursor.
After each calculation of *d* you can quit this function or proceed.

PSTH (peri-stimulus time histogram)

This button is used to automatically or semi-automatically calculate peri-stimulus time histograms. This requires correct setting of the stimulus duration ($\rightarrow$ page 72) and that each start of a rotation

is indicated by a vertical line in the POLstim channel.

If you click this button, you first have to chose which mode you want to chose *(semi-auto or auto)*. The PSTHs are automatically saved as ASCII files in the same directory as the recording. Their names contain the filename of the recording, a trailing number and the data range that has been analyzed.

Semi-automatic   Semi-automatic PSTH means that you are able to calculate single PSTHs and you can influence bin size and number of bins. To do so, you have to place the cursors around the stimulus you want to analyze. Then you are asked to enter the bin size and the number of bins. After each PSTH you can quit the function or proceed.

Automatic   IntraCell can automatically calculate PSTHs for an entire data file. You can select whether you only want the results to be saved (one ASCII file per PSTH, naming as in semi-automatic mode) or if IntraCell shall also display the graphs. In this mode you can not influence the PSTH. A default of 36 bins is used, and the bin size is 1/36 of the duration of the stimulus (as defined in the settings dialogue ($\rightarrow$ page 72)). This is the fastest way to evaluate your data, however you have to be aware that for each event in the POLstim channel a PSTH is calculated, which can result in a lot of PSTHs when the POLstim channel contains artifacts.

ManPSTH (manual peri-stimulus time histogram)

This function is also used to calculate PSTHs but it does not rely on the POLstim channel. During the evaluation process you are asked to set the beginning of each stimulus with a cursor. It also allows to set the number of bins and can, in addition, calculate the response strength R (Labhart, 1996). R measures the summed deviation of spiking activity within each bin of the PSTH from the mean spiking activity. For a PSTH with 18 bins, with n_i being the number of spikes in bin i and $\bar{n}$ being the mean number of spikes per bin, R is defined as:

$$R = \sum_{i=1}^{i=18} |n_i - \bar{n}|$$

Checkboxes allow you to decide if you want the PSTH to be displayed and saved and if the histogram should be scaled as spikes/s (otherwise spike counts/bin are used). If you chose to calculate the response strength R, the result will appear in a message box and will be written to a text mark ($\rightarrow$ page 69) in a channel named R.

After each PSTH you can quit the function or proceed.

INTH (interval histogram)

An interval histogram displays the frequency histogram of the intervals between events on a selected channel. To calculate an interval histogram, you have to indicate the region of interest by setting cursors 1 and 2. Then select *INTH*. If there are no cursors (or only one) within the data file, they are inserted when you click *INTH*. Then you can choose the region of interest and click *OK*. The histogram appears at the bottom of the spike2 window. A dialogue allows you to select whether you want to save the histogram and whether this histogram window should be automatically closed when you finish evaluating.

Unpoleval

This function was added to facilitate the evaluation of neuronal responses to unpolarized light. To use this function, you need a channel that indicates light on/of stimuli by voltage steps. *Unpoleval* calculates a PSTH with three bins, that is displayed to the right side of the recording. In the dialogue that comes up after clicking *unpoleval*, you have to do four settings:

Stimulus channel Chose the channel that contains the stimulus trace from the drop-down menu.

Trigger mode You can either trigger to the *rising edge* or to the *falling edge* of the stimulus, depending on the polarity of the stimulus trace. If you want to evaluate both the responses during the stimulus and after-stimulus effects, you can also chose to trigger to *both* edges.

Stimulus duration Here you can enter the duration of the stimulus. The value you enter here will be the width of the PSTH bins. So you can also enter values that are smaller than the duration of your stimulus.

Copy results to clipboard The PSTH values are copied to the clipboard. Here you can specify the format. Possible values are: *as a column* (One value below the other), *TAB delimited, comma delimited, space delimited.*
After completion of the *settings* dialogue, you have to set the threshold to trigger the stimulus times. This works exactly as spike triggering ($\rightarrow$ page 74). After you have set the threshold and clicked *OK* the threshold crossings are written to a new memory channel named "stimstart" and a new toolbar appears. It contains the buttons *y optim* ($\rightarrow$ page 76), *x full* ($\rightarrow$ page 76), $<<, <, >, >>$, *PSTH*, and *finished*. The arrow symbols are used navigate between the events in the "stimstart" channel. Single arrows move the cursor to the next or previous stimulus event, double arrows move the cursor 10 events forward or backward. When *PSTH* is clicked, a PSTH is generated that consists of three bins each displaying spike counts within the duration that was specified in the *settings* dialogue. The first bin of the PSTH displays the number of spikes before the topical cursor position, bins 2 and 3 show the spike counts after the cursor. The numbers of spikes are copied to the clipboard.

Record

Version

The current version number of the script is 0.5.2.

Purpose

This script is used to record from polarization sensitive neurons. It organizes the data in folders, provides threshold based online display of the mean frequency and online evaluation of the data. In addition it communicates with the programs Steuerung.exe (that controls a filter unit with grey and interference filters) and Beleuchtungssteuerung.exe (controls the stimulus device for polarized light and unpolarized light spots). Both programs were written by Sebastian Richter from the electronics workshop of the Philipps-University Marburg.
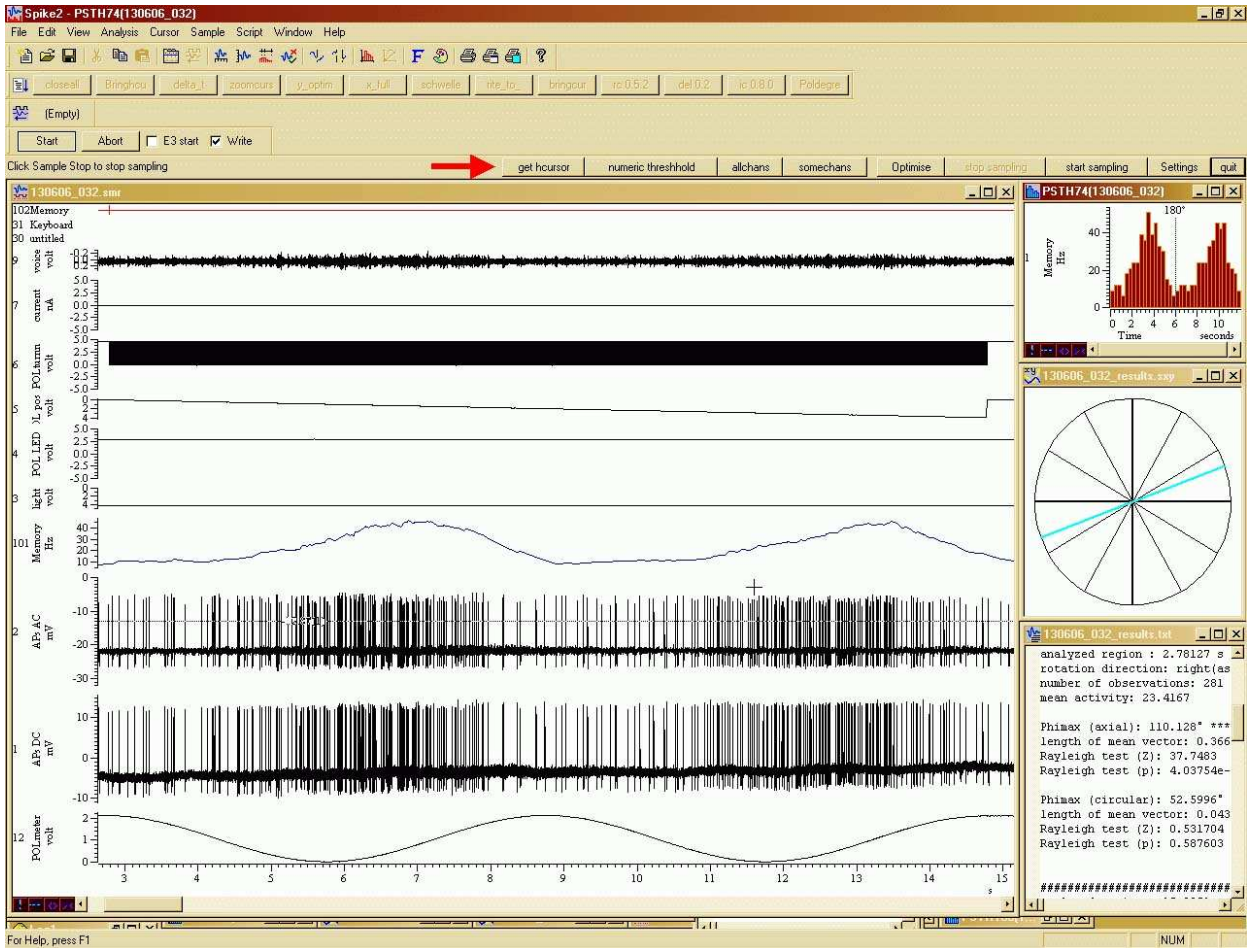
Figure 2: Typical appearance of spike2 during a recording session with the script Record. The tool bar (arrow) provides access to several functions. The main window displays the spike train and several stimulus traces, as configured in the sampling configuration. The right window on top holds the PSTH ($\rightarrow$ page 84) of the last stimulation. The middle window indicates the Φ_{max} values of all stimulations within the topical recording. Φ_{max} values from stimulation with polarized light are indicated by blue bars, Φ_{max} values from stimulations with unpolarized light are represented by circles in the color of the stimulus light (violet for 330 and 350 nm, blue for 400 to 450 nm, green for 500 to 550 nm, orange for 600 nm, grey for "white" light). The text window logs all results of the online analysis and every change within the stimulation regime or the trigger threshold.

File naming and Folder organization

Each spike2 data file that is created by Record is named according to the date of creation with a three-digit counter at the end of the filename: `ddmmyy_nnn.smr` (with nnn being the counter starting with 000). For example the second recording on July 10th 2006 would be called: `100706_002.smr`. Each data file is placed in a folder with the same name (without the smr extension), together with the log- and result files that are created by Record. This folder is stored within a folder that is named `ddmmyy`. All folders of a whole month are stored in a folder with the name `mm_yyyy`. All folders that do not exist are created by the script. The root directory for the folders is `F:\Pfeiffer\Ableitungen\`. As to the current version this can only be changed within the source code.

Tool bars

Record provides a tool bar with the following buttons:

button name	full name	page
quit		82
settings		82
start sampling		83
stop sampling		83
optimize		83
somechans	show some channels	84
allchans	show all channels	84
numeric threshold	set numeric threshold	84
get hcursor	get horizontal cursor	84

Table 4: Buttons of the main toolbar.

Functions

Quit

Click this button to terminate the script.

Settings

This button brings you to the *settings* section. A new tool bar leads you to four categories of changeable settings:

Colors   Here you can set the background and foreground colors of the application. You can choose between 25 colors (including black, white and 6 greyscales) from two drop-down menues. A checkbox allows to switch between color mode and black and white.

Y-scales You can enter the y-range that is displayed for each channel defined in the topical sampling configuration. First you have to select a channel, then you can enter the upper and lower limits. In addition you can specify a channel weight ($\rightarrow$ page 76).

X-range Here you can set the length of the x-axis. If you use the program Beleuchtungssteuerung.exe, this setting is ignored and the length of the x-axis is scaled to the duration of the stimulus rotation automatically.

Online triggering This button opens a settings dialogue. The following settings can be made:

- *Spike channel:* Select the channel that contains your electrophysiological data that shall be analyzed during recording.

- *Threshold:* Select the polarity of your spikes. This should be set to *positive* for intracellular recordings.

- *Initial threshold:* Spike times are detected by threshold crossings, the value of which is set by a horizontal cursor. Here, you can determine where this cursor shall be positioned on startup of the script.

- *Action:* What shall the script do, when it detects a threshold crossing? It can output a TTL pulse (I did not test this feature) or write a marker to a memory channel. The latter is necessary for online evaluation and should be selected.

- *Stimulus channel:* Select the channel that indicates the rotation of the stimulus device. This channel is used to determine the beginning of the rotation. The signal within this channel must fall through 2.5 V at the beginning of a rotation. The motor-control signal for some stepping motors is suited for this.

- *Stimulus direction:* Select the channel that indicates the direction of rotation of the stimulus device. This channel is used to determine the direction of rotation. It has to contain a ramp-like signal.

When you are content with the settings, click *OK* to return to the main tool bar.

Start sampling

To begin the recording of data you have to click this button.

Stop sampling

If you click this button, the current recording is stopped and the data file is saved. A fresh set of empty windows appears (see Figure for the types of window).

Optimize

This function optimizes all y-axes. To use this function you have to make sure that the window that holds the recording is the current view ($\rightarrow$ page 69).

Somechans (some channels)

If you have to record a lot of channels but you do not need to observe all channels during recording, you can click this button. Only the channels that are provided in the `vischans%()` function within the source code are displayed. These are currently channels 1, 2, 101 and 102, which can only be changed by editing the source code. The contents of channels 1 and 2 depend on your local sampling configuration. Within Record, channel 101 displays the mean frequency of the spikes and channel 102 indicates the beginnings of the stimulus rotation.

Allchans (all channels)

Click this button to display all channels.

Numeric threshold

This allows you to enter a numeric value for the threshold based spike triggering, just as in IntraCell ($\rightarrow$ page 74).

Get hcursor (get horizontal cursor)

Click this button to bring the horizontal cursor, which defines the threshold for spike triggering, into the visible y-range.

Online analysis

Record automatically analyzes your electrophysiological data during recording. The basis of all analyses that are performed is a threshold based event detection. The threshold can be adjusted at any time during the recording by moving the horizontal cursor in the spike channel, that has been defined in the settings section ($\rightarrow$ page 82) or by entering a numeric threshold value ($\rightarrow$ page 84). The event times that are extracted are written to a memory channel.

The most basic analysis that is done by Record is to calculate the mean activity, which is displayed in real-time in the memory channel.

When the stimulus device is being rotated, Record starts several kinds of analyses:

PSTH   While the stimulus device rotates, Record calculates a PSTH in realtime. Thus, the PSTH window in the upper right corner of the spike2 window ($\rightarrow$ page 81) is continuously updated as new spikes occur. At the end of the rotation, the PSTH is saved in ASCII format in the same folder as the recording.

Φ_{max} and Rayleigh test   At the end of a rotation of the stimulus device, Record calculates the Φ_{max} for this rotation and performs the Rayleigh test of uniformity. The algorithm that converts spike times to angles and the subsequent calculations are identical to those performed by IntraCell ($\rightarrow$ page 77), but the direction of rotation is determined automatically. The results of the calculations are printed to the log window in the lower right corner of the main window. In addition, they are plotted in a circular diagram in the right middle of the main window. For

stimuli that contained polarized light, a light blue line is plotted at the angle of the calculated Φ_{max} . For unpolarized light stimuli, a circle in the color of the light is plotted at the Φ_{max} angle. When the Rayleigh test indicates that the distribution of data differs significantly from uniformity, i.e. they are directed, the system exclamation sound is played via the soundcard. Depending on the p-value, this happens three times ($p < 0.001$), twice ($p < 0.01$) or once ($p < 0.05$).

Communication with other programs

Steuerung.exe

Steuerung.exe is a program that allows to control an electromagnetic shutter, two filter units and a neutral density wedge that is attached to a stepping motor. One filter unit contains a set of neutral density filters, the other contains small-band interference filters. Steuerung.exe allows to move different filters into the beam path and to adjust the light intensity by attenuating the neutral density wedge. At startup and after any change it writes the topical filter settings to the Windows registry. All keys are stored in the following path:
\HKEY_CURRENT_USER\CED\Spike2\myscripts\Filtersteuerung\
The keys (REG_DWORD) that are used are:

- *Filter_A:* This is the current interference filter that is used. The value of the key can range between 0 and 9. Currently 0 is no filter and 1 to 9 are increasing wavelengths between 330 nm and 600 nm.

- *Filter_B:* This is the current neutral density filter. The value of the key can range between 0 and 9. Currently 0 is no filter and 1 to 9 are decreasing transmission rates between 79% and 0.01%.

- *Shutter:* This key indicates whether the shutter is opened (1) or closed (0).

- *wedge:* This key holds the topical position of the neutral density wedge and can range between 0 and 1599. The value simply reflects the step number of the stepping motor. With the current configuration, the value 920 positions the wedge to the highest transmission rate.

All registry keys are permanently monitored by Record. When the shutter opens for the first time within a recording or if any of the filter settings has changed, the script writes a text mark ($\rightarrow$ page 69) to channel 30. The color of the text mark indicates the color and type of stimulus. The unpolarized light stimuli are indicated by grey ("white"), violet (330 and 350 nm), blue (400 - 450 nm), green (500 - 550 nm) and orange (600 nm) text mark. When you move the mouse pointer over the text mark, wavelength transmission of the neutral density filter and position of the neutral density wedge are displayed.

Beleuchtungssteuerung.exe

Beleuchtungssteuerung.exe controls the device that is used to apply polarized and unpolarized light stimuli. The polarized light is produced by a combination of LED and polarizer. The intensity of the LED is controlled by 8bit PWM (pulse width modulation). The stimulation device can rotate clockwise or counterclockwise at angular velocities between 10°/s and 40°/s. All keys are stored in the following path:

`\HKEY_CURRENT_USER\CED\Spike2\myscripts\Steuerung\`

The keys that are stored are:

- *LED_intensity* (REG_DWORD): This can be a value between 0 and 255. A value of 255 means, the LED is switched off, the remaining values indicate increasing intensity from 254 to 0 (full intensity).

- *Position* (REG_SZ): This key indicates the topical position of the stimulus device. It is not continuously updated during rotation, but written when the position is reached. The range of this variable lies between 0 and 360. This key is currently not used by Record.

- *rotation_intenion* (REG_SZ): Yes! *"intenion"*. This is a typo in Beleuchtungssteuerung.exe. This key is written before the rotation starts to indicate direction and angle of rotation. Right rotations are indicated by positive values. This key is currently not used by Record.

- *rotation_velocity* (REG_DWORD): This key indicates the topical rotation velocity and can range from 10 to 40.

The keys *LED_intensity* and *rotation_velocity* are monitored by Record. When the LED is switched on or its intensity (actually the pulse width modulation) is changed, Record stores a bright blue text mark ($\rightarrow$ page 69) in channel 30, which contains the LED intensity in %.
The rotation_velocity key influences the x-axis of both the data file window (the recording) and the PSTH window. When this value changes, the x-axis of the recording is immediately rescaled. Its x-range is always the duration of a 360° rotation plus 0.5 s. To change the x-axis of the PSTH, a new PSTH window with the correct scaling is created.

FileDelete

Version

The current version number of the script is 0.2.

Purpose

This script helps to clean up the hard drive after a recording session. It is especially helpful when recordings were made using the script "Record" ($\rightarrow$ page 80). The Record script places each recording in a separate folder and stores results of online evaluated data and a log file. It is very time consuming to check each data file of a recording session for usability, remember its name, close it and delete the folder of the recording within a file manager. With FileDelete, you can check the data file within spike2 and if its useless you can close it and move the whole folder of the recording to a predefined folder by a single click. Then the original files are deleted.
FileDelete 0.2 calls the Windows command shell which then performs the actions on the filesystem. It does not run under Windows 9x.

Tool bar

Filedelete provides a tool bar with the following buttons (from right to left):

- quit (Terminate the script.)

- settings

- show all

- y-optimize

- closefile

- DELETE FILE

Functions

Settings

To prevent loss of data, files will be backed up before deletion. So in case you accidentally click *DELETE FILE* you can restore your data. Here you can set up the path where the files shall be moved. Attention! **Make sure you enter a valid drive letter within the path you provide here.** FileDelete has no control about the success of copying the files and will delete the original files anyway. If you enter a path that does not exist, but with a valid drive letter, the windows command shell will ask you if you entered a file name or a folder name. Please answer *folder*. Then the missing folders will automatically be created.

Show all

To provide an overview about the whole recording, the x-axis is scaled from 0 to the end of the recording and all y-axes are optimized.

Y-optimize

Click this button to optimize all y-axes.

Closefile

Closes the front view, but does not delete it.

DELETE FILE

If you click this button, the script first closes the front view. Then it calls the Windows command shell and makes it copy all files that lie within the same folder as the front view to the folder that was provided in the *settings* dialogue. After that, **even if copying was not successful,** all files from the original folder and the original folder itself are deleted.

Warning: Be aware of what you are doing! If the destination drive does not exist or has no space left, your files will be lost! Only use this script if you have stored each recording in a separate folder and if you are sure that the destination drive is set up correctly and has enough space. This script has been tested and used many times and it always worked well. However I do not take responsibility if you lose all your data while using this script.

Solar Altitude

Version

The current version number of the script is 0.1.

Purpose

This script calculates the elevation of the sun (solar altitude), for a given geographical location and time. It can work in two modes and upon startup, the user is asked to choose one.

Whole day mode

In this mode, the user has to enter geographical coordinates and a date. The script will then calculate the solar altitude for the given parameters in the course of a day with a resolution of 1 min 26.4 s (0.001 d). Elevations smaller than 0° are neglected. The result is plotted in a graph window.

After that, the user is asked if another graph is to be plotted. If yes is chosen, the parameter settings can be changed and the new graph is plotted on top of the old one. This is repeated until the user chooses not to plot another graph.

The graph window can be saved as a picture (bitmap or metafile), as an XY File (the native, proprietary format of spike2 XY views), or as a text file. The latter contains all data points as a tab-separated table. This is useful if the data shall be further processed or plotted by a different program.

One time mode

If this mode is chosen the user has to enter geographical coordinates, date and time. Then the solar altitude is calculated for the given parameters. Besides the solar altitude, the script calculates the number of the day, the local apparent time, the equation of time, the declination and the hour angle ($\rightarrow$ page 46).

The input parameters and the results of the calculation are printed to a text window.

```
Input:
Date: 24.6.2005
Time: 13 h 18 min
Latitude: 23.4°
Longitude: 6.5°
```

```
Output:
number of day: 175
true local time (local apparent time):
12.7003 h = 12h 42 min 1.08042 s
equation of time: -1.98199 min
declination: 23.4237°
hour angle:10.5045°
solar altitude: 80.3624°
```

Figure 3: Appearance of a typical output from solar altitude using the one time mode.

The spike2 script POLdegree

Version

The current version number of the script is 0.1.

Purpose

This script calculates the degree of polarization from a channel that holds polarimeter data. Its functionality is similar to that of the *poldegree* function within IntraCell ($\rightarrow$ page 78) and it uses the formula described there. However it does not write text marks to the data file but instead displays the degree of polarization in a text window that is constantly updated.

Usage

The script places three horizontal cursors into channel 1 of the front view. Then it creates a text window that displays the degree of polarization in percent. Set the cursors at the dark value, minimum and maximum of the polarimeter response as explained in the section *poldegree*($\rightarrow$ page 78). When you are finished, click *OK* to leave the script.

References

Batschelet, E. (1981). Circular Statistics in Biology. Academic Press, 111 Fifth Ave., New York, NY 10003, 1981, 388.

Labhart, T. (1996). How polarization-sensitive interneurones of crickets perform at low degrees of polarization. J Exp Biol, 199, 1467–75.

CV
KERAM PFEIFFER

ADDRESS

Cappeler Str. 32

35039 Marburg

Germany

Office: +49 6421 28-23494

Home: +49 6421 948476

email: Pfeiffer@staff.uni-marburg.de

web: http://cgi-host.uni-marburg.de/∼omtierph/neuro/

PERSONAL

Born:	Mönchengladbach, Germany, July 10th 1975
Citizenship:	German
Marital status:	unmarried

EDUCATION

1986 - 1995	High school: staatliches Otto-Hahn-Gymnasium, Saarbrücken, Germany
1995 - 2001	Undergraduate: Philipps-Universität Marburg, Germany
2001 -	PhD: Philipps-Universität Marburg, Germany

DEGREE

2001:	Diploma Title of thesis: Characterization of interneurons with ramifications in the anterior optic tubercle of the locust *Schistocerca gregaria*

AWARDS

2002	Travel allowances, Boehringer Ingelheim Fonds, Germany, €3,000
2002	Marine Biological Laboratory Scholarship funded by Howard Hughes Medical Institute, USA, $3,450
2002	Travel allowances, Foundation of the Philipps-Universität Marburg, Germany, €489

ACADEMIC APPOINTMENT

2001 - 2005	Research Assistant, Philipps-Universität Marburg, Germany

TEACHING

Tutor in undergraduate courses:

Animal Physiology	Subject: Fundamentals of Neurophysiology Method: Extracellular recordings from earthworm giant fibers
Animal Physiology	Subject: Fundamentals of Sensory Physiology Method: ERG from locust eye
Neurophysiology	Subject: Sensory Physiology Method: Intracellular recordings from visual interneurons of the locust brain
Biology for medical students	Subject: Circadian rhythms Method: Behavioural experiments

SCIENTIFIC MEETINGS

2004   Organizing Committee, 15th Neurobiological
                       PhD-Students Workshop, Marburg, Germany

INVITED PRESENTATIONS

2003   "Polarization vision: Behavioural and electro-
                       physiological studies in the locust *Schistocerca
                       gregaria*", University of Zürich, Switzerland, In-
                       stitute of Zoology, Group of Prof. Dr. Rüdiger
                       Wehner, (shared talk with Martina Mappes)

2005   "Polarization vision and sky compass in the
                       desert locust", 30th Göttingen Neurobiology
                       Conference, Germany, (shared talk with Prof.
                       Dr. Uwe Homberg)

2005   "Processing of sky compass signals in the lo-
                       cust brain", Neurobiological Arthropod Semi-
                       nar, Bielefeld, Germany

SPECIAL TRAINING

2002   Neural Systems and Behavior Course, Marine
                       Biological Laboratory, Woodshole, MA, USA

PUBLICATIONS

Reviewed Articles:

1. Homberg U, Hofer S, Pfeiffer K, Gebhardt S (2003): Organization and neural connections of the anterior optic tubercle in the brain of the locust, *Schistocerca gregaria*, J Comp Neurol, 462:415-430

2. Pfeiffer K, Kinoshita M, Homberg U (2005): Polarization-sensitive and light-sensitive neurons in two parallel pathways passing through the anterior optic tubercle in the locust brain, J Neurophysiol, 94:3903-3915

Review:

1. Homberg U, Hofer S, Mappes M, Vitzthum H, Pfeiffer K, Gebhardt S, Müller M, Paech A (2004): Neurobiology of polarization vision in the locust *Schistocerca gregaria*, Acta Biol Hung, 55:81-89

Abstracts:

1. Pfeiffer K, Homberg U (2002): Visual signal processing in neurons of the anterior optic tubercle of the locust, *Schistocerca gregaria*, 95. DZG meeting Halle Zoology 105 Suppl. V, p45

2. Pfeiffer K, Homberg U (2003): Neurons of the anterior optic tubercle of the locust *Schistocerca gregaria* are sensitive to the plane of polarized light, NWG Göttingen Proc 5th German Neurosci Soc Conf, Thieme Verlag, Stuttgart, New York, 492 p567

3. AbstractPfeiffer K, Kinoshita M, Homberg U (2004): POL neurons of the anterior optic tubercle in the brain of the desert locust, *Schistocerca gregaria* receive multiple inputs from different regions of the compound eye, 7th International Congress of Neuroethology, Nyborg/Denmark P161, p132

4. Kinoshita M, Pfeiffer K, Homberg U (2004): Spectral sensitivity of POL neurons in the desert locust *Schistocerca gregaria*, 7th International Congress of Neuroethology, Nyborg/Denmark P162, p132

5. Pfeiffer K, Kinoshita M, Homberg U (2005): Integration of celestial orientation cues in an identified neuron in the brain of the desert locust *Schistocerca gregaria* NWG Göttingen, Proc 6th German Neurosci Soc Conf, Thieme, Stuttgart 21B, p218

6. Homberg U, Pfeiffer K (2005): Polarization vision and sky compass in the desert locust NWG Göttingen, Proc 6th German Neurosci Soc Conf, Thieme, Stuttgart S16-5, p210

Marburg, March 8th 2006   Keram Pfeiffer

Danksagung

Zunächst möchte ich mich bei Prof. Dr. Uwe Homberg für die Vergabe des spannenden und ertragreichen Themas und für die gute Zusammenarbeit bedanken. Er war jederzeit helfend und unterstützend zur Stelle, wenn es nötig war und hat mir ansonsten ein freies arbeiten ermöglicht.

Der Zweitgutachterin Apl. Prof. Dr. Monika Stengl, die durch die Fähigkeit ihre Begeisterung für die Neurophysiologie anderen Menschen zu vermitteln mein Interesse an diesem Themengebiet geweckt hat danke ich ebenfalls herzlich.

Den weiteren Mitgliedern der Prüfungskommission, Prof. Dr. Monika Hassel und Prof. Dr. Lothar Beck danke ich für die Mithilfe bei der Einhaltung meines Zeitplanes.

Bei meinem Elektrophysiologie Mentor Dr. Jan Dolzer möchte ich mich für seine stete Hilfs- und Diskussionsbereitschaft bedanken. Er hat mein wissenschaftliches Denken mitgeprägt.

Bei meinen Büromitbewohnern Martina Mappes und Dr. Nils Schneider (Doc Snyder), sowie unserem Untermieter Nico Werner Funk möchte ich mich für die lustige Atmosphäre bedanken; für ungezählte sinnvolle und sinnlose Gespräche innerhalb und ausserhalb der Universität.

Bei allen POL-seherInnen bedanke ich mich für gewinnbringende Diskussionen zu unserem gemeinsamen Thema. Es sind dies: Stephan Gebhardt, Martina Mappes, Sascha Gotthardt und Stanley Heinze.

Herrn Dr. Benjamin Funke danke ich für den TEXnischen Onlineservice.

Dr. Nils-Schneider hat durch seine große technische Versiertheit, manches Problem beim Umbau des Elektrophysiologie Messstandes mit großer Freude beseitigt. Dadurch hat er wesentlich zum Gelingen dieser Arbeit beigetragen. Dafür vielen Dank.

Ohne die Mitarbeiter der Elektronik- und der Feinmechanikwerkstatt, allen voran Sebastian Richter und Horst Schmidt wäre diese Arbeit nicht möglich gewesen. Ich bedanke mich für die Geduld und die gute Zusammenarbeit bei der Umsetzung meiner und ihrer eigenen Ideen zur Reizapparatur, die in den Versuchen zu Kapitel zwei und drei verwendet wurde.

Der Fachschaft Biologie danke ich für die Bereitstellung des Kickertisches, der für manche nichtwissenschaftliche Stunde sorgte. In diesem Zusammenhang danke ich auch Basil El Jundi, Christian Flecke, Nico Werner Funk, Dr. Nils Schneider, Julia Schuckel, Achim Werckenthin, Wolf Hütteroth sowie den Mitgliedern der Arbeitsgruppe Stoffwechselphysiologie, die die Kicker-Leidenschaft mit mir teilen.

Wolf Hütteroth gilt ausserdem mein Dank für die Einführung in die Geheimnisse der konfokalen Laser Raster Mikroskopie und für das Korrekturlesen.

Der Zentralkomplexexpertin Angela Kurylas danke ich für geduldige Antworten auf Fragen zum CX und zu Literatur.

Allen Mitgliedern der Arbeitsgruppen Homberg, Schachtner, Stengl und Wegener danke ich für die schöne Arbeitsatmosphäre.

Ein großer Dank gilt meinen Eltern und meiner Familie, die mich immer auf meinem Weg unterstützt haben.

Bei meiner Freundin Julia Schuckel möchte ich mich besonders herzlich bedanken. Durch ihre Liebe und tatkräftige Unterstützung hat sie viel zum Gelingen dieser Arbeit beigetragen. Insbesondere hat sie mir ermöglicht mich in den letzten Wochen vor der Abgabe voll auf meine Dissertation zu fokussieren.

Erklärung

ich versichere, daß ich meine Dissertation

Coding of sky-compass information in neurons of the anterior optic tubercle of the desert locust *Schistocerca gregaria*
(Kodierung von Himmelskompassinformationen in Neuronen des anterioren optischen Tuberkels der Wüstenheuschrecke *Schistocerca gregaria*)

selbständig, ohne unerlaubte Hilfe angefertigt und mich dabei keiner anderen als der von mir ausdrücklich bezeichneten Quellen und Hilfen bedient habe.

Die Dissertation wurde in der jetzigen oder einer ähnlichen Form noch bei keiner anderen Hochschule eingereicht und hat noch keinen sonstigen Prüfungszwecken gedient.

Marburg, den 4.August 2006 _____

(Keram Pfeiffer)